

The University of Nottingham

UNITED KINGDOM · CHINA · MALAYSIA

Spatio-Temporal Dynamics and Role of NIMA-related Kinase 1 (NEK1) in *Plasmodium berghei*

George McKeown B.Sc

Professor Rita Tewari PhD

Dr Mohammed Zeeshan

Date: 01/03/2021

Thesis submitted to the University of Nottingham

for the degree of Master of Research

Abstract

Eukaryotic cell division is reliant on a plethora of protein kinases required for the progression and completion of mitosis and meiosis. The NIMA-related Kinase family represent one such group of proteins that are known to play vital roles in cell division; implicated in centrosomal dynamics, axonemal assembly and chromosome segregation to name a few. *Plasmodium* species owe their success to the flexibility and speed in which cell progeny can be produced in both host and vector organisms, and it is thought that the regulative phosphorylation by the *Plasmodium* NEK equivalents are vital to this process, however, their exact roles are poorly understood. This study characterises the spatio-temporal dynamics of NEK1 expression, to a greater degree than has previously been achieved in *Plasmodium* parasites. NEK1-GFP protein was observed in the rodent malaria model, *Plasmodium berghei*, during blood stage schizogony, in addition to mosquito stage male endoreduplication and ookinete development using live cell imaging. The results reveal a highly specific pattern of NEK1 focal expression and localisation to the perinuclear space in all proliferative stages, where its divide atypically in a highly specific sequence. Additionally, the study of colocalization between NEK1 and preestablished cell division proteins, exposes an extensive association between NEK1 foci and centrosomal-related structures. Finally, protein pulldown assays and mass spectrometry of NEK1 in addition to conditional knockdown procedures, both specific to male gametocytes, reveals an extensive interaction between the kinase and various protein constituents of cell division and microgamete axonemal machinery. The dual patterns of NEK1 expression in both host and mosquito proliferative stages, where it plays a vital role in both, highlights the kinase as an attractive target for future interventionist strategies to combat the malaria parasite.

Acknowledgements

First and foremost, I would like to thank my supervisor, Professor Rita Tewari, for providing me with a very interesting and rewarding project in addition to her continued support in and outside of the lab over the course of this study. I would also like to thank my secondary supervisor, Professor Liz Sockett, for assisting me in the administrative background of my degree. Thirdly, I would like to thank Dr Mohammed Zeeshan for his seemingly endless supply of knowledge with respect to both scientific background and lab technique, provided on a daily basis. I would also like to extend my gratitude to Declan Brady, for his continued mentoring of lab procedure, in addition to his behind-the-scenes technical support, which was invaluable to this project.

Abbreviations

α	alpha
β	beta
µl	microlitre
µm	micrometre
acc/dec	acceleration/deceleration
AID	Auxin-inducible degron
ARK	Aurora-related kinase
ATP	Adenosine triphosphate
BB	basal body
bim	blocked in mitosis
Bp	base pairs
CDK	cyclin-dependent kinase
Cen	centrin
CF11	Cellulose Fibre 11
Cyc	cyclin
DDR	DNA damage response
DIC	differential interference contrast
DNA	Deoxyribonucleic acid
G_1	Gap 1
G_2	Gap 2
GFP	green fluorescent protein
HDAC	histone deacetylase
hDHFR	human dihydrofolate reductase
HP1	heterochromatin protein 1
HSPG	heparan sulphate proteoglycans
IFA	immunofluorescence assay
IMC	inner membrane complex
Kb	kilobase
Kc	Kupffer cells
kDa	kilodalton

M	mitosis
Mg	milligrams
MS	mass spectrometry
MSP	merozoite surface protein
MTOC	microtubule organising centre
Mut	mutant
NAG	non-activated gametocytes
NEK	NIMA-related kinase
nim	never in mitosis
OAD	outer-arm dynein
PCR	polymerase chain reaction
Pen/Strep	Penicillin Streptomycin
PK	protein kinase
PV	parasitophorous vacuole
qRT-PCR	quantitative PCR
RBC	red blood cell
RNA	Ribonucleic acid
RON	rhoptry neck protein
rpm	revolutions per minute
S	synthesis
SDS	sodium dodecyl sulphate
SPB	spindle pole body
V	volt
WT	wild-type

Table of Contents

Abstract ..... **i**

Acknowledgements ..... **ii**

Abbreviations ..... **iii**

Table of Contents ..... **v**

List of Figures ..... **viii**

List of Tables ..... **ix**

1.0 Introduction **10**

1.1 *Plasmodium* Life Cycle 11

1.1.1 Pre-erythrocytic Stages 13

1.1.2 Erythrocytic Stages 15

1.1.3 Sexual Stages 19

1.1.4 Mosquito Stages 20

1.2 Cell Cycle and Division 23

1.2.1 Eukaryotic and *Plasmodium* Cell Cycles 23

1.2.2 Strategies and Mechanisms of Eukaryotic and *Plasmodium* Cell Division 25

1.2.3 *Plasmodium* Endomitosis 27

1.3 Alternative Methods for Apicomplexan Asexual Cell Division 28

1.3.1 *Toxoplasma* Endodyogeny 28

1.3.2 *Sarcocystis* Endopolygeny 29

1.3.3 *Plasmodium* Male Gametogenesis 31

1.4 Cell Regulation 33

1.4.1 Microtubule Organising Centres 33

1.4.2 Cyclins and Kinases Implicated in Cell Division 34

1.4.3 NIMA-related Kinases 39

1.4.4 *Plasmodium* NIMA-related Kinases 42

2.0 Aims and Objectives **45**

3.0 Materials and Methods **47**

3.1 Ethics Statement 51

3.2 Mouse and Mosquito Maintenance 51

3.3 Generation of Transgenic Parasites 51

3.3.1 Isolation of NEK1 C-terminal Regions for use in Alternative Transgenic Parasites 51

3.3.2 Ligation 52
3.3.3 Transformation 52
3.3.4 Isolation of Plasmid DNA from *E. coli* 53
3.3.5 Transfection 54
3.4 Genotypic Analysis 54
3.4.1 Isolation of asexual *Plasmodium* Stages from Mouse Blood 54
3.4.2 Extraction of *Plasmodium* DNA from Parasite Pellets 55
3.4.3 Diagnostic PCR 55
3.5 Analysis of Gene Expression 57
3.5.1 RNA Extraction 57
3.5.2 cDNA Synthesis 57
3.5.3 Quantitative PCR (qRT-PCR) 57
3.6 Proteomic Analysis 58
3.6.1 Protein Preparation and Western Blotting 58
3.6.2 Immunoprecipitation Pulldown 59
3.7 Phenotypic Analysis 60
3.7.1 Giemsa Staining 60
3.7.2 Schizont Media and Purification 60
3.7.3 Gametocyte Host Preparation 60
3.7.4 Exflagellation Counts 61
3.7.5 Gametocyte and Ookinete Purification 61
3.7.6 Fluorescent microscopy 62
3.7.7 Immunofluorescent Assays 62
4.0 Results 64
4.1 Expression and Localisation of NIMA-related Kinase 1 in *P. berghei* 64
4.1.1 Genotypic Analysis Confirms Integration of NEK1-GFP Parasite Lines 64
4.1.2 NEK1 is Temporally Expressed in Both Asexual and Sexual Stages Where it Localises to the Nuclear Periphery and Divides in Specific Sequence 66
4.1.3 NEK1 Localisation in Asexual Blood Stages 67
4.1.4 NEK1 Localisation in Activated Male Gametocytes 69
4.1.5 NEK1 Localisation in Ookinete Stages 71
4.2 NEK1 Localises at Centriole-related Structures During Schizogony and Male Gametogenesis 74
4.2.1 NEK1 Localises with Centrin-2 Markers 74

4.2.2 NEK1 Partially Colocalises with α-tubulin During the Dividing Stages of Gametogony, However, not Schizogony 76

4.2.3 NEK1 Localises with NDC80 and Shares a Similar Pattern of Focal Duplication During Genome Replication 80

4.3 Proteomic Analysis Reveals a Large Number of Interactive Partnerships Between NEK1 and other Proteins Implicated in Cell Division and Axonemal Functioning 82

4.3.1 NEK1 Interacts with a Number of Motor Proteins During Male Gametogenesis 83

4.4 Functional Analysis of NEK1 Implicates it as an Essential Kinases for *Plasmodium* Sexual Development 85

4.4.1 Analysis of NEK1 Function in Gametogenesis and Ookinete Formation..... 85

4.4.2 Confirmation of Clag1 Integration into the NEK1 Gene for use in Conditional Knockdown 85

4.4.3 Nek1 is Essential for the Progression of the Sexual Stages 88

4.4.4 NEK1 is Essential for Male Exflagellation 88

4.4.5 No Ookinete Development was observed in NEK1clag Parasites 90

4.4.6 No Oocyst Formation was Observed in NEK1clag Parasites 92

4.4.7 NEK1 may act as an Upstream Regulator of MAPk2 93

5.0 Discussion..... 95

5.1 Localisation and Expression of NEK1 in Proliferative Stages 96

5.2 Colocalization of NEK1 Proteins 102

5.3 Interacting Partners of NEK1..... 107

5.4 Functional Analysis of NEK1 in *Plasmodium berghei* 109

5.5 Concluding Remarks..... 115

References 116

Appendices 128

List of Figures

Figure 1 - The life cycle of *Plasmodium*. 12
Figure 2 - Sporozoite inoculation and subsequent exoerythrocytic development of *Plasmodium*. 14
Figure 3 - Cell morphologies of the three invasive stages in the *Plasmodium* life cycle.. 18
Figure 4 - Progression of the mosquito ookinete from the onset of male exflagellation, fertilisation and zygote maturation. 21
Figure 5 - Development of *Plasmodium* parasites within the midgut of a female *Anopheles* mosquito. 22
Figure 6 - Comparative views of the conventional cell cycle vs the Apicomplexan cell cycle. 24
Figure 7 - Traditional cell mitosis compared to *Plasmodium* mitosis as occurs in the blood stage. 26
Figure 8 – The strategies of asexual cell division utilised by Apicomplexan parasites. 30
Figure 9 – Formation of the axonemes during *Plasmodium* male gametogenesis. 32
Figure 10 - Genotypic analysis of NEK1-GFP genes to confirm successful integration. ... 65
Figure 11 - NEK1-GFP expression (green) in intraerythrocytic asexual stages viewed under a fluorescent microscope. 68
Figure 12 - Fluorescent microscopy of NEK1-GFP focal expression and localisation during male gametogenesis. 70
Figure 13 - NEK1-GFP expression in exflagellating males and the resultant flagella approximately ~15 minutes post activation, as seen using fluorescent microscopy. 71
Figure 14 - NEK1-GFP expression in males compared to female gametocytes and the two zygote phenotypes observed. 72
Figure 15 - NEK1-GFP expression during ookinete development. 73
Figure 16 - Localisation studies using NEK1-GFP with centrin markers in fixed IFA blood stage schizonts. 75
Figure 17 - Localisation studies using NEK1 and α-tubulin in fixed IFAs samples of blood stage schizonts. 77
Figure 18 - Localisation studies using NEK1 and α-tubulin in fixed IFAs samples of activated male gametocytes. 79
Figure 19 - Spatio-temporal patterns of NEK1-GFP relative to NDC80-mCherry proteins in live imaged cells. 81
Figure 20 - Genotypic analysis of NEK1clag genes to confirm successful integration. 87
Figure 21 - Number of NEK1clag and WT exflagellating males observed after activation. 89
Figure 22 - NEK1clag and WT ookinete development and phenotypic analysis. 91
Figure 23 - NEK1clag and WT oocyst development. 92
Figure 24 - Normalized expression of cDNA encoding proteins implicated in male gametogenesis, in the presence or absence of NEK1 wild-type and NEK1clag respectively. 94

List of Tables

Table 1 – Summary table of CDKs and ARK proteins identified in *Plasmodium*. 38
Table 2 – NEKs identified in human cells. 41
Table 3 – Neks identified in *Plasmodium* 44
Table 4 – List of materials 47
Table 5 – List of solutions 48
Table 6 – List of antibodies 49
Table 7 – List of commercial kits 49
Table 8 – List of enzymes 49
Table 9 – List of primer sequences 50
Table 10 – Mass spectrometry results of NEK1-GFP in male gametocytes. 84

1.0 Introduction

The Apicomplexan subphylum is an extensive grouping of heterotrophic species belonging to the eukaryotic domain, of which all have evolved parasitic strategies used as a means for survival and reproduction. The infection and exploitation of the host by various species is responsible for a plethora of diseases including babesiosis, toxoplasmosis and cryptosporidiosis. *Plasmodium,* which are mosquito-borne, intracellular, Apicomplexa, are the agent responsible for causing malaria, arguably the most clinically important Apicomplexan disease infecting vertebrate species including humans. Malarial pathology is attributed to the destructive intraerythrocytic life cycle exhibited by the parasite required for asexual reproduction, causing erythrocytic death and associated symptoms. It is as a result of the manifestation of these malarial symptoms in humans that the disease continues to pose a threat to billions of individuals, thus making the parasite of great importance to medical science. To date, 250 species of *Plasmodium* have been documented, of which five are known human pathogens: *Plasmodium falciparum*, *P. vivax*, *P. malariae*, *P. ovale* and *P. Knowlesi (WHO, 2019).* Despite a marked decline in disease incidence and mortality being achieved throughout the last few decades, albeit at varying rates, in 2018, 228 million cases and 405,000 deaths were recorded (WHO, 2019). *P. vivax* is responsible for around half of all recorded cases of malaria (WHO, 2015), evidenced by the fact it is the most dominant species outside of Sub-Saharan Africa. The parasite exhibits the greatest geographical range compared to that of its counterparts; attributed to its potential to trigger a state of dormancy whilst in the liver phase. This ensures the parasite's survival until the return of optimum conditions (Menkin-Smith and Winders, 2020), the presence of which allows for the continuation of hepatocytic asexual schizogony and a relapse in infection (Tuteja, 2007). The parasite demonstrates a consistently high prevalence throughout South-East Asia, the Western Pacific and the Americas, regions collectively accounting for 3.5 billion people, many of whom are at risk

of infection (Howes et al., 2016). Despite *P. vivax* and *P. falciparum* sharing common vectors and environmental optima, the former plays a subsidiary role compared to the latter within the African continent. This is attributed to the percentage of native Africans displaying a Duffy-negative blood phenotype, an essential antibody required for *P. vivax* erythrocytic recognition, attachment and invasion by the merozoite stages (Gunalan et al., 2016; Langhi and Bordin, 2006). In spite of *P. vivax* accounting for most malarial cases, *P. falciparum* infections are responsible for the greatest amount mortality as a result of a higher virulence (Geleta and Ketema, 2016). Whilst *P. vivax* and *P. ovale* can cause anaemia in chronic forms of the disease, most severe symptoms concomitant with acute malaria are resultant from *P. falciparum* (Trampuz et al., 2003). Mortality within the African continent accounts for 90% of all malaria associated deaths (Bannister and Sherman, 2009), the most impacted demographic being children under the age of five. Major health complications include cerebral malaria and acute renal failure (Ghosh and Ghosh, 2007; Tuteja, 2007), both brought about in part due to the blockage of the host's vasculature in conjunction with alterations in blood viscosity and red blood cell (RBC) decline.

1.1 *Plasmodium* Life Cycle

The *Plasmodium* life cycle alternates between a primary vertebrate host and a mosquito vector, specifically a female *Anopheles* mosquito in the case of human malaria parasites. After host inoculation, two rounds of asexual replication proceed, consisting of sporozoite exoerythrocytic and merozoite erythrocytic schizogony, the latter continuing indefinitely due to repeated invasion of host RBCs. A subset of the blood stage parasite population differentiates into male and female gametocytes and activate upon entering the mosquito's midgut. This culminates in male gametogenesis, during which, three rounds of genomic replication produces eight identical haploid flagella (1n), egressing from the male microgamete after exflagellation. These flagella fertilise female macrogametes (1n)

producing zygotes (2n), similar to the mechanisms involved in sperm and egg fertilisation events. The zygote undergoes developmental stages, culminating in a motile ookinete which develops into an oocyst along the mosquito midgut basal lamina and proliferates producing thousands of sporozoites, which invade the vectors salivary glands to continue the life cycle (Menard et al., 2013) (Figure 1).

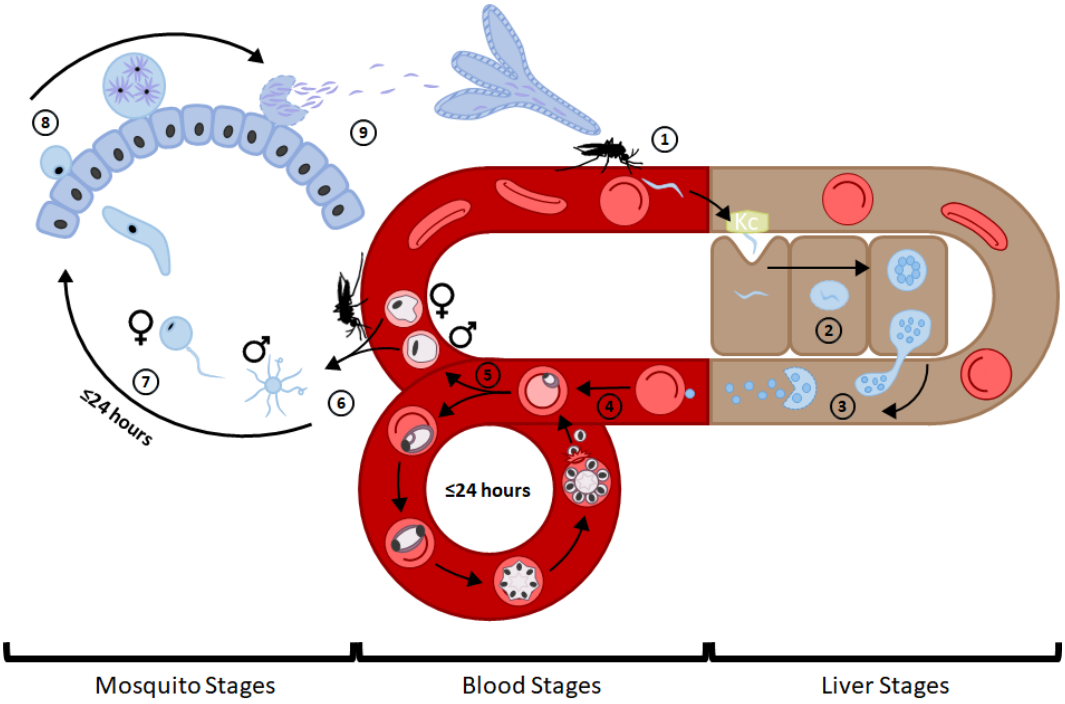


Figure 1 - The life cycle of *Plasmodium*.

The life cycle of *Plasmodium* begins when a female *Anopheles* mosquito injects motile sporozoites into the host, which travel to the sinusoid and enter the hepatocytes **(1)** (KC = Kupffer cell). The sporozoite travels through multiple cells before undergoing pre-erythrocytic asexual schizogony, producing thousands of invasive merozoites **(2)** which are released into the blood stream via the sinusoid **(3)**. Merozoites invade erythrocytes **(4)**, and undergo asexual schizogony, releasing more merozoites. A subset of the population may differentiate into male and female gametes **(5)** which enter female mosquitoes during blood meals **(6)**. Activated males produce flagella and fertilise females to form a zygote, which develops into a motile ookinete **(7)**. Ookinetes exit the midgut through the epithelium, and produce a cyst in which sporozoites develop **(8)**. Sporozoites are released and invade the mosquito salivary glands, ready for host inoculation **(9)**. Adapted from **(CDC, 2019)**.

1.1.1 Pre-erythrocytic Stages

Transmission of the parasite is achieved prior to the commencement of a blood meal by a female *Anopheles* mosquito, during which a few nanolitres of anti-coagulant containing saliva is injected into the dermis of the host (Hopp and Sinnis, 2015) (see Figure 2). If the mosquito is carrying the parasite, it is this injection of the saliva that inoculates the host with the invasive motile sporozoites. After the initial injection, the parasite migrates toward the host's vasculature, which is required for the transportation of the parasite to the liver. Hepatocytes are the final destination for the sporozoite, which access these cells by traversing through the liver sinusoid, before entering Kuppfer cells to emerge in the space of Disse (Barnwell, 2001; Coppi et al., 2007).

The parasite's ability to distinguish between various host cells is highly important, as failure to locate and invade the appropriate hepatocyte, would prevent it from establishing its exoerythrocytic form. Certain environmental stimuli are therefore exploited by the sporozoite to aid in cellular recognition, including the presence of heparan sulphate proteoglycans (HSPG). These ubiquitous glycoproteins, covalently bound to heparan sulphate chains, display a highly diverse range of functions dictated by their operative locations; the surfaces of membranes, within secretory vesicles or in the extracellular matrix (Roskams et al., 1995; Sarrazin et al., 2011). It is the level of proteoglycan sulphation that appears to alter the behaviour of the sporozoite, with low sulphate expressing cells causing a migratory response in the parasite, in contrast to high sulphated cells, which triggers parasitic invasion (Coppi et al., 2007). The HSPGs associated with the hepatocyte membrane, bind with the densely packed circumsporozoite protein found on the parasite's surface, which triggers sporozoite invasion and the onset of enzymatic secretions from the rhoptries and micronemes (Vaughan and Kappe, 2017) (see Figure 3).

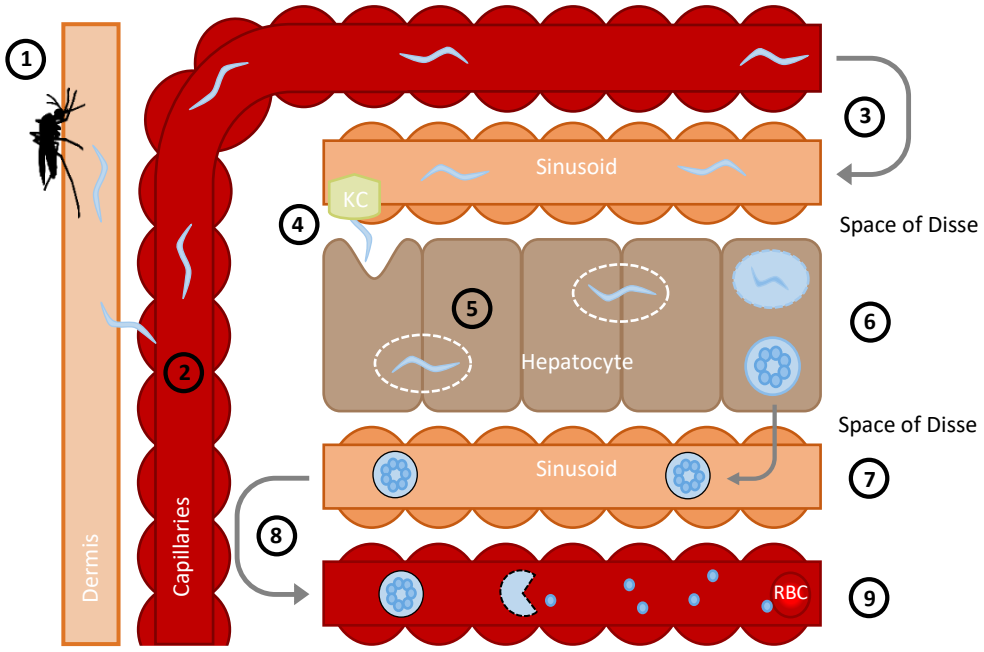


Figure 2 - Sporozoite inoculation and subsequent exoerythrocytic development of *Plasmodium*.

Sporozoites are injected into the skin by a female *Anopheles* mosquito **(1)** and proceed to the capillaries **(2)** which subsequently transport them to the liver sinusoid **(3)**. They access the hepatocytes via the Kupffer cells (KC) and invade from the space of Disse **(4)**, before travelling across numerous cells inside a transient vacuole **(5)**. A PV is formed inside the chosen cell, in which asexual schizogony produces up to 40,000 merozoites **(6)**. The vacuole ruptures, releasing the merozoites in a merosome, which enters the sinusoid **(7)** and is transported to the blood vessels **(8)**. Here, the merosome ruptures, releasing the merozoites into the blood **(9)** which within 60 seconds, may attach to an erythrocyte prior to invasion.

The parasite may enter multiple hepatocytes before establishing an exoerythrocytic infection, gliding through the cytoplasm whilst contained inside a transient vacuole (Govindasamy et al., 2016; Menard et al., 2013). When the sporozoite locates the appropriate hepatocyte cell, it forms a parasitophorous vacuole (PV), which offers protection from the host's immune system in conjunction with providing the subsequent proliferative stages with a niche compartment in which they can develop (Coppi et al., 2007; Risco-Castillo et al., 2015). In addition, the parasite has also been implicated in the alteration of internal cellular conditions, specifically the up-regulation of aquaporin-3, a protein associated with solute transportation across the membrane. The deletion of this

protein results in a decline in the parasite content within the liver, indicating that increased nutrient transport during the exoerythrocytic phase is highly important to *Plasmodium* development (Posfai et al., 2018).

Asexual schizogony within the PV can produce between 2000 to 40,000 uninucleate merozoites, each with the propensity to invade a single RBC (Crutcher and Hoffman, 1996; Hisaeda et al., 2005). The merozoites are ovoid in shape and represent the smallest form of *Plasmodium* in its life cycle. Rhoptries, micronemes and dense granules make up the cell's invasive arsenal, with the former two being attached at the polar rings and the latter being suspended in the cytoplasm. A coat of bristle-like structures associated with various proteins are present on the outer membrane, and aid in RBC attachment (Bannister et al., 2000a) (see Figure 3).

Merozoites are released when the PV ruptures, however, at the point where the parasites enter the blood vessels, they are still contained within a vacuole known as a merosome (Sturm et al., 2006). Single merozoites are highly susceptible to phagocytosis, of which there is an elevated risk within the liver due to the incredibly high concentration of the Kupffer cells, immune macrophages located within the lumen of the sinusoid (Baer et al., 2007; Terzakis et al., 1979). The merosome, being a derivative of the hosts own cell membrane, allows the merozoites to avoid detection and subsequent engulfment by the body's immune orientated macrophages, thus allowing them to enter the bloodstream (Burda et al., 2017).

1.1.2 Erythrocytic Stages

The merosome ruptures within the blood vessels, realising the merozoites and thus starting the phase of the *Plasmodium* lifecycle with which the pathology of malaria is associated (Burda et al., 2017). The membrane bound cell receptors of the host's RBCs provide the parasite with a means of identifying the appropriate cells for invasion. Upon

finding an erythrocyte, the merozoite attaches to its surface via receptor-ligand interactions, with glycophosphatidylinositol anchored merozoite surface proteins (MSP-1) being implicated (Beeson et al., 2016). Specific components of the ligand reactions concerned with RBC attachment are not fully understood, however, it has been implied that many different pathways for attachment exist. The range of invasive pathways available to the merozoites likely stems from the need for diversity in invasive techniques, driven by selection pressures exerted by the host's immune system, in conjunction with the polymorphisms in RBCs seen across different human groups (Jaskiewicz et al., 2019; Maier et al., 2003).

Once attached, the merozoite positions itself with its apical end perpendicular to the plasma membrane, required due to the concentration of the invasive organelles within the apical complex. Secretions from the rhoptries and micronemes, including RON proteins (rhoptry neck proteins) and AMA1 respectively, form a junction between the two cells known as the moving junction (Koch and Baum, 2016). Deformation of the RBC plasma membranes is mediated by the use of actin-myosin motors located within the inner membrane complex (IMC), which are associated with membrane bound adhesins (Besteiro et al., 2011). The membrane of the RBC is not cleaved during this process, as the parasite uses it to encapsulate itself in a PV, similar to that of the sporozoite exoerythrocytic stage.

After invading an erythrocyte, the merozoite no longer has use for its invasive organelles, resulting in the loss of the rhoptries, micronemes and dense granules. The parasite undergoes a number of morphological changes, which culminates in the formation of the ring stage, so named due to the infected RBC developing a hollow centre, with the parasite developing around the periphery into a flattened discoidal structure (Bannister et al., 2000a; Bannister et al., 2004). Erythrocyte cytoplasm is ingested through the cytostome

and broken down by the parasite resulting in the formation of hemozoin crystals, a derivative of the ferriprotoporphyrin constituent of haemoglobin, which is packaged in food vacuoles due to its toxicity (Tuteja, 2007). Parasitic expansion and the presence of visible food vacuoles within the RBC, denotes the onset of the trophozoite stage. Atypical nuclear division results in the formation of the schizont, which over the course of 24 hours produces between 10 to 36 merozoites (Crutcher and Hoffman, 1996). For the RBC to rupture, the secondary structure of MSP-1 must change to increases its affinity to bind with spectrin (erythrocyte cytoskeletal protein), achieved by interactions with serine proteases known as SUB1 (Das et al., 2015). Upon merozoite release into the bloodstream, a cycle of repeated erythrocytic invasion and asexual schizogony takes place.

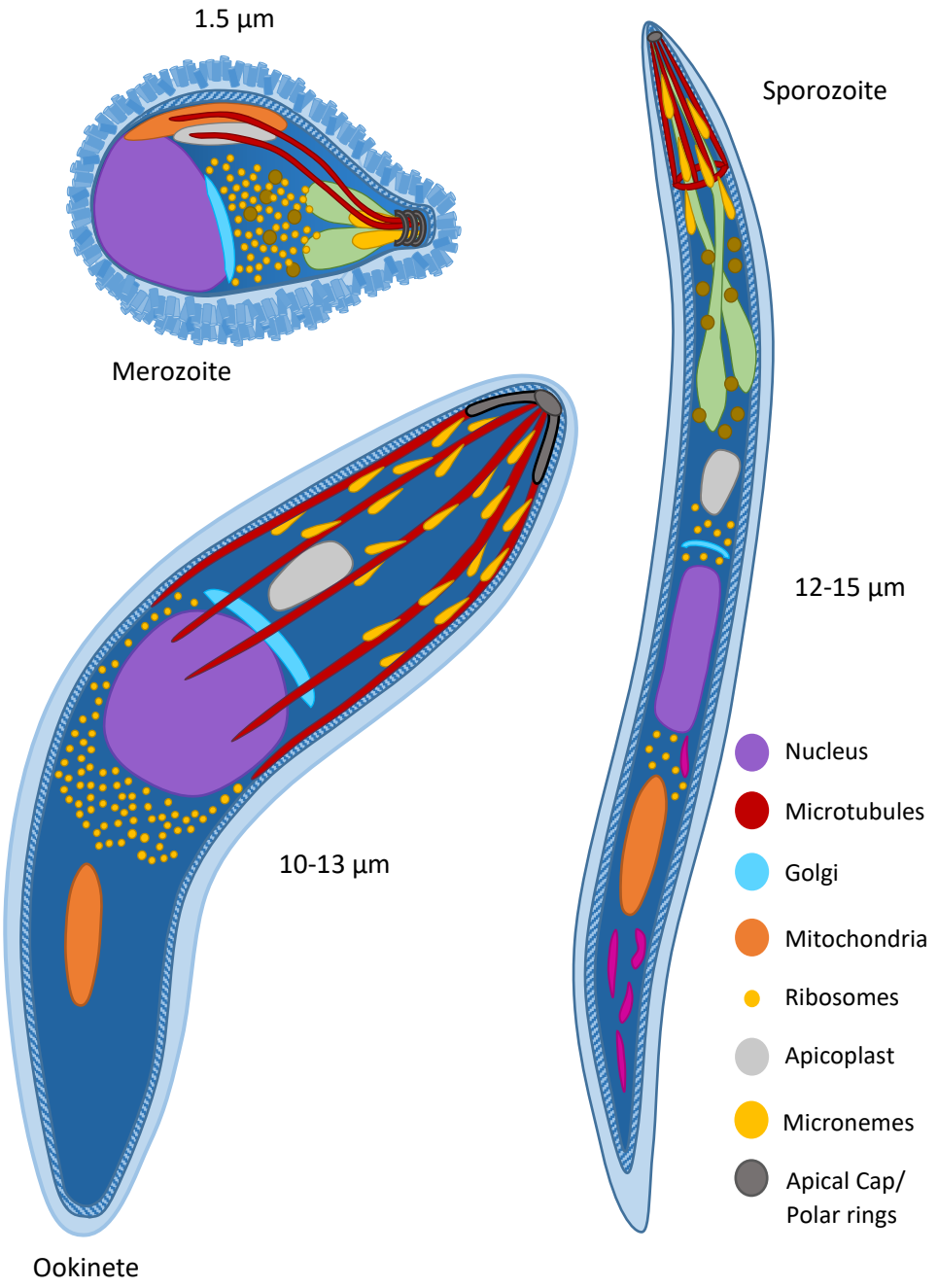


Figure 3 - Cell morphologies of the three invasive stages in the *Plasmodium* life cycle.

Plasmodium invasive stages include the merozoite (top left), sporozoite (right) and ookinete (bottom left). The structures conserved across the three stages include: nuclei (purple), microtubules (red), Golgi apparatus (light blue), mitochondria (orange), ribosomes (golden-yellow), apicoplasts (light grey), micronemes (yellow) and apical rings (dark grey) with the ookinete having an additional apical collar. The zoite stages also possess rhoptries (green) and dense granules (brown) which are lost in the ookinete stage. The ookinete does not form a PV within the cells of mosquitoes as it exists extracellularly, and thus does not need rhoptries for cell attachment or the formation of the moving junction. Diagrams adapted from **(Bannister et al., 2003; Bannister et al., 2000a; Brown et al., 2017; Harding and Frischknecht, 2020)**.

1.1.3 Sexual Stages

Repeated invasion of RBCs continues indefinitely, however, a small stochastic number of parasites (<10%) undergo differentiation to produce male and female gametes, which represents the mature and transmissible form of the organism (Guttery et al., 2012; Josling and Llinas, 2015). It has been demonstrated that the DNA-binding transcription factor, AP2-G, is the main component responsible for initiating sexual commitment in both *Plasmodium berghei* and *P. falciparum*, acting as the master transcriptional regulator for this process (Filarsky et al., 2018; Kafsack et al., 2014). Further demonstrations have shed light on the activities involved upstream of AP2-G, implicating various other components in gametocytogenesis. The histone deacetylases (HDAC) are responsible for the promotion of transcriptional silencing by the deacetylation of histone proteins (Coleman et al., 2014). This results in the binding of heterochromatin protein 1 (HP1) in *P. falciparum*, which recruits chromatin modifying histone methyltransferases, subsequently altering histone density and forming the gene suppressing variety of chromatin, heterochromatin, as opposed to euchromatin (Bui et al., 2019). HDAC2 and HP1 have consequently been implicated as epigenetic regulators of AP2-G preventing sexual differentiation (Filarsky et al., 2018; Rea et al., 2018), substantiated by reports that the removal of either significantly increases gametocytaemia (Bui et al., 2019; Coleman et al., 2014). To counter HP1 and initiate sexual commitment by the activity of AP2-G, the gametocyte development 1 protein has been shown to evict HP1 activity in heterochromatin, derepressing AP2-G transcription and thus inducing the necessary changes to allow for the signalling pathway to progress towards sexual commitment (Filarsky et al., 2018; Usui et al., 2019). Deletion or over expression of this gene has been reported to terminate gametocyte production or drastically increase gametocyte production respectively (Eksi et al., 2012; Usui et al., 2019). The exact causes for the release of these factors remains unidentified, however, it is likely that a combination of

host and environment mediated stressors are responsible for triggering gametocytogenesis, with immune response to infection and drug treatment being a few examples that have been shown to have a positive feedback on this process (Talman et al., 2004).

1.1.4 Mosquito Stages

Gametocytes enter the midgut of female *Anopheles* mosquitoes during blood meals, where the change in conditions results in their activation. Implicated signals for activation include a drop in temperature, an increase in pH from 7.3 to 8.0 and the presence of xanthurenic acid (Bennink et al., 2016; Billker et al., 1997). Within 15 minutes post activation, males undergo DNA replication and exflagellation. Three rounds of consecutive genomic duplication produce a polyploid nucleus containing up to 8 identical genomes. Individual nuclei containing haploid genomes bud from parent nucleus after the formation of the flagellar axonemes, and are packaged into the developing flagella, producing eight motile haploid microgametes which fuse with the haploid female macrogamete to produces the diploid zygote (Bannister and Sherman, 2009; Kuehn and Pradel, 2010; Sinden, 2009; Sinden et al., 1976). Developmental stages in ookinete formation were first described by Janse et al. (1985), who observed the in vitro progression of *P. berghei* zygotes over a 24 hour period, formulating a six step process between the onset of female fertilisation and zygote maturation. His observations placed an emphasis on the spatio-temporal patterns of the nucleus and dense granules in Giemsa-stained cells, with cell morphology playing a subsidiary role in stage description. The characterisation of ookinete development has since been rationalised by Wall et al. (2016), who placed a greater emphasis on cell morphologies at determined time points, made possible by the use of Cy3-labelled antibodies associated with P28 proteins expressed on zygote and ookinete membranes. During maturation, an extension of the membrane

progresses into a visible protrusion which grows longer over time (see Figure 4); a product of essential microtubule elongation (Shahabuddin, 1998). Eventually, the round segment of the cell from which the protrusion originated begins to shrink, incorporating itself into the elongated structure bringing the nuclear material with it.

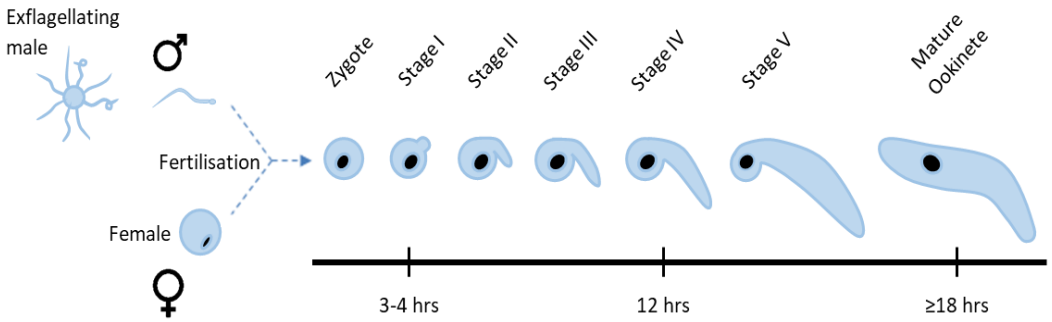


Figure 4 - Progression of the mosquito ookinete from the onset of male exflagellation, fertilisation and zygote maturation.

Progression of the mosquito ookinete from the onset of male exflagellation, fertilisation and zygote maturation through six developmental stages, first observed by **Janse et al. (1985)**. Male exflagellation produces eight flagella which fuse with the female macrogamete to fertilise. Females and zygotes are morphologically similar, however, zygotes have a larger and more rotund nucleus, as they are diploid. A small protrusion in the cell is visible after 3-4 hours (Stage I), which forms the basis of the new "banana-shaped" ookinete morphology and continues to elongate (Stage II to IV). Stage V ookinetes consist of a main body with the remnants of the zygote at the apical end, still containing the nuclear material. Mature ookinetes incorporate the round cell into its structure, bringing with it the nucleus which relocates to the centre of the cell.

The ookinete lacks the rhoptries present on early invasive stages (see Figure 3), however, as this form exists and functions extracellularly, they are not required due to the absence of a PV post invasion (Kats et al., 2006). Micronemes and actin-myosin based motility mechanisms are present however. Various secretions from the micronemes are used for epithelial attachment and cell cleavage, whilst gliding motility allows the parasite to swiftly enter the ruptured cell and exit the midgut (Bannister and Sherman, 2009; Lal et al., 2009). Further secretions produce the walls of the oocyst, which implants itself into the basal lamina. Within the cyst, endomitotic nuclear divisions result in the formation of

between 2000-8000 sporozoites over a 21 day period (Sinden, 2009), which upon release, migrate to the mosquito's salivary glands in preparation for the invasion of the next host (see Figure 5).

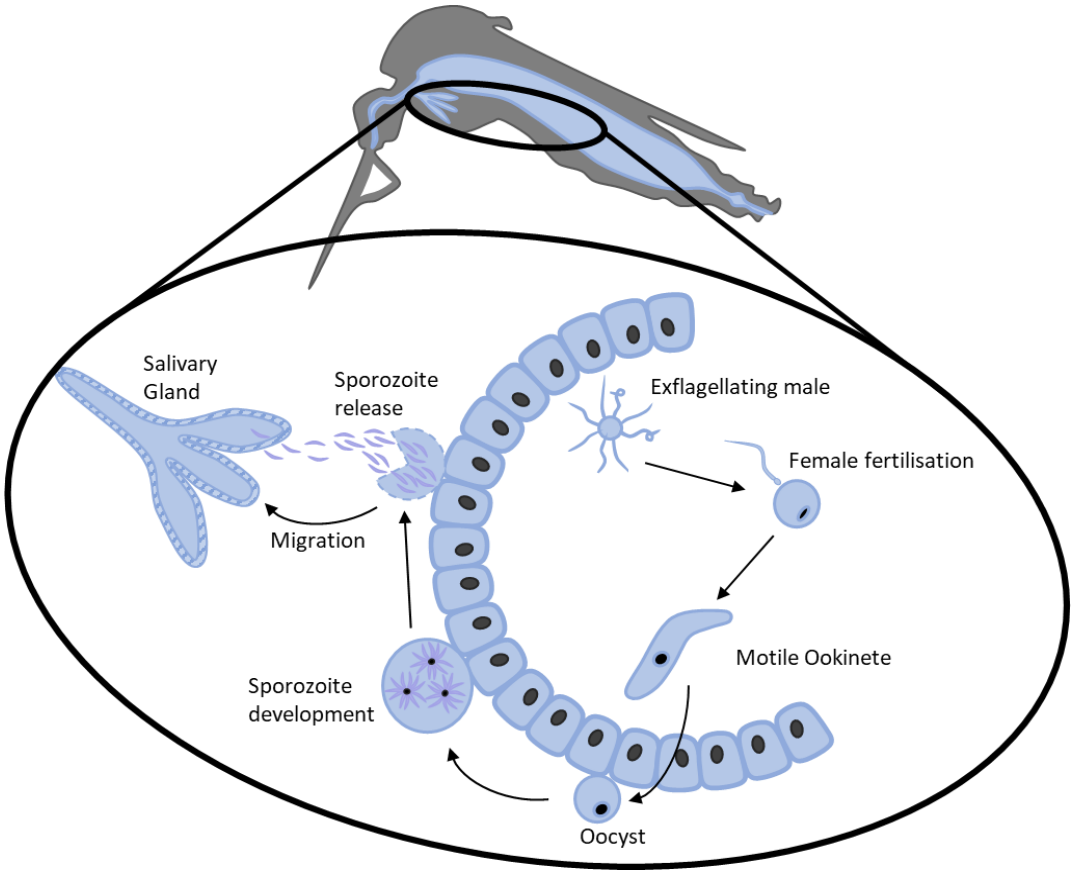


Figure 5 - Development of *Plasmodium* parasites within the midgut of a female *Anopheles* mosquito.

Mature ookinetes are formed after a six-stage process lasting 24 hours. Motile cells then proceed to exit the midgut interior by forcing through the epithelial cells. An oocyst develops on the midgut exterior wall, which undergoes endomitotic divisions and produces up to 8000 sporozoites over a 21-day period. The oocyst ruptures, and the motile sporozoites travel to the salivary gland, whereupon they are injected into the host during a blood meal, carried in the anti-coagulant saliva of the vector and thus reinitiating the cycle.

1.2 Cell Cycle and Division

1.2.1 Eukaryotic and *Plasmodium* Cell Cycles

The general eukaryotic cell cycle is a coordinated four-phase process in which cells grow, metabolise and replicate within an approximate 24-hour window. At its most basic interpretation, it is split into two distinct stages consisting of mitosis (M) and interphase, the latter being further divided into Gap 1 (G_1), synthesis (S) and Gap 2 (G_2), collectively accounting for 95% of the cycle duration (Cooper, 2000). During mitotic division, condensed DNA is separated into daughter chromatids and divided amongst opposite cell hemispheres. Cytokinesis results in cell cleavage producing two identical haploid daughter cells. Interphase represents the cycles preparatory intermission, required prior to the onset of DNA replication and mitosis. G_1 and G_2 intervals occur at the start and end of interphase, with the former in preparation for DNA replication during the S phase, and the latter prior to mitosis. During these two periods, cells grow, metabolise and synthesize proteins ready for the proceeding stage.

The cell cycle model observed in most eukaryotic organisms can be adapted to *Plasmodium* erythrocytic schizogony. In contrast to the four-phases observed in eukaryotes, Apicomplexans display a three-phase process consisting of G_1, S and M, with the G_2 phase between DNA replication and the onset of mitotic division in eukaryotes, being either insignificant or not present at all in *Plasmodium* (Francia and Striepen, 2014). Invading merozoites and the subsequent early ring stages of *Plasmodium*, represent the G_0 phase (Ishiyama et al., 2008), existing in a state of quiescence where the parasite is non-dividing nor in preparation for division. Early trophozoites represent the G_1 phase, where the breakdown of erythrocyte cytoplasm is used for the synthesis of proteins in preparation for DNA replication during the S phase, which takes place in mature trophozoites. The onset of the M phase denotes the formation of the schizont and the

A)

B)

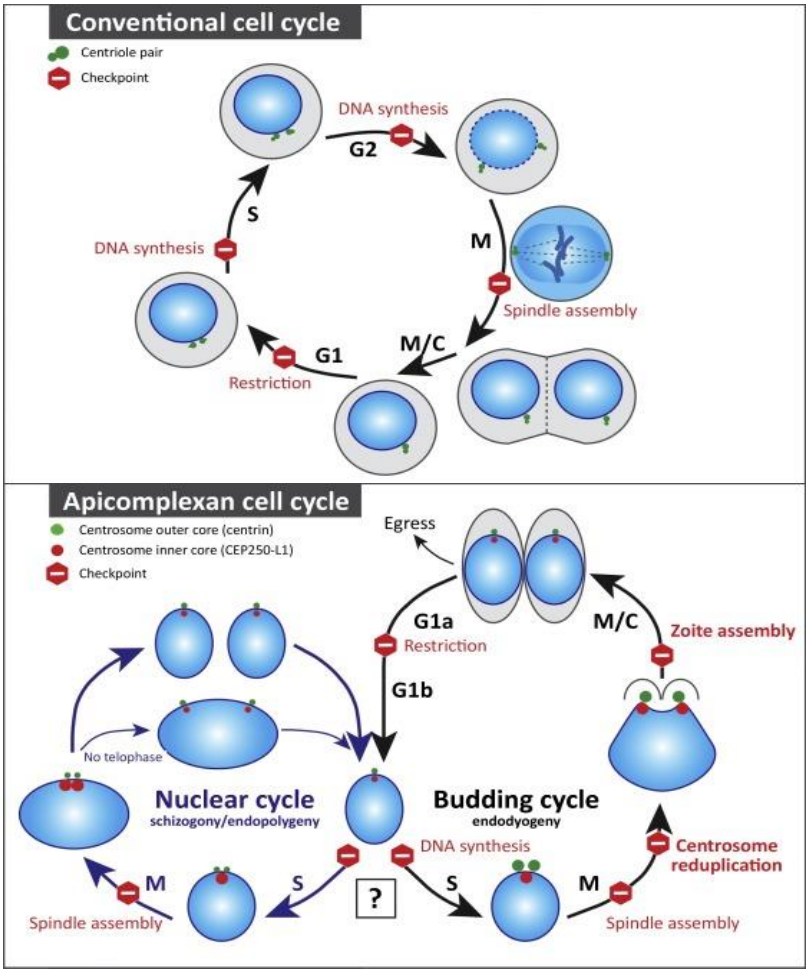


Figure 6 - Comparative views of the conventional cell cycle vs the Apicomplexan cell cycle.

The conventional cycle **(A)** involves four phases: G_1, S, G_2 and M. G_1 and G_2 phases occur in preparation for the two main events of the cells lifecycle, namely the synthesis of DNA (S) and the mitotic division of the cell (M). The culmination of mitosis results in the formation of two daughter cells and the reestablishment of cell functionality until the onset of the next mitotic event, governed by the "once only rule" of chromosome and associated centrosome duplication **(White and Suvorova, 2018)**. Contrasting this, *Plasmodium* erythrocytic schizogony **(B,** left, external arrows**)** operates a nuclear cycle system whereby the replication and division of the MTOC and DNA during S and M phases is accompanied immediately by karyokinesis, which thereafter continues asynchronously in a cycle culminating in a multinucleate cell prior to budding. Endopolygeny differs from schizogony, as synchronous genomic duplication occurs in the absence of karyokinesis, resulting in a polyploid nucleus until the final division and subsequent egress of the daughter cells (left, internal arrows). *Toxoplasma* operates a budding cycle (endodyogeny), in which MTOC and genome replication during the S and M phases is accompanied by the budding of daughter cells. This is somewhat more akin to the conventional cycle, however, under the caveat that said daughters are assembled from within the mother **(B,** right**)**. Figure taken from **(White and Suvorova, 2018)**.

beginning of schizogony, where atypical cell division and subsequent cytokinesis culminates in the release of up to 36 merozoites in blood stages.

1.2.2 Strategies and Mechanisms of Eukaryotic and *Plasmodium* Cell Division

Traditional cell division as seen in higher eukaryotes, is a multifaceted process consisting of prophase, metaphase, anaphase and telophase. During prophase, the nuclear material condenses, forming chromosomes made up of sister chromatids conjoined at the centromere. The disintegration of the nuclear envelope followed by the association of microtubules with kinetochores, marks the onset of metaphase. Extensions and contractions of the microtubules originating at the centrioles, align the chromosomes along the cell equator ready for anaphase, during which, a coordinated contraction of the tubules results in the separation of the sister chromatids and their relocation to opposite poles of the cell. The nuclear envelope is reassembled around the separated chromatids during telophase, and the cleaving of the cells during cytokinesis results in uninucleate, identical daughter cells.

The above-mentioned mechanism for cell division, does not apply to all members of the eukaryotic domain, with variant mitoses having developed inside the incredibly diverse taxon. “Open mitosis” is the method in which the nuclear envelope encasing the chromosomes, disintegrates at the boundary between prophase and metaphase (Cooper, 2000). For this to be completed, the three components of the nuclear envelope: the nuclear membrane, nuclear pore complexes and the nuclear lamina (Wiese et al., 1997) must collectively dissemble via fragmentation, dissociation and depolymerisation (Wiese et al., 1997). As a result, the processes of microtubule-kinetochore association, chromosome alignment and the separation and relocation to opposite poles during open mitosis, occurs in the cytoplasm of the cell (Arnone et al., 2013). This necessitates the forming of two nuclear envelopes around the newly deposited chromatids, which occurs

during telophase (De Souza and Osmani, 2007). In contrast, most lower eukaryotes undergo the more ancient "closed mitosis", which involves the maintenance of the nuclear envelope throughout the entire mitotic event. Thus, centrosome-equivalent structures, acting as centres for the organisation of microtubules involved in chromosome manipulation, tend to operate differently compared to those in organisms practising open mitosis.

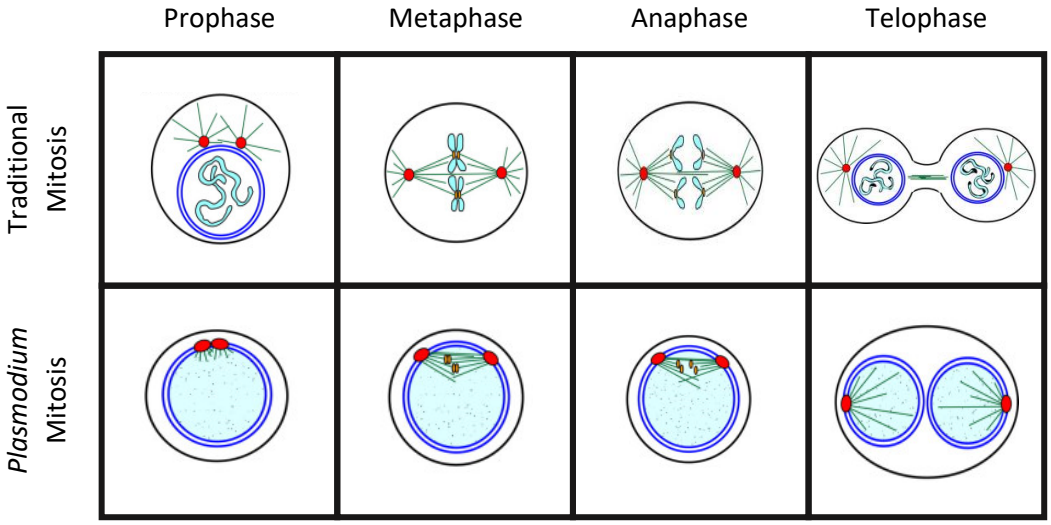


Figure 7 - Traditional cell mitosis compared to *Plasmodium* mitosis as occurs in the blood stage.

The nuclear membrane (blue), MTOCs/centrioles (red circles), condensed chromosomes (light blue), uncondensed *Plasmodium* chromosomes (light blue textured pattern), microtubules (green lines) and kinetochores (brown ovals) are all shown on the diagram. The most obvious differences between the two views include the absence of nuclear disassembly, association of the MTOCs with the nuclear membrane and lack of chromosome condensation in *Plasmodium* cells. Figure adapted from **(Gerald et al., 2011)**.

1.2.3 *Plasmodium* Endomitosis

Plasmodium schizogony is an example of a closed mitotic system which divides via asynchronous endomitosis. In open mitotic systems, a single round of mitosis occurs before the formation of two identical daughter cells after cytokinesis. In schizogony, multiple rounds of mitotic division occur, each ending in telophase and karyokinesis, however, the lack of any cytokinesis and commitment to assemble true daughter cells, results in a polyploid cell containing multiple nuclei (Gerald et al., 2011; Striepen et al., 2007). It is not until the final synchronised division, that the schizont buds and undergoes cytokinesis, releasing up to 10-fold its original number in identical progeny (Francia and Striepen, 2014).

The microtubules begin to assemble inside of the nucleus during prophase, necessitated by the nature of closed mitosis, however, the DNA does not condense into distinct shapes resembling chromosomes and thus appear diffused. The point of origin for microtubule growth, is at the microtubule organising centres or MTOCs, which are seemingly amorphous structures, however, have been described as electron dense masses embedded within the nuclear envelope and associated with nuclear pores (Bannister et al., 2000b), which will discussed in greater depth later. This structure is the centriole equivalent of Apicomplexa, and nucleates the spindles, providing them with a point of anchorage to grow and contract for the necessary manipulation of the DNA (Gerald et al., 2011; Roques et al., 2019). Similar to human mitosis, the association of microtubules with the kinetochores takes place in metaphase, though the DNA is not intentionally aligned along the equator of the cell. It has been suggested that the centromeres remain readily available for microtubule attachment (despite the intranuclear space being crowded with uncondensed chromatin), by remaining tethered to the MTOCs throughout the cell's lifecycle (Francia and Striepen, 2014). The localisation of the centromeres to a distinct apical region within the nucleus where the MTOCs are believed to reside, has been

demonstrated in *Toxoplasma gondii* and is hypothesized to aid in the abovementioned microtubule-centromere attachment, in addition to maintaining genomic integrity (Brooks et al., 2011). Contraction of the spindles separate the sister chromatids in anaphase, allowing them to be relocated to within close proximity of their respective MTOC. During telophase, the nucleus divides in two, equally segregating the daughter genomes into their own nuclei, each with a single MTOC present. This process is then repeated with emphasis on asynchrony, allowing the parasite to expand its numbers faster than would be expected during synchronous geometric nuclei duplication (Gerald et al., 2011).

1.3 Alternative Methods for Apicomplexan Asexual Cell Division

It is important to understand the alternative methods to asexual Apicomplexan division, as by doing so it may provide a better understanding of the mechanisms involved in the *Plasmodium* equivalent. Whilst *Plasmodium* cell division may differ significantly from the conventional system, more obvious and relevant similarities may be drawn between species belonging to the same phylum. *Toxoplasma gondii* for example is considered the best model for the study of Apicomplexan biology, having been the focus of both extensive forward and reverse genetic studies, in addition its "user-friendliness" in laboratory conditions (Kim and Weiss, 2004). Thus, knowledge that has been gained from the well-established study of *Toxoplasma*, can provide firm scientific backing to any assumptions or questions raised in regards to how similar cell mechanisms or proteins function in *Plasmodium* proliferation *(Roos et al., 1999)*.

1.3.1 *Toxoplasma* Endodyogeny

Toxoplasma gondii, responsible for toxoplasmosis in humans, undergoes endodyogeny in feline intestinal cells, a relatively simple process compared to that of *Plasmodium* schizogony (Striepen et al., 2007). In contrast to the development of polyploid cells at

the conclusion of schizogony, endodyogeny culminates in the formation two identical daughter cells after a single round of DNA replication and nuclear mitosis, similar to that seen in human cells (Francia and Striepen, 2014). In contrast to humans however, where two new cells arise from cytokinesis, the daughter cells are assembled within the mother itself. An IMC, separate to the mothers own located adjacent to the cell membrane, first forms the basis of the conoid anteriores of the two daughters (Hu et al., 2002). MTOCs separate the sister kinetochores, pulling DNA into opposite regions, before the nucleus and mitochondria are equally divided between the cells. The formation of a cleavage burrow down the length of the cell centre, forces the cells apart producing two identical daughter cells (Black and Boothroyd, 2000). The progeny resulting from this single mitotic event, have the capacity to immediately invade new host cells, a benefit of endodyogenic division, however, may also repeat this process in the existing cell, allowing them to produce more parasites.

1.3.2 *Sarcocystis* Endopolygeny

Endopolygeny draws similarities to schizogony, with respect to the number of daughter cells produced during a single cell cycle. Contrasting this however, is the manner in which it is achieved, as the former undergoes synchronised DNA replication within a single nucleus, which is not interrupted by karyokinesis (Vaishnava et al., 2005). In *Plasmodium* schizogony, the polyploid nucleus will contain a maximum of two genomes, before nuclear division results in the distribution of the genetic material into two separate nuclei. The asynchronous divisions of these newly formed nuclei, concluding with a single synchronised division, results in up to 36 identical nuclei within a single cell. In endopolygeny, DNA and MTOC replication occurs within a single nucleus following a geometric sequence, with the last mitotic division coinciding with karyokinesis. The beginnings of separate, haploid nuclei radiate out from the central nucleus and form at

the surface of the mother cell before being packaged into daughter cells and released via budding (Francia and Striepen, 2014).

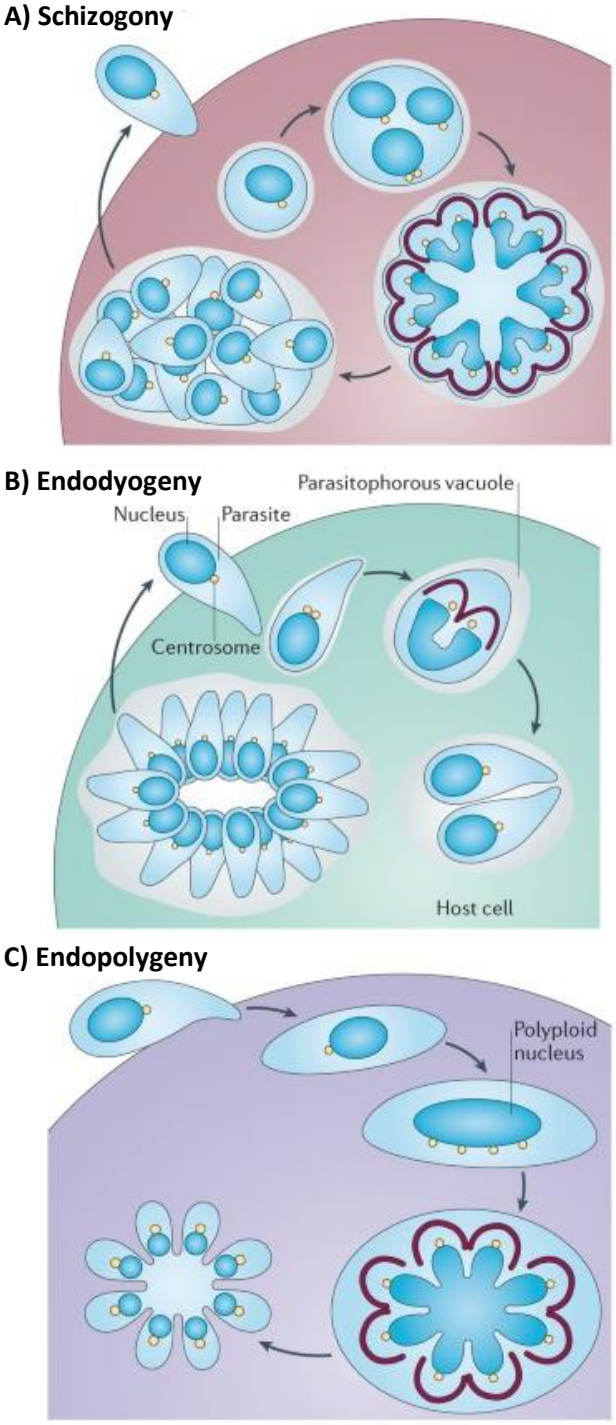


Figure 8 – The strategies of asexual cell division utilised by Apicomplexan parasites.

A) Schizogony begins after the first mitotic event, which is followed by multiple successive rounds of asynchronous nuclear division, culminating in the formation of a multinucleated cell. The final nuclear division occurs synchronously and corresponds to the budding of the daughter merozoites. **B)** Endodyogeny, as used by *T. gondii*, occurs within the mother tachyzoite and culminates in the formation of two identical daughter cells after a single mitotic division. **C)** Endopolygeny, as utilised by *Sarcocystis* species, involves multiple rounds of synchronised DNA replication, however, the conservation of a mononucleate cell arrangement, resulting in a polyploid nucleus which buds to form the daughter cells. Figure adapted from **(Francia and Striepen, 2014)**.

1.3.3 *Plasmodium* Male Gametogenesis

Changes in environmental stimuli, most notably in temperature and the presence of xanthurenic acid, initiates the process of male endoreduplication (Billker et al., 1997; Guttery et al., 2015; Smith and Lefebvre, 1997). This strategy involves the replication of DNA in the absence of any mitotic division in the forms of karyokinesis or cytokinesis, altering nuclear ploidy, however, maintaining a mononucleate arrangement. Three rounds of successive genomic replication produce an 8N nucleus, giving rise to eight, haploid, motile, microgametes in the form of simple flagella, composed only of a cell membrane, nucleus, cytoplasm and axoneme (Sinden et al., 1976; Zeeshan et al., 2019a). The axoneme is an integral part of all flagella, most commonly existing in a 9+2 arrangement of doublet microtubules surrounding a central pair known as C1 and C2 (Mitchell, 2004). Flagella motility occurs independent of the central microtubules, evidenced by reports of fully functioning flagella utilising 9+0 arrangements, in certain spermatozoa (Michalik, 2009), however, the central apparatus is still required to maintain axonemal uniformity. Dynein molecules anchored along the peripheral doublets face clockwise in the direction of their neighbours, the interaction with which provides the mechanical movement necessary for motility (Wilson et al., 2013).

The basal bodies (BB) in *Plasmodium* provide the foundation on which the axonemes are formed, and are absent until the onset of gametogenesis. Apicomplexan BB structure deviates somewhat from the traditional arrangement of triplet microtubules displaying nine-fold symmetry, instead being reported as nine single microtubules surrounding a hollow core, associated with an electron dense mass in place of the C1 and C2 tubules (Francia et al., 2015; Sinden et al., 2010). *Plasmodium* BB and axoneme assembly, defies the conventional method of flagellation. Axoneme formation occurs within the cytoplasm of the male, thus negating the need for an intra-flagellar transport system (IFT). This is an integral part of axoneme assembly in cells that initiate microtubule doublet construction

inside membranous protrusions, and thus rely on the anterograde transport of axoneme components for its formation (Briggs et al., 2004).

Basal body and axoneme assembly occur de novo in gametogenesis alongside the replication of the genomic DNA. A tetrad of BBs is recruited at the MTOC within the first minute of male activation (Sinden et al., 2010). After the first endomitotic event, a further four BBs are formed at the opposite MTOC, which coincides with the initiation of axoneme assembly. Basal bodies will maintain an equal distribution amongst MTOCs, culminating in a 1:1 ratio at the end of the cycle. The continued growth of the axonemes within the microgamete, results in the formation of a "basket-like" structure around the nucleus, due to the nature of cytoplasmic axonemal assembly (see Figure 9) (Zeeshan et al., 2019a). The axonemes remain unassociated with the cell membrane until exflagellation, where karyokinesis and cytokinesis, assisted by rapid flagellar movement, results in the separation of an independent microgamete, ready for female fertilisation (Straschil et al., 2010).

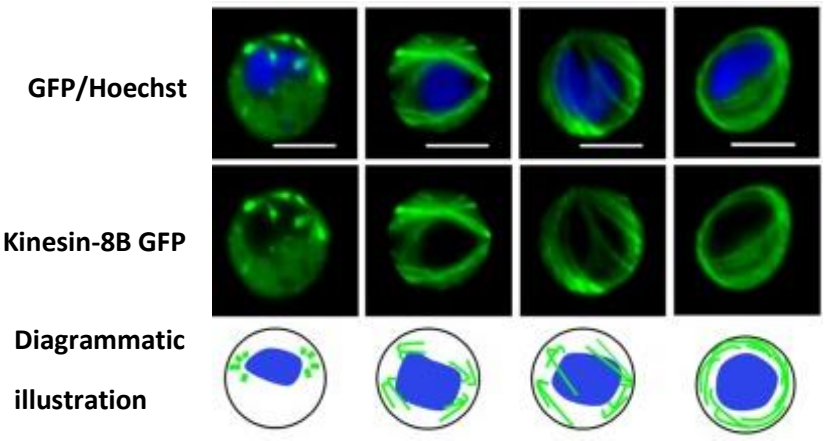


Figure 9 – Formation of the axonemes during *Plasmodium* male gametogenesis.

Plasmodium axonemes, visualised here in live cell imagery of activated male gametocytes using the basal body and axoneme marker, Kinesin-8B GFP (green fluorescent protein), are formed in the cytoplasm. This differs from the conventional method of axonemal assembly, which involves the formation of the axonemes directly into membranous protrusions which represent proto-cilia or flagellar. As such, the *Plasmodium* axonemes form the abovementioned "basket-like" structure around the nucleus as they are assembled, before exflagellation results in their insertion into the male microgametes. Figure taken from **(Zeeshan et al., 2019a)**.

1.4 Cell Regulation

1.4.1 Microtubule Organising Centres

Plasmodium MTOCs are described as electron dense masses embedded within the nuclear envelope, with visible plaque-like structures present either side (Arnot et al., 2011; Gerald et al., 2011). It is therefore often termed the "centriolar plaque", however, the circular arrangement of microtubules concurrent with centriole structures are absent in *Plasmodium* (Francia and Striepen, 2014; Wall et al., 2018), with exception to those visible in the previously described BBs. Centriole-related structures have been implicated as integral components in the regulation of the cell cycle in mammalian and Apicomplexan cells, demonstrated by the significant correlation between centriole/MTOC duplication and mitotic division (Arnot et al., 2011). This implication has been compounded by the observed arrestation of the cell cycle at the G_1 phase, in experimentally generated mutant cells lacking centrosomes (Khodjakov and Rieder, 2001). Disruption of the MTOC in *Plasmodium* has also been shown to prevent successful parasite replication in the blood stages.

Centriole/MTOC duplication occurs at the boundary between the G_1 and S phases of the cycle (Francia and Striepen, 2014), at which point, the daughter MTOC is situated adjacent to the mother. The subsequent segregation of the genomes does not take place until the daughter MTOC has relocated to the opposite cell hemisphere, allowing the necessary mitotic spindles to form. As in higher eukaryotic organisms, where the procentriole (daughter) represents an immature version of the mother centriole (Avidor-Reiss and Gopalakrishnan, 2013), a visible dimorphism is present between the daughter and mother MTOC, which are inherited by separate nuclei. This is responsible for the asynchronicity displayed during endomitotic and endoreduplicative divisions within *Plasmodia*, as the daughter MTOC represents a smaller, immature form of the organelle, for which more time is required before the onset of the S phase can initiate (Arnot et al., 2011; Matthews

et al., 2018). Nuclear and genomic division thus occurs regardless of the state of other daughter nuclei, and as mentioned above, allows the parasite to multiply quicker than would be expected if replicating in geometric sequence (Gerald et al., 2011).

Centrins are calcium-binding phosphoproteins found in the centrosomes and centriole-related structures of eukaryotes. Four centrins, Cen-1, -2, -3 and -4, have been identified in *Plasmodium*, where Cen-1, -2 and -4 are concerned with centriole replication and mitotic division, and Cen-3 with microtubule binding (Mahajan et al., 2008). Cen-1, -2 and -3 are recognised as essential for the completion of asexual development, as proven by various attempts to delete the genes using C-terminal tagging approaches (Roques et al., 2019).

1.4.2 Cyclins and Kinases Implicated in Cell Division

Progression through the eukaryotic cell cycle is facilitated by the cyclin proteins, which are expressed in oscillatory waves of upregulation and downregulation dictated by their transcriptional activation and proteolytic degradation. Upregulation of a specific cyclin at a determined time point coincides with its association with a complimentary cyclin-dependent kinase (CDK) with which it forms a complex. This results in the conformational change of the tertiary structure located at the C-terminal end of the CDK, concluding in a state of activation (Barbash and Diehl, 2008). The complex is responsible for the coordinated phosphorylation of specific target proteins required for the promotion of crucial cell division processes (Costa-Guda and Arnold, 2013). Conversely, the anaphase-promoting complex, E3 ubiquitin ligase, targets specific regulatory proteins made redundant by the progression of the cycle, resulting in their selective degradation (Matthews et al., 2018). It is through the combined interaction of protein upregulation and their subsequent inhibition, that is responsible for the sequential advance through the four phases of the cell cycle.

Three cyclins have been identified in *Plasmodium*, consisting of Cyc1, Cyc3 and Cyc4. Major contrasts between the canonical mammalian and *Plasmodium* cyclins can be drawn, chief among which being the complete lack of homology between the sets, with *Plasmodium* species lacking the Group one cyclins entirely (Roques et al., 2015). In addition, waves of cyclin expression are not evident in *Plasmodium* species, with the proteins instead displaying an omnipresent expression in the parasite's lifecycle. To compliment these cyclins, seven CDKs and have been identified, consisting of MRK1, PK5, PK6, CRK-1, CRK-3, CRK-4 and CRK-5 (Matthews et al., 2018).

Robbins et al. (2017) identified an interactive partnership between MRK1, MAT1 and Cyc1 proteins, and implicated the resultant complex as a regulator of the cell cycle required for the progression of schizogony. Cyc1 itself has been recognised as an essential component in schizont cytokinesis and subsequent merozoite egression, supporting the hypothesis that the cyclin either regulates or phosphorylates transcripts or proteins that are yet to be identified, however, are essential for this process (Robbins et al., 2017). The unknown interactions between *Plasmodium* cyclins and CDKs is a common theme, as no data currently exists on Cyc4, and whilst Cyc3 is implicated as essential for oocysts and subsequent sporozoite development, it is not currently known what the cyclin interacts with to achieve this (Robbins et al., 2017; Roques et al., 2015). Having said this, PK5 autophosphorylates in the presence of Cyc1, however, this has only been demonstrated in vitro (Le Roch et al., 2000). Regardless, PK5 has been implicated in the phosphorylation of ORC1, which results in its expulsion from the nucleus where it is involved in DNA replication, suggesting PK5 activity is required for the completion of DNA synthesis and potential progression beyond the S checkpoint, however, the existence of such a checkpoint is yet to be confirmed in *Plasmodium* (Deshmukh et al., 2015; Matthews et al., 2018). Less is known of PK6, however, its expression has been shown to be upregulated

between the ring and trophozoite stages, corresponding to its supposed role in the onset of DNA synthesis (Bracchi-Ricard et al., 2000).

CRK-1 has been implicated as essential for the completion of intraerythrocytic proliferation, however, its role has not yet been established in these stages (Rangarajan et al., 2006; Tewari et al., 2010). The peak presence of CRK-1 mRNA in the gametocytes though, has to led the suggestion that the protein may be involved in the differentiation of gametocytes and active in the subsequent sexual stages, however, this is yet to be seen (Doerig et al., 1995; Rangarajan et al., 2006). CRK-3 has been demonstrated localising with histone HP1 kinases in blood stages, and as such is presumed to play a role in the modification of chromatin, responsible for a multitude of roles including the regulation of gene transcription (Halbert et al., 2010; Rossetto et al., 2012). CRK-4, in common with CRK-1, has also been implicated as essential for the completion of blood stage schizogony, specifically involved in DNA replication evidenced by its knockout resulting in the complete termination of this process (Ganter et al., 2017). Further similarities are evident by the presence of CRK-4 in the gametocytes, however, the protein is redundant during gamete differentiation and male exflagellation, only proving refractory to deletion in ookinete stages, most likely due to a role in ookinete meiosis (Ganter et al., 2017). Interestingly, CRK-5 deletion in schizogony does not prevent its completion, though, due to the subsequent reduction in the speed in which nuclei divide, fewer daughter merozoites are formed by each schizont (Dorin-Semblat et al., 2013). The deletion of CRK5 in gametocytes however, has be shown to result in the prevention of endomitotic division due its role in the phosphorylation of a plethora of proteins involved in the early stages of DNA replication (Balestra et al., 2020).

Two families of Cyclin-independent kinases have been recognised, namely, the NIMA-related kinases (to be discussed later) and the Aurora-related kinases (ARK). *Plasmodium*

Aurora-related kinases are a family of three (ARK1, ARK2, ARK3) conserved serine/threonine protein kinases (Reininger et al., 2011). Multiple reports have implicated ARK1 in mitotic spindle formation and nucleation during endomitosis. This has been substantiated by evidence of paired focal localisation at recently divided MTOCs, flanking the mitotic spindle at the G_2/M transition (Carvalho et al., 2013; Reininger et al., 2011). Interestingly, only a subset of nuclei exhibit foci association in select cells. In addition, visible foci only remain present until the conclusion of bi-polar spindle establishment. These two observations support the model of asynchronous cell division, in conjunction with the specific recruitment of ARK1 to centriole-related structures for the purpose of spindle formation respectively (Carvalho et al., 2013). Correspondingly, the metazoan homolog, Aurora kinase A, promotes centriole maturation and the assembly of the mitotic spindle at the G_2/M boundary and thus is observed at duplicated centrioles (Carvalho et al., 2013; Willems et al., 2018). In contrast, ARK2 and ARK3 are unique to Apicomplexans, with the former being exclusive to *Plasmodium*. The roles of ARK2 and ARK3 are yet to be established, however, ARK3 focal expression has been documented in late stage schizogony with a supposed MTOC association, suggesting a role in merozoite ontogeny (Carvalho et al., 2013). All ARK proteins have been shown to be refractory to deletion in asexual blood stages, suggestive of individual roles during division (Carvalho et al., 2013; Dwivedi et al., 2017; Reininger et al., 2011; Roques et al., 2015).

Table 1 – Summary table of CDKs and ARK proteins identified in *Plasmodium*.

The Seven CDK and three ARK proteins identified in *Plasmodium* including their role. **1) Robbins et al. (2017); 2) Chen et al. (2006); 3) Deshmukh et al. (2015); 4) Matthews et al. (2018); 5) Bracchi-Ricard et al. (2000); 6) Rangarajan et al. (2006); 7) Tewari et al. (2010); 8) Doerig et al. (1995); 9) Halbert et al. (2010); 10) Rossetto et al. (2012); 11) Ganter et al. (2017); 12) Dorin-Semblat et al. (2013); 13) Balestra et al. (2020); 14) Carvalho et al. (2013); 15) Reininger et al. (2011); 16) Dwivedi et al. (2017).** Table adapted from **(Matthews et al., 2018)**.

CDKs	Stage Active	Role	Ref
MRK1	Erythrocytic schizogony	Forms a complex with MAT1 and Cyc1, implicated as a cell cycle regulator of schizogony	**1, 2**
PK5	Erythrocytic schizogony	Phosphorylation of ORC1, implicated in the role of DNA synthesis and checkpoint transition	**3, 4**
PK6	Erythrocytic schizogony	Upregulation between ring and trophozoite stage suggests role in DNA synthesis	**5**
CRK-1	Erythrocytic schizogony + gametocytogenesis	Essential for completion of erythrocytic schizogony however role unknown Suggested role in gametocytogenesis and subsequent stages evidenced by high mRNA expression	**6,7,8**
CRK-3	Erythrocytic schizogony	Localises with histone HP1 kinases, implicated as a transcriptional regulator	**9, 10**
CRK-4	Erythrocytic schizogony + ookinesis	Implicated in DNA replication during schizogony Refractory to deletion in ookinetes, potential role during meiosis	**11**
CRK-5	Erythrocytic schizogony + gametogenesis	Refractory to deletion in endomitosis, potential role in the phosphorylation of proteins essential for early DNA replication	**12, 13**
ARKs			
ARK1	Erythrocytic schizogony + gametogenesis	Implicated in mitotic spindle formation and nucleation at recently divided MTOCs	**14, 15**
ARK2	Erythrocytic schizogony + gametogenesis	Refractory to deletion in asexual parasites however role unknown	**14, 16**
ARK3	Erythrocytic schizogony + gametogenesis	Localisation in late stage schizogony to vicinity of suspected MTOCs, potential role in merozoite ontogeny	**14**

1.4.3 NIMA-related Kinases

NIMA-related kinases (NEK) are a family of serine/threonine protein kinases, implicated as major components involved in the functioning of cellular division. The name derives from the NIMA gene, initially identified in *Aspergillus nidulans* fungi by Morris (1975), during an experiment using temperature-sensitive cells displaying cell cycle mutations. Fungal cells were categorised on the basis of this cycle mutation, of which two types were observed; "bim" (blocked in mitosis) mutants, which arrested during mitosis with evidence of chromosomes condensing and microtubule activity, and "nim" (never in mitosis) mutants, which arrested during interphase (Oakley and Morris, 1983). The NIMA gene, being the first identified gene in the nim mutants of *Aspergillus*, hence the name NIMA (Never-in-mitosis *Aspergillus*), was later found to encode for a serine/threonine protein kinase (Osmani et al., 1988). Under permissive temperatures, which allowed for the expression of NIMA, mitotic division was observed. However, suboptimal temperatures which inhibited protein synthesis in the NIMA mutants, resulted in the arrestation of the cycle at G_2, whilst overexpression resulted in the premature initiation of mitosis regardless of the current cycle phase.

Of the 11 identified NIMA-related kinases in humans, NEK2, NEK6, NEK7 and NEK9 are recognised as components involved in mitotic initiation. As demonstrated by its cellular localisation, NEK2 has been identified as a constituent of the human centrosome, exhibiting peak expression during interphase between the S and G_2 phases (Fry et al., 1998; Fry et al., 1995). The kinase has been implicated as a key component in the regulation of the centrosomal cycle, evidenced by its overexpression resulting in the premature decoupling of the centrioles (Fry et al., 1998). As such, it is believed that NEK2 is responsible for the initiation of tether disassembly during G_1, ultimately allowing for the separation of the mother and procentriole, essential for the successive formation of the mitotic spindles (Andersen et al., 2003; Fry et al., 1998; Fry et al., 2012; O'Regan et al.,

2007). The onset of mitosis coincides with the degradation of NEK2 via the action of ubiquitin ligases, followed by the initiation of a signalling pathway that results in the activation of NEK9; achieved via the sequential phosphorylation of sites along the kinase by CDK1 and PLK1 (Bertran et al., 2011; Hames et al., 2001; Sdelci et al., 2011). Subsequent alterations in protein structure permits it to bind with both NEK6 and NEK7, allowing for their activation (Belham et al., 2003; Roig et al., 2002). As a result of this, NEK9 is suspected of playing an indirect role in the functions undertaken by the two NEKs immediately downstream of it, however, the level of dependency exhibited by NEK6 and NEK7 on their upstream regulator is unknown (Fry et al., 2017; Fry et al., 2012). The phosphorylation and subsequent localisation of Kinesin Eg5 to the centrosome by both NEK6 and NEK7, is believed to be required for the separation of the centrioles following their previous disjunction by NEK2 activity (Bertran et al., 2011; Rapley et al., 2008). Additionally, both kinases are implicated in the formation of the mitotic spindle, demonstrated by their removal resulting in cell arrestation at metaphase, with evidence of increased microtubule fragility and decreased density (O'Regan and Fry, 2009). Whilst the specific role of NEK7 remains unidentified, the association of HSP72 with the mitotic spindle has been shown to be a product of NEK6 phosphorylation (O'Regan et al., 2015b). HSP72 is responsible for the recruitment of stabilising proteins to the kinetochore-fibre, a grouping of microtubules which span the distance between the kinetochore and the centrioles, thus allowing for their robust assembly (O'Regan et al., 2015a; O'Regan et al., 2015b). In addition to the abovementioned role of NEK9, the kinase has been implicated as an associate of the γ—tubulin ring complex, a structure responsible for the nucleation of the microtubules at the centrosome (Moritz et al., 2000; Sdelci et al., 2012). NEK9's phosphorylation of NEDD1, the adaptor between the microtubules and the γ-tubulin ring complex, results in the recruitment of γ-tubulin for spindle assembly (Roig et al., 2005;

Sdelci et al., 2012). Table 2 breakdowns the roles and locations of all the NIMA-related kinases identified in human tissues.

Table 2 – NEKs identified in human cells.

The 11 NEKs identified in human cells including their cytogenetic location, the factors required for their activation, the location of their cellular activity and the functional role of the proteins. Little is known of NEK5, however, it has been heavily involved in carcinoma-based research. It has been suggested that it participates in cell apoptosis and the regulation of cell respiration due to the reported colocalization of NEK5 with the mitochondria **(Melo Hanchuk et al., 2015)**. Table modified from **(Fry et al., 2012)**.

NEK	Cytogenetic Location	Activation	Localisation	Function
NEK1 (1258 aa)	4q33	Genotoxic Insults (IR, UV, oxidative injury)	Cytoplasm, centrosomes, cilia, damaged DNA sites	Cilia and DDR
NEK2 (445 aa)	1q32.3	S, G_2-M	Centrosomes	Mitosis
NEK3 (459 aa)	13q14.3	Prolactin receptor stimulation	Cytoplasm	Prolactin signalling
NEK4 (841 aa)	3q21.1	?	Basal bodies	Cilia
NEK5 (889 aa)	13q14.3	?	?	?
NEK6 (313 aa)	9q33.3	Activated by NEK9, mitosis	Mitotic spindle	Mitosis
NEK7 (302 aa)	1q31.3	Activated by NEK9, mitosis	Weakly to spindle poles	Mitosis
NEK8 (703 aa)	17q11.2	Serum starvation	Nucleus, centrioles, cilia	Cilia
NEK9 (979 aa)	14q24.3	Mitosis	Cytoplasm, spindle poles	Mitosis
NEK10 (1125 aa)	3q24.1	UV, G_2-M	?	DDR
NEK11 (645 aa)	3q22.1	DNA replication inhibitors and genotoxic insults, S to G_2-M transition	Nucleus	DDR

1.4.4 *Plasmodium* NIMA-related Kinases

Four NEK proteins have been identified in *Plasmodium*: NEK1; NEK2; NEK3; and NEK4, distributed between chromosome 12, 5, 12 and 7 respectively (Carvalho et al., 2013). Syntenic orthologues of all four NEKs are present in all species of the *Plasmodium* genus, however, NEK1 and NEK4 display a higher level of conservatism between species (97-98%) compared to NEK2 and NEK3 (72-78%) (Carvalho et al., 2013). NEK2, NEK3 and NEK4 are expressed predominantly in the gametocytes, evidenced by the high expression of their mRNA in these stages, however, detectable levels of the kinases have been identified in asexual parasites (Reininger et al., 2009). Whilst NEK2 and NEK4 are recognised as dispensable in asexual proliferation, they have been identified as non-redundant in the female gametocytes, evidenced by attempts to knockout the genes resulting in the inability of the parasite to complete its life cycle (Solyakov et al., 2011). Specifically, disruption of the NEK2 gene in mutant clones, results in a parasite that is capable of gametogenesis, but which is unable to develop into an ookinete after fertilisation, with an observed disruption in pre-meiotic DNA replication (Reininger et al., 2009; Tewari et al., 2010). The absence of female-introduced NEK2 into the zygote is believed to disrupt the functioning of the MTOC, which NEK proteins are believed to be associated with (Dorin-Semblat et al., 2011), ultimately preventing the meiotic event that sees 2N divided into 4N (Reininger et al., 2009) and thus preventing ookinete formation. Expression of NEK4 in asexual schizonts correlates to a high level of gametocyte cell conversion, demonstrating that its presence may act as an indication of sexual commitment (Reininger et al., 2012). Despite this, NEK4 knockout parasites are observably capable of gametocytogenesis and gametogenesis, however again, are unable to undergo meiosis in ookinetes, implicating the protein as essential for cell cycle completion (Reininger et al., 2005). Concurrent with the previous examples, NEK3 is also crucial for cell cycle completion, however, contrast can be drawn due to it being refractory to deletion in both

asexual and sexual parasites (Tewari et al., 2010). Little is known of the role of NEK3 in *Plasmodium*, though it is implicated as an upstream regulator of the MAPK proteins, specifically MAPk2 in *P. falciparum* (Lye et al., 2006; Wierk et al., 2013).

NEK1 has also been shown to be involved in the upstream signalling of the MAPK2 pathway (Dorin-Semblat et al., 2011; Dorin et al., 2001). Of the four NEKs, NEK1 is the largest consisting of two coiled-coil motifs. Whilst this is a mainstay for most NEK proteins, the non-catalytic C-terminal region, in which said motifs are found, is relatively long compared to its counter parts (Carvalho et al., 2013). Additionally, NEK1 is the only *Plasmodium* NEK that displays orthology with species outside of the Apicomplexan phylum, that being the NEK2 proteins of humans and NIMA in *Aspergillus* (Reininger et al., 2009). Whilst human NEK2 is non-essential for mitosis or meiosis (O'Regan et al., 2007), *Plasmodium* NEK1 has proven to be refractory to deletion in both asexual and sexual stages, indicating its importance to the cycle and suggesting its role as a general cell cycle regulator (Dorin-Semblat et al., 2011; Tewari et al., 2010). Upregulation of NEK1 specific to early asexual stages and male gametocytes is interesting, as both stages are proceeded by periods of relatively fast DNA replication during schizogony and endoreduplication respectively (Dorin-Semblat et al., 2011; Tewari et al., 2010). As Human NEK2 is associated with the centrosome, an organelle heavily involved in cell cycle regulation, it is possible that *Plasmodium* NEK1 may play a similar role with the *Plasmodium* MTOC. Despite evidence implicating NEK1 as essential at all stages of the life cycle, limited research has been conducted on the exact function of the protein. This provides an opportunity to expand the wealth of knowledge in this field by the documentation of the real-time dynamics of the protein to expose its functioning in *Plasmodium berghei*.

Table 3 – Neks identified in *Plasmodium*.

The four NIMA-related kinases identified in *Plasmodium* species including the stages they are active, cellular localisation and their implicated functions. **1) Dorin-Semblat et al. (2011); 2) Tewari et al. (2010); 3) Dorin et al. (2001); 4) Reininger et al. (2005); 5) Reininger et al. (2009); 6) Lye et al. (2006); 7) Reininger et al. (2012)**. Table adapted from **(Carvalho et al., 2013)**.

NEK	Stage Active	Localisation	Function	Ref
NEK1	Erythrocytic schizogony + male gametogenesis	Centriole-equivalent structures in schizonts Unknown in gametes	Refractory to deletion in both stages Potential involvement in MTOC functioning Implicated in MAPK2 expression	**1, 2, 3**
NEK2	Zygote meiosis	Microtubules in macrogametes	Implicated in ookinete meiosis, specifically pre-meiotic genome replication	**2, 4, 5**
NEK3	Erythrocytic schizogony + male gametogenesis	Unknown	Refractory to deletion during both stages yet role unknown Implicated in MAPK2 expression	**2, 6**
NEK4	Schizogony? + gametocytogenesis + zygote meiosis	Centriole-equivalent structures in schizonts + ookinetes	Redundant in asexual parasites Implicated in parasite sexual differentiation Implicated in ookinete meiosis	**4, 7**

2.0 Aims and Objectives

The ability to undergo rapid proliferation in both host and vector organisms plays a vital role in the *Plasmodium* lifecycle, and is in large part responsible for their success. As such, the proliferative stages are highly attractive targets for anti-malarial strategies, and thus require an in depth understanding of the biochemical processes involved. The main focus of this lab is the identification of the roles and interactions of the regulatory proteins that have either been previously implicated in cellular processes, or are currently unknown to science, by means of biochemical, proteomic and reverse genetic techniques.

NIMA-related kinases have been implicated as essential regulators of the aforementioned proliferation of *Plasmodium* species. This has been confirmed by attempts to knockout the genes resulting in the inability of the parasite to complete its lifecycle, with NEK1 in particular proving refractory to deletion in both asexual and sexual stages (Tewari et al., 2010). Whilst live cell imagery of asexual parasites has demonstrated a specific pattern of NEK1 localisation to the perinuclear space (Dorin-Semblat et al., 2011), the characterisation of NEK1 in the sexual and later ookinete stages has not yet been attempted. Localisation during schizogony is suggestive of a possible association between NEK1 and the MTOC, which is far better understood between the human centrioles and human NEK2 (Fry, 2002; Fry et al., 2012). Therefore, the aim of this project is to characterise the expressive patterns of NEK1 in all proliferative stages, with the intention of identifying the role of the kinase during proliferation.

For the completion of the experimental aim, four main objectives are set. First and foremost, the localisation of NEK1 in all proliferative stages is to be characterised using fluorescent microscopy of NEK1-mCherry and Scarlet, which will be generated by endogenously tagging the C-terminus end of the kinase with the fluorescing protein. Secondly, NEK1 will be used in IFA studies alongside centrin and α-tubulin markers to

characterise the potential colocalization between the proteins. Adding to this, the genetic crossing of NEK1 fluorescing proteins and NDC80-mCherry parasites, the latter courtesy of Zeeshan et al. (2020), will be undertaken to breed a line of cells that express both, in order to track their relative real-time dynamics in live cell imagery. Thirdly, protein pulldown experiments will be undertaken on activated male gametocytes, to extract NEK1 and its interacting partners which will be identified by mass spectrometry. Finally, a NEK1clag parasite line will be generated to allow for the conditional knockdown of the kinase specific to the male gametocytes. The results gathered will expose the interactions between NEK1 and various cell division orientated machinery, in addition to its over-arching role in the regulation of *Plasmodium* asexual and sexual proliferation.

3.0 Materials and Methods

Table 4 – List of materials

Material	Manufacturer
Agarose	Invitrogen
β-mercaptoethanol	Sigma-Aldrich
Bovine serum albumin	Melford
CF11	Whatmann
DEPC-treated water	Invitrogen
Ethanol	Sigma-Aldrich
Ethidium bromide	Fisher Scientific
Foetal bovine serum	Sigma-Aldrich
Giemsa	Sigma-Aldrich
GoTAQ buffer	Promega
Hyperladder (1Kb)	Bioline
Hoechst	Sigma-Aldrich
Isopropanol	Fisher Scientific
Methanol	Sigma-Aldrich
Nucleofector	Lonza
Nycodenz	Axis-shield
Paraformaldehyde	Fish Scientific
Penicillin/Streptomycin	Sigma-Aldrich
Phenol/chloroform	Sigma-Aldrich
Phenylhydrazine	Sigma-Aldrich
Poly-L-Lysine Slides	Sigma-Aldrich
Pyrimethamine	Sigma-Aldrich
RPMI	GIBCO
Sulphadiazine	Sigma-Aldrich
SYBR Green	Sigma-Aldrich
Triton	Sigma-Aldrich
XL1-BLUE competent *E. coli* cells	Stratagene

Table 5 – List of solutions

Solution	Mixture
Coelenterazine loading buffer (CLB)	20 mM Hepes, 20 mM Glucose, 4 mM $NaHCO_3$, 1 mM EDTA, 0.1% BSA, pH 7.5 in PBS
Electrophoresis buffer	25 mM Tris-base, 250 mM glycine, 0.1% SDS
Freezing Solution	9-parts Alseverver's solution, 1-part glycerol
Laemmli buffer	0.5 M Tris/HCl pH 6.8, 0.8 ml glycerol, 10% SDS, 2-mercaptoethanol, H_20, bromophenol blue
Luria Bertani (LB) medium	10 g bacto-tryptone, 5 g bacto-yeast extract, 0.5 g NaCl in 950 ml H20
Microtubule-stabilising buffer (MTSB)	10 mM MES, 150 mM NaCl, 5 mM EGTA, 5 mM $MgCl_2$, 5 mM glucose
Nycodenz	5 mM Tris, pH 7.2, 3 mM KCl, 0.3 mM EDTA, 27.6% w/v Nycodenz
Ookinete media	2 g $NaHCO_3$, 10 ml Pen/Strep, 1 ml 100 mM xanthurenic acid in RPMI pH 7.4
Red blood cell lysis buffer (10x)	1.5 M NH_4Cl, 0.1 M $KHCO_3$, 0.01 M EDTA, pH8
Schizont media	8 ml foetal calf serum, 0.5 ml Pen/Strep, 40 ml RPMI
TE buffer	10 mM Tris-Cl, pH 7.5, 1 mM EDTA
Solution I	50 mM glucose, 25 mM Tris-HCl pH8, 10 mM EDTA pH8, 100 µg/ml RNase A
Solution II	10 mM NaOH, 10% SDS in H20
Solution III	60% 5 M CH_3COOK, 11.5% acetic acid in H20
Transfer buffer (10x)	3 g/l Tris, 14.4 g/l glycine, 20% methanol
Tris-buffered saline (TBS) (10x)	80 g NaCl, 2 g KCl, 30 g Tris-base, pH 7.4
Tris-glycine electrophoresis buffer	15 g, Tris, 72 g, glycine, 25 ml 20% SDS
Tris-NaCl-EDTA (TNE) buffer (10x)	100 mM Tris, 1 M NaCl, 50 mM EDTA, pH 7.5

Table 6 – List of antibodies

	Antibody	Host	Manufacturer	Concentration
1º Antibody	*Anti-GFP*	Rabbit	Thermofisher	1:250
	Anti-centrin	Mouse	Sigma	1:500
	Anti-α-tubulin	Mouse	Sigma	1:1000
2º Antibody	*Anti-rabbit (488)*	Goat	Invitrogen	1:1000
	Anti-mouse (568)	Goat	Invitrogen	1:1000
Other	*Anti-P28 (13.1)*	Mouse	Tewari et al., 2005	1:1000
	Vectashield with DAPI	N/A	Vector Labs	N/A

Table 7 – List of commercial kits

Kit	Manufacturer
Fast SYBR® Green Master Mix	Applied Biosystems
GenElute™ Plasmid Miniprep Kit	Sigma-Aldrich
GFP-Trap_A®	Chromotek
High-Capacity RNA-to-cDNA™ Kit	Applied Biosystems
QIAquick® PCR purification kit	QIAGEN
Rneasy® Mini Kit	QIAGEN
WesternBreeze ™ Chemiluminescent kit	Invitrogen

Table 8 – List of enzymes

Enzyme	Manufacturer
Apa1	Promega
Xcm1	New England Biolabs
Kpn1	New England Biolabs
RNase A	Sigma-Aldrich
Proteinase K	Sigma-Aldrich
T4 DNA Ligase	New England Biolabs
T4 DNA Ligase Buffer	New England Biolabs

Table 9 – List of primer sequences

Primer	Sequence
For generation of tag lines:	
NEK1tgFW	CCCCGGTACCGGGAAACCAGTAATAATAGTGCTCG
NEK1tgRV	CCCGGGCCCTCTACAAGAATATAATTTTCTATCATATATAT
Ol492-GFP	ACGCTGAACTTGTGGCCG
IntNEK1tg	GAACGGGCGATGATGGAAAAAACTAGAAG
For generation of knockdown lines:	
PTD0141	GAGACCGCGGCAAGTTTCCCCAAAAGATGATGAAA
PTD0142	GAGACTGCAGTTTAATAATTTTTTTTTCACACACACATATATATA
PTD0143	GAGACTCGAGATGCCAAGTAAATATGACGATGGAG
PTD0144	GAGAGCGGCCGCGATATCCAAAATCACCAATTTTTGCAATAG
5'IntPTD014	GTATATAACGAATTGTTTTTTACACAAAGT
5' Int RV	TCTACTTTATTTGCTAATTCTGG
3' IntClag	GTGTGTACCATATTTTCACATATAAGTTT
3' IntPTD014	CGCACGAATGTGCCATACTTTC
For quantitative PCR:	
NEK1 FW	CTGCGAAAAGGAAGGCTATG
NEK1 RV	CGCTCTCTTTCCACTCTTCC
Hsp70 FW	GTATTATTAATGAACCCACCGCT
Hsp 70 RV	GAAACATCAAATGTACCACCTCC
Arginyl Fw	TTGATTCATGTTGGATTTGGCT
Arginyl RV	ATCCTTCTTTGCCCTTTCAG

3.1 Ethics Statement

All animal work has passed an ethical review process and was approved by the United Kingdom Home Office. Work was carried out in accordance with the United Kingdom 'Animals (Scientific Procedure) Act 1998' and in compliance with the 'European Directive 86/609/EEC' for the protection of animals used for experimental purposes under the project licence No. 30/3248 and PDD2D5182.

3.2 Mouse and Mosquito Maintenance

This project used *P. berghei* ANKA 2.34 parasites which were maintained in six-to-eight week old female Tuck-Ordinary outbred mice. Mice were kept in well ventilated containers at room temperature (21-23°C) with simulated 12-hour day/night cycles. Blood samples from daily tail bleeds were fixed on slides using 99.8% methanol and used in Giemsa staining (as described in 3.7.1) to assess parasitaemia levels. Intraperitoneal injections of Ketamine (0.75 µl, Sterlin) and sodium pentobarbital (200 mg, Vetoquinol) were used to induce terminal anaesthesia before blood was extracted via cardiac puncture.

Anopheles stephensi mosquitoes (Strain SD500) were raised in an insectary and maintained at 26 to 28°C with a humidity of 30 to 40%. Larvae were grown in trays of salt water and fed pond pellets, and transferred into netted cages upon pupation. Mature mosquitoes were nourished with a 2% glucose solution via a saturated filter paper, which was maintained in the cage.

3.3 Generation of Transgenic Parasites

3.3.1 Isolation of NEK1 C-terminal Regions for use in Alternative Transgenic Parasites

NEK1-GFP plasmid constructs (pOB277, Appendix A) that had been previously generated by single homologous recombination (unpublished data, Tewari et al.), were selected for

the donation of their C-terminal regions (of NEK1), which were to be used in the generation of alternative NEK1-mCherry and NEK1-Scarlet lines. Before this however, a diagnostic PCR was undertaken to confirm that the sample contained the correct GFP tagged gene before committing to its use (see section 3.4.3). Upon confirmation of successful integration, the NEK1-GFP plasmids were transformed into calcium competent *Escherichia coli* XL1 BLUE cells (Stratagene) by heat shock, and inoculated on 0.1% LB-ampicillin agar to produce colonies (same method used in section 3.3.3). Single colonies were selected and cultured in an LB broth overnight, with the subsequent isolation of the plasmids achieved using the GenElute Plasmid Miniprep Kit (Sigma-Aldrich) as per the manufacturer's instructions. Purified plasmids were incubated at 37°C for 2 hours with the enzymes Apa1 and Kpn1, to complete a double restriction digest of the NEK1 C-termini from the vectors (same method used in section 3.3.4). Digested samples were loaded on a 1% agarose gel for gel electrophoresis to separate the desired NEK1 region from the vector. The band produced was visualised using UV light of wavelength 302 nm whilst in a dark room, and excised using a scalpel. The NEK1 fragment was extracted from the gel using the QIAquick Gel Extraction Kit (Qiagen) as per the manufacturer's instructions.

3.3.2 Ligation

The purified NEK1 C-terminal inserts were ligated into mCherry and Scarlet vectors (pOB277 Appendix B and C) in a 10 µl reaction mixture consisting of 2 µl of insert, 1 µl of vector, 1 µl of T4 ligase, 1 µl of T4 ligase buffer and 5 µl of distilled water. Negative control reactions were set up, in which the inserts were replaced with an additional 2 µl of distilled water (7 µl total volume). Ligation reactions were incubated at 25°C for 2 hours.

3.3.3 Transformation

Newly ligated plasmids were mixed with 30 µl of calcium competent *E. coli* XL1 BLUE cells and incubated on ice for 20 minutes. Heat shock treatment, intended to increase the

permeability of cell membranes, was used for transformation. Samples were incubated at 42°C for 1 minute, before being returned to the ice for another 2 minutes. Cells were then incubated at 37°C for 25 minutes, after the addition of rich SOC medium, to allow the *E. coli* cells to recover. Following this, samples were inoculated, practising aseptic technique, on 0.1% LB-ampicillin agar (1 µl ampicillin/ml) and incubated for 24 hours at 37°C to promote colony growth. The selective growth of the cells that contained the desired construct was achieved via the use of the ampicillin antibiotic supplemented in the agar. All vectors contained an ampicillin cassette, inferring resistance to the antibiotic, thus promoting the growth of this specific bacteria whilst preventing the formation of contaminants.

3.3.4 Isolation of Plasmid DNA from *E. coli*

Colonies from the inoculated agar plate were selected and incubated overnight at 37°C in separate 5 ml LB broth tubes to further promote bacterial growth. 750 µl from each sample was taken and centrifuged at 13000 rpm for 1 minute, with resultant supernatant being removed. The pellet was resuspended in 100 µl of Solution I, followed by the addition 200 µl of Solution II (lysis) and 150 µl of Solution III (neutralisation) (Table 5), which were mixed by inversion (6x). Samples were spun at 13000 rpm for 10 minutes, and added to 350 µl of Isopropanol (Fisher Scientific). This centrifugation step was repeated with liquid being discarded and replaced with 170 µl of 70% ethanol. Samples were spun for 1 minute; supernatant was removed and pellets were resuspended in 30 µl of distilled water. Gel electrophoreses of double restriction digested plasmids were used to confirm the successful ligation of the NEK1 C-termini into the mCherry and Scarlet vectors. 5 µl of plasmid was mixed with 1 µl of the enzymes Apa1 and Kpn1 with 2 µl of CutSmart buffer (NEB) in 20 µl distilled water. Samples were incubated at 37°C for 1 hour before being run on the gel (100 ml TAE, 1 g agarose powder, 1 µl ethidium bromide).

Plasmids from samples that tested positive for successful ligation were purified using the GenElute Plasmid Miniprep kit as per the manufacturer's instruction.

3.3.5 Transfection

NEK1-mCherry and Scarlet constructs were digested overnight at 37°C in reaction mixtures containing EcoRV and ClaI respectively, in order to linearize them, thus promoting their integration into the *Plasmodium* genome. WT-ANKA schizonts were selected for transfection, as the formation of the subsequent transgenic merozoite stages, provided an efficient means of replicating the tag via repeated host cell invasions. Schizonts were purified from blood (see section 3.7.2) and resuspended in 100 µl of Nucleofector containing 10 µl of the linearized construct in electroporation cuvettes. Vessels were inserted into a Nucleofector 2b Device (Lonza) and run using the 'Zap Program U-033', before being incubated in 150 µl of blood at 37°C for 15 minutes. This blood was extracted from uninfected mice that had been injected intraperitoneally with phenylhydrazine (6 mg/L, 100-150 µl) two days prior. This served to kill mature RBCs and promote reticulocyte generation, thus providing the parasite ample opportunity to invade these susceptible cells. Blood samples were injected intraperitoneally into mice which were subsequently dieted on water supplemented with pyrimethamine (70 µg/ml). All tag constructs contained a hDHFR (human dihydrofolate reductase) cassette to a infer resistance to the pyrimethamine drug, thus allowing for the selective survival of the parasites containing the desired construct. Confirmation of successful integration was achieved using diagnostic PCR on isolated transgenic parasite DNA (see section 3.4).

3.4 Genotypic Analysis

3.4.1 Isolation of asexual *Plasmodium* Stages from Mouse Blood

Infected mouse blood was extracted via cardiac puncture into a heparin anticoagulant. This blood was filtered through a column containing CF11 (cellulose fibre) saturated with

PBS, in order to separate host white blood cells. Filtered blood was then centrifuged at 1900 rpm for 10 minutes, with the resulting pellet being resuspended in 1 ml of RBC lysis buffer (Table 5) before an additional 14 ml of buffer was added. Samples were incubated on ice for 1 hour to allow for RBC lysis, before being centrifuged at 1900 rpm for 10 minutes, with the resulting pellet being washed in 750 µl of PBS at 5000 rpm for 6 minutes. The final pellet was either frozen at -20°C or used immediately.

3.4.2 Extraction of *Plasmodium* DNA from Parasite Pellets

Parasite pellets were resuspended in 400 µl of 1x TNE buffer (Table 5), 50 µl of 10% sodium dodecyl sulphate (SDS) and 10 µl of RNase A (10 mg/ml stock). Samples underwent two incubations, the first at 37°C for 10 minutes, and the second at 50°C for 1 hour after the addition of 10 µl of Proteinase K (10 mg/ml stock). 50 µl of 3 M sodium acetate and 500 µl of phenol:chloroform were added, the latter under a fume hood, and mixed by inversion (20x) before samples were centrifuged at 13000 rpm for 5 minutes with resultant supernatant being transferred into new Eppendorfs. Another 50 µl of 3 M sodium acetate was added in addition to 1 ml of ice cold 100% ethanol. Samples were inverted (20x) and centrifuged at 13000 rpm for 15 minutes with resultant supernatant being discarded. Pellets were washed with 170 µl of 70% ethanol and centrifuged at 13000 rpm for 1 minute. Supernatant was discarded and the sample was centrifuged again for 30 seconds to remove remaining ethanol. The DNA pellet (not always visible) was resuspended in 30 µl of TE buffer (Table 5).

3.4.3 Diagnostic PCR

Diagnostic PCRs were used to confirm the successful integration of the tags downstream of the NEK1 coding region. NEK1-mCherry and NEK1-Scarlet integration was checked using the forward primer IntNEK1tg and reverse primer ol492 (Table 9). WT (wild-type) genomic DNA was used alongside transgenic DNA with the aforementioned primers to act

as a negative control. IntNEK1tg binds inside of the NEK1 coding sequence, present on WT and mutant DNA, whilst ol492 binds inside of the tag sequence. NEK1tgRV (Table 9) was used as a positive control with IntNEK1tg, both binding inside of the NEK1 and thus confirming the presence of DNA. mCherry and Scarlet constructs failed to integrate into NEK1, and as such NEK1-GFP was used in all experiments. Integration PCR of NEK1-GFP to confirm the correctly tagged gene was present in sample provided, was achieved using the same primers (See Figure 10).

A diagnostic PCR was also used to confirm the correct integration of the previously generated NEK1clag DNA (unpublished data, Tewari et al.; used for the conditional knockdown of NEK1). 5' integration was confirmed by 5' IntPTD014 and 5' IntRV primers (Table 9), binding upstream and inside of the selectable hDHFR marker respectively. 3' integration was confirmed by 3' IntClag and 3' IntPTD014 (Table 9), binding inside of the inserted clag promoter trap and NEK1 gene respectively. 5' to 3' integration or gene Knock-in was confirmed using 5' IntPTD014 and 3' IntPTD014 primers, both sites being present in WT and mutant DNA.

Each PCR reaction mixture consisted of 1µl of gDNA, 1µl of the forward and reverse primer, 12.5µl of GoTaq and 9.5µl of water (25µl total). A Thermal Cycler PCR machine (Alpha Laboratories) was used with preprogramed cycling conditions: 94°C for 5 minutes, 94°C for 45 seconds (Step 2), 50°C for 45 seconds, 62°C for 2 minutes followed by the return and repeat of all steps after and including step 2 another 29 times, finishing with a 62°C 10-minute cycle. 5µl of the amplified samples were added to the wells of a 1% agarose-gel with ethidium bromide (1µl) (99 ml water, 1 g agarose powder), which was submerged in TAE buffer for gel-electrophoresis and run for 30 minutes at constant 120 V. The agarose-gel was visualised using a Gel-Doc XR+ Gel Documentation System (BioRad).

3.5 Analysis of Gene Expression

3.5.1 RNA Extraction

A RNeasy® Mini Kit (Qiagen) was used to extract RNA from parasites as per the manufacturer's instructions. The pellet was resuspended in RLT lysis buffer with β-mercaptoethanol, before an equal amount of 70% ethanol was added. Samples were transferred to spin columns and centrifuged at 13000 rpm for 30 seconds, with flowthrough being discarded. RW1 washing buffer was added before repeating centrifugation. DNase was added to the column which was left at room temperature for 15 minutes, before RPE buffer was used to wash the column following the same centrifugation steps. Remaining RNA was eluted with 50 µl of DEPC-treated water and quantified using a Nanodrop (ThermoFisher) before being run through gel-electrophoresis (1% agarose gel in TBE buffer) to ascertain RNA quality.

3.5.2 cDNA Synthesis

A High-Capacity RNA-to-cDNA™ Kit (Applied Biosystems) was used as per the manufacturer's instructions to transcribe the RNA into cDNA for use in quantitative PCRs, intended to examine stage-specific mRNA expression of WT-GFP and NEK1clag. Reaction mixtures (10 µl 2x RT buffer, 1 µl 20x RT enzyme mix, 3 µl RNA sample and 7 µl distilled water) were run in a thermal cycler (37°C for 1 hour, 95°C for 5 minutes, 4°C until removed) before being diluted to 800 ng/µl (stock) or 80 ng/µl (working).

3.5.3 Quantitative PCR (qRT-PCR)

For every cDNA sample run, three reaction mixtures were required for each of the three primer pairs used (ARG, HSP70 and NEK1 forward and reverse primers; Table 9). 0.5 µl of the forward and reverse primer were added to a reaction mixture containing 10 µl of SYBR green master mix (Applied Biosystems™) and 9 µl DEPC-treated water (20 µl total per sample). 18 µl of reaction mixture was added to 4 µl of cDNA sample which was split into

two technical replicates on the 96 well-plate (10 µl each) before the plate was sealed with an air tight lid. Target gene amplification was achieved by subjecting the plate to 40x 95°C 3 second and 60°C 30 second heating cycles. An unpaired t-test was conducted to examine significant differences between WT and NEK1clag mutant strains.

3.6 Proteomic Analysis

3.6.1 Protein Preparation and Western Blotting

Western blotting was used to confirm the correct expression of NEK1-GFP proteins in mutant parasites. Previously extracted asexual parasite pellets (see section 3.7.2) were resuspended in 1 ml of RBC lysis buffer containing 60 µl of PBS with EDTA free protease inhibitors and 1% NP40, before being incubated on ice for 20 minutes. 10 µl of 10x laemmli buffer (Table 5) was added, vortexed and centrifuged at 6000 rpm for 30 seconds, before a 5-minute incubation in a 95°C heating block was used to denature secondary and tertiary protein structures.

A SDS-polyacrylamide gel (BioRad) with a dynamic gradient of 4 to 12% was placed inside of a Protean Tetra-Cell system (BioRad) with the resultant chambers being filled with 1x tris-glycine electrophoresis buffer (Table 5). Alternating wells were filled to prevent cross contamination of samples, with 10 µl of protein ladder, 10 µl of WT control, and 20 µl of sample injected into the gel. The system was run at a constant voltage of 175V until the dye had reached the bottom. A Protran Nitrocellulose membrane (Amersham) and two blotting papers (Whatman) were soaked in 1x transfer buffer (Table 5) for 2 minutes. The gel was extracted and the top and bottom sections were removed to discard excess dye and cell debris. The Trans-Blot SD Semi-Dry cell (BioRad) was loaded in sequence (blotting paper, Nitrocellulose membrane, SDS-polyacrylamide gel, blotting paper) and run at a constant voltage of 25V for 1.5 hours at 0.33 amps. A WesternBreeze Chemiluminescent kit (Invitrogen) was used to block the membrane using the blocking solutions provided,

and to detect the protein bands using the anti-GFP polyclonal antibody (1:1250), as per the manufacturer's instructions. Membranes were developed in a darkroom on Hyperfilm ECL sheets (Amersham) using a film cassette. All attempts to visualise NEK1-GFP were unsuccessful, however, the NEK1 protein had been confirmed in a previous experiment (Figure 10).

3.6.2 Immunoprecipitation Pulldown

Previously extracted male gametocytes (see section 3.7.5) were activated for 1.5 minutes in an ookinete media (Table 5) before being resuspended in 1 ml of ice-cold PBS. 27 µl of 37% formaldehyde was added and tumbled for 10 minutes, before being centrifuged for 5 minutes at 5000 rpm, with supernatant being discarded. A 20 ml PBS solution containing 0.125 M glycine was added before being mixed on a rocker at 40 rpm for 5 minutes. Samples were centrifuged at 1900 rpm for 10 minutes before undergoing two washing processes using PBS.

The previously generated pellet was resuspended in 200 µl of lysis buffer with 1x protease inhibitor (50x stock) and left on ice for 30 minutes, before being sonicated to completely lyse the cells. Lysate was spun at 13000 rpm for 20 minutes at 4°C with the resultant supernatant being added to 300 µl of dilution buffer with 1x protease inhibitor, before being incubated on ice. GFP-Trap beads from the GFP-Trap_A kit (Chromotek) were vortexed and washed in dilution buffer (5000 rpm, 2 minutes at 4°C) three times before 20 µl of beads were added per sample. Lysates were tumbled at 4°C for 2 hours and centrifuged at 5000 rpm for 2 minutes. 1 ml of dilution buffer was added, before samples were vortexed and centrifuged with resultant supernatant being removed, which was repeated three times. Final samples were sent to Dr Andrew Bottrill and colleagues (University of Warwick) to undergo mass spectrometry (MS) analysis.

3.7 Phenotypic Analysis

3.7.1 Giemsa Staining

Parasite smears were fixed in 99.8% methanol for one minute before being air dried. Slides were then submerged in a 1:5 Giemsa:water solution for 5 minutes to stain parasite nuclei, before being washed with water and then dried again. Resultant stains were observed using a light microscope at 40x magnification with immersion oil.

3.7.2 Schizont Media and Purification

Schizont media was prepared in 500 ml conical flasks containing 60 ml RPMI, 12 ml foetal bovine serum (FBS) and 0.5 ml penicillin streptomycin (Pen/Strep), suitable for 1 to 2 ml of blood sample. Gas (5% CO_2, 90% N_2, 5% O_2) was pumped into the flask for 20 seconds before and after the inoculation of the medium with infected mouse blood. Bungs were used to create an air tight seal on the flasks, which were incubated at 37°C in orbital shakers running at 90 rpm for a predetermined time depending on the required age of the schizonts. Giemsa stains were used to determine schizont age prior to purification. Schizont cultures were split equally between 50 ml falcon tubes and spun at 1900 rpm for 10 minutes, with the removal of resultant supernatant leaving 1 ml of volume. This was layered on a 60% Nycodenz gradient (3 ml Nycodenz, 2 ml PBS) in 15 ml falcon tubes and centrifuged for 25 minutes at 1200 rpm with acceleration/deceleration (acc/dec) set to 4. Schizont layers were transferred into 1.5 ml Eppendorfs, and centrifuged for 5 minutes at 5000 rpm to remove remaining liquid.

3.7.3 Gametocyte Host Preparation

In order to cultivate and extract gametocytes, preparation of the host was required. Mice were injected intraperitoneally with phenylhydrazine (6 mg/L, 100-150 µl) two days prior to the inoculation of the parasite, to kill mature RBCs and promote the formation of reticulocytes, which are more susceptible to parasite invasion. Four days post inoculation,

sulfadiazine (20 mg/L) was fed to the mice via their water supply to kill pre-existing asexual blood stages, and apply a stress on remaining parasites to encourage their differentiation into male and female gametocytes. Blood was extracted 5 days after the initial inoculation of the parasite.

3.7.4 Exflagellation Counts

Prior to gametocyte purification, samples of blood were smeared to observe the number of exflagellating centres, described as rosette-like structures with occasional visible flagella. Samples were activated by imitating the conditions of the mosquito midgut using an ookinete medium (Table 5) derived from the work of Billker et al. (1997), which was incubated at 20°C for 10-15 minutes. Field of view dictated counts were made using a light microscope at 40x magnification with immersion oil.

3.7.5 Gametocyte and Ookinete Purification

The prepared gametocyte-infected blood was added to 4 ml of coelenterazine loading buffer (CLB) (Table 5) in a 15 ml falcon tube and spun at 1900 rpm for 10 minutes to reduce it to a volume of 1 ml. A 48% Nycodenz gradient was made (2.4 ml Nycodenz, 2.6 ml CLB) with the blood subsequently layered on top, which was spun at 2345 rpm for 10 minutes at acc/dec 4. Gametocyte layers were transferred to 1.5 ml Eppendorfs and spun for 2 minutes at 6000 rpm, with resulting supernatant being discarded. These were either frozen immediately at -80°C for inactivation and storage, or resuspended in ookinete media to observe microgamete formation (10-15 minutes) and subsequent ookinete maturation (<24 hours).

Infected blood samples left in ookinete media for 24 hours at 20°C resulted in the development of mature ookinetes, which was confirmed by live-cell imaging prior to purification. Samples were first spun down at 1900 rpm for 10 minutes to separate and remove RBCs. A 15ml RBC solution was added and the sample was incubated at 4°C for

30 minutes before being centrifuged at 1495 rpm for 10 minutes. The remaining media was removed and the pellet washed in 1 ml of RPMI before being transferred to an Eppendorf and spun at 6000 rpm for 3 minutes. RPMI was removed and replaced with 1 ml of ookinete medium, which was layered on top of a 65.2% Nycodenz gradient (2.5 ml Nycodenz, 1.5 ml PBS). The centrifuge was precooled to 4°C and the sample spun down at 1495 rpm for 30 minutes with acc/dec set to 4. The middle layer was removed and added to an Eppendorf which was centrifuged at 4°C for 5 minutes at 5000 rpm. Supernatant was removed leaving the pellet, which was resuspended in 50 µl of ookinete media ready for further usage.

3.7.6 Fluorescent microscopy

Fluorescent microscopy was used to observe the expression of fluorescent tagged proteins in all life stages, in addition to immunofluorescent assay (IFA) slides (see section 3.7.7) using a Zeiss AxioImager M2 microscope and associated ICc1 digital camera, visualised on Carl Zeiss AxioVision Rel. 4.8.2 software (Carl Zeiss inc). Purified pellet samples were mixed with Hoechst solution (1:1000) directly on the slide (2 µl each) to stain the nuclei. When observing ookinetes, 13.1 antibodies were used to highlight the cell morphology due to its association with the surface protein P28. A 60x magnification with immersion was used for most imaging.

3.7.7 Immunofluorescent Assays

Immunofluorescent assays allowed for the characterisation of proteins in relation to NEK1-GFP, which had not been endogenously tagged with fluorescent proteins. Schizont/gametocyte smears were fixed with 2%/4% paraformaldehyde in microtubule stabilising buffer (MTSB) (Table 5) on poly-L-lysine coated slides (Sigma). Slides were washed in tris-buffered saline (1x TBS) (Table 5) before and after cell permeabilization using 0.1% Triton in TBS, and subsequently blocked with a blocking solution consisting of

10% goat serum (GS) and 3% bovine serum albumin (BSA) in TBS. Primary antibodies consisting of polyclonal anti-GFP rabbit (1:250, Thermofisher), primary mouse monoclonal anti-α-tubulin and primary mouse monoclonal anti-centrin (1:500/1:200, Sigma; Table 6) were diluted in 1% BSA and 1% GS in TBS and incubated on the slides for 1 hour. AlexaFluor 488 anti-rabbit (1:1000, green) and 568 anti-mouse (1:1000, red) (both Invitrogen; Table 6) secondary antibodies were also diluted in 1% BSA and 1% GS in TBS and incubated in the dark for 45 minutes. Slides were washed with 1x TBS at the end of each incubation, and were mounted in VectaShield with DAPI (Vector Labs) before being enclosed with a slip which was sealed with nail polish.

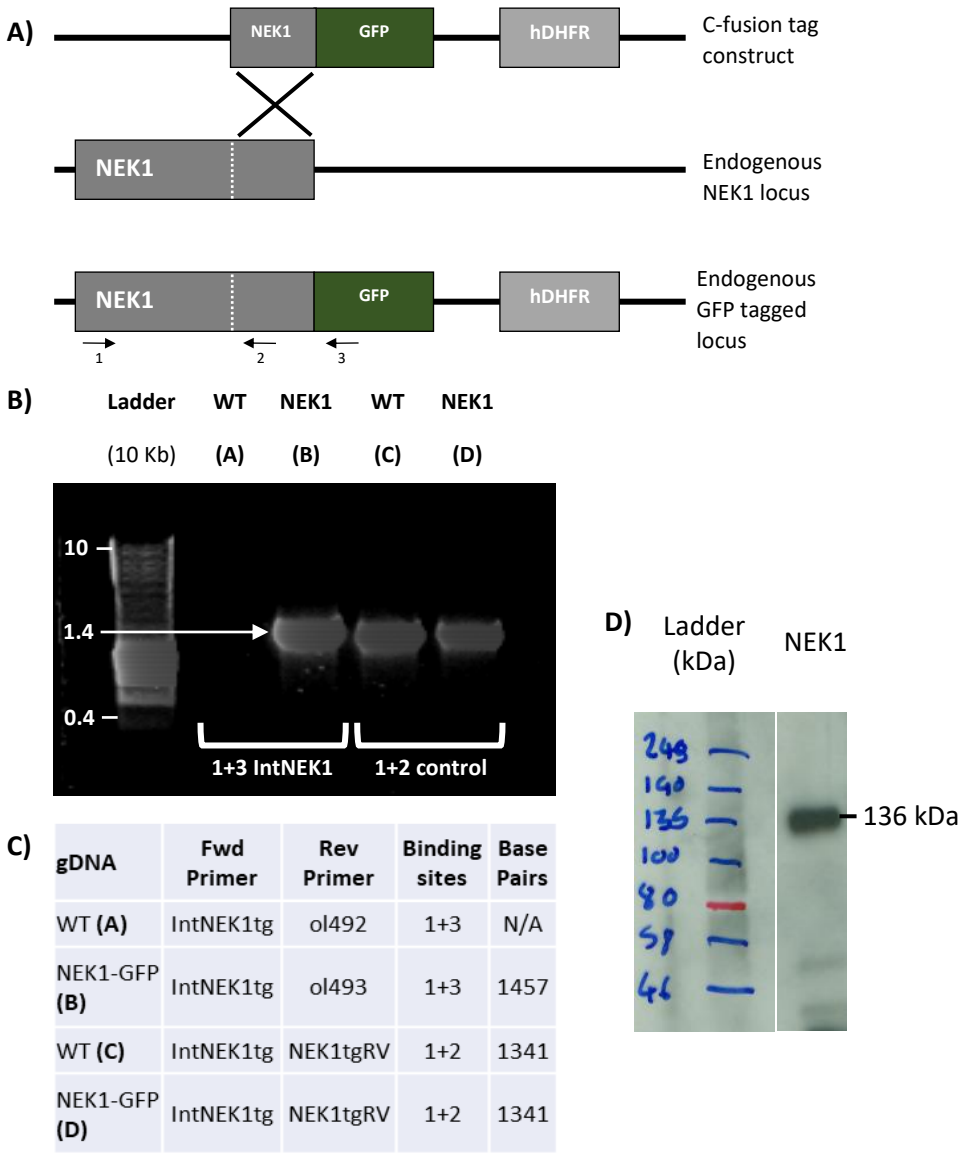
4.0 Results

4.1 Expression and Localisation of NIMA-related Kinase 1 in *P. berghei*

The spatio-temporal patterns of *Plasmodium* NEK1 expression (PBANKA_1443000) remain relatively unidentified, with few localisation studies having been carried out on the protein to date. In order to report the patterns of NEK1 localisation during schizogony, gametogenesis and ookinesis, NEK1-GFP, which had been previously generated by endogenously tagging the C-terminal end of the NEK1 gene with GFP by single homologous recombination (unpublished date, Tewari et al.), was used. The expression of this protein thus allowed for the characterisation of its localised patterns throughout the parasite's life cycle using live cell fluorescent microscopy.

4.1.1 Genotypic Analysis Confirms Integration of NEK1-GFP Parasite Lines

As attempts to generate alternative NEK1-mCherry and NEK1-Scarlet lines by single homologous recombination were unsuccessful, NEK1-GFP was instead used for all live cell phenotypic analysis. Whilst diagnostic PCR had been performed on the NEK1-GFP at the time of its generation and confirmed its successful integration, the procedure was repeated to confirm that the stock sample stored in the -80°C freezers, contained the desired NEK1-GFP locus, before committing to its use in further experiments. This confirmation was achieved using IntNEK1tg and ol492 primers (Figure 10) on NEK1-GFP and WT gDNA, resulting in the amplification of NEK1-GFP fragments expected to be 1457bps in size, which were represented as a band on the agarose-gel at the expected position along the 10 Kb ladder. Additionally, IntNEK1tg forward primers were used with NEK1tgRV primers to perform a positive control, which produced bands in both mutant and WT samples as was to be expected.



C)

gDNA	Fwd Primer	Rev Primer	Binding sites	Base Pairs
WT **(A)**	IntNEK1tg	ol492	1+3	N/A
NEK1-GFP **(B)**	IntNEK1tg	ol493	1+3	1457
WT **(C)**	IntNEK1tg	NEK1tgRV	1+2	1341
NEK1-GFP **(D)**	IntNEK1tg	NEK1tgRV	1+2	1341

Figure 10 - Genotypic analysis of NEK1-GFP genes to confirm successful integration.

A) Schematic representation of the single homologous recombination procedure that was used to endogenously tag the NEK1 C-terminus region with a construct containing the GFP and hDHFR cassette used for selectability. The numbers under the GFP tagged locus represent the binding sites of the primers used in the PCR. **B)** Agarose-gel electrophoresis of the diagnostic PCR, demonstrating the confirmed presence and integration of NEK1-GFP (1457bps), evidenced by the band in the NEK1 (B) lane. IntNEK1tg primers bind at the region of the NEK1 locus represented by 1 on the schematic, whilst ol492 primers bind inside the GFP at 3; WT lacks GFP, thus no band is visible in the (A) lane. The NEK1tgRV primer (binds at 2), was used as a positive control with IntNEK1tg as both regions are present in the WT and mutant, evidenced by the two bands in the WT (C) and NEK1 (D) lanes. **C)** Table containing the list of primers used. **D)** Western blot analysis confirming correct expression of NEK1-GFP protein as evidenced by a 136 kDa band, as was to be expected.

The lysates of NEK1-GFP blood stage parasites were used in multiple western blot procedures, however, all attempts at displaying the correct expression of the NEK1-GFP protein failed. Western blots conducted in previous experiments have demonstrated this correct expression however (unpublished data, Tewari et al.), producing a band of approximately 136 kDa (NEK1 = 107 kDa + GFP = 27 kDa). Furthermore, confirmation of NEK1-GFP protein was achieved in protein pulldown and subsequent mass spectrometry of activated male gametocytes, which demonstrated the presence of NEK1-GFP associated with the bait, and thus identified in the parasite.

4.1.2 NEK1 is Temporally Expressed in Both Asexual and Sexual Stages Where it Localises to the Nuclear Periphery and Divides in Specific Sequence

Little work has been done to elucidate the temporal patterns of NEK1 during blood stage proliferation in its entirety, especially with an emphasis on the patterns of division undertaken by the protein in relation to nuclear karyokinesis. In addition to this, NEK1 temporal profile during male gametogenesis, exflagellation and the subsequent ookinete development remains poorly understood. Therefore, the patterns of NEK1 localisation throughout blood stage schizogony in addition to male endoreduplication and the proceeding ookinete formative stages are studied here.

To determine the patterns of NEK1 localisation during the parasite's life cycle, fluorescent microscopy of GFP-tagged NEK1 proteins in *P. berghei* was performed. Blood stages were observed over a 24-hour window at predetermined time points, to account for all stages leading up to and culminating in intraerythrocytic proliferation. The same technique was applied to the sexual stages, where the temporal profile of NEK1-GFP was observed in activated male gametocytes in an ookinete media over a 15-minute window. Male microgametes were allowed to fertilise female cells to produce zygotes which were subsequently observed over a 24-hour period. Cy3-conjugated P28 antibodies were used to stain the surfaces of these female and zygote cells during ookinete development. Liver

stage schizogony was not observed, due to the lab lacking the required equipment to accomplish this. Strong NEK1 expression was observed in all proliferative asexual and sexual stages with exception to most ookinetes stages, and displayed specific patterns of localisation and divisional sequences with respect to the nuclei and presumed genomes.

4.1.3 NEK1 Localisation in Asexual Blood Stages

NEK1 foci were initially absent in ring and trophozoite stages, however, green-stained cytosol was observed in late stage trophozoites, indicative of diffused NEK1 proteins (Figure 11). Strong NEK1-GFP expression was only present after the commencement of endomitosis, which was evidenced by the first observed division of the nuclei concurrent with *Plasmodium* schizont formation, where visible foci localised in the perinuclear space. These results are supported by the previous findings published by Dorin-Semblat et al. (2011). A specific and predictable sequence of focal and nuclear division was recorded; NEK1 foci always divided into two distinct entities and separated to opposite nuclear hemispheres prior to the onset of karyokinesis. Each nucleus inherited a single dot, with no nuclei being observed with more than two NEK1 foci at any one time. Interestingly, NEK1 dots associated with recently divided daughter nuclei, demonstrated atypical focal division relative to each other. Reductions in protein fluorescence and defined NEK1 foci were observed in late and mature schizonts, with the kinase appearing diffused as was observed in late trophozoites. Some disparity in NEK1 expression was observed in free merozoite stages as the level of NEK1-GFP fluorescence varied in different cells, however, diffused NEK1 was absent in most. The patterns of NEK1 localisation and division with respect to the nuclei provides strong evidence implicating NEK1 in schizogony, specifically with the MTOC, known to operate and divide in the same space and sequence.

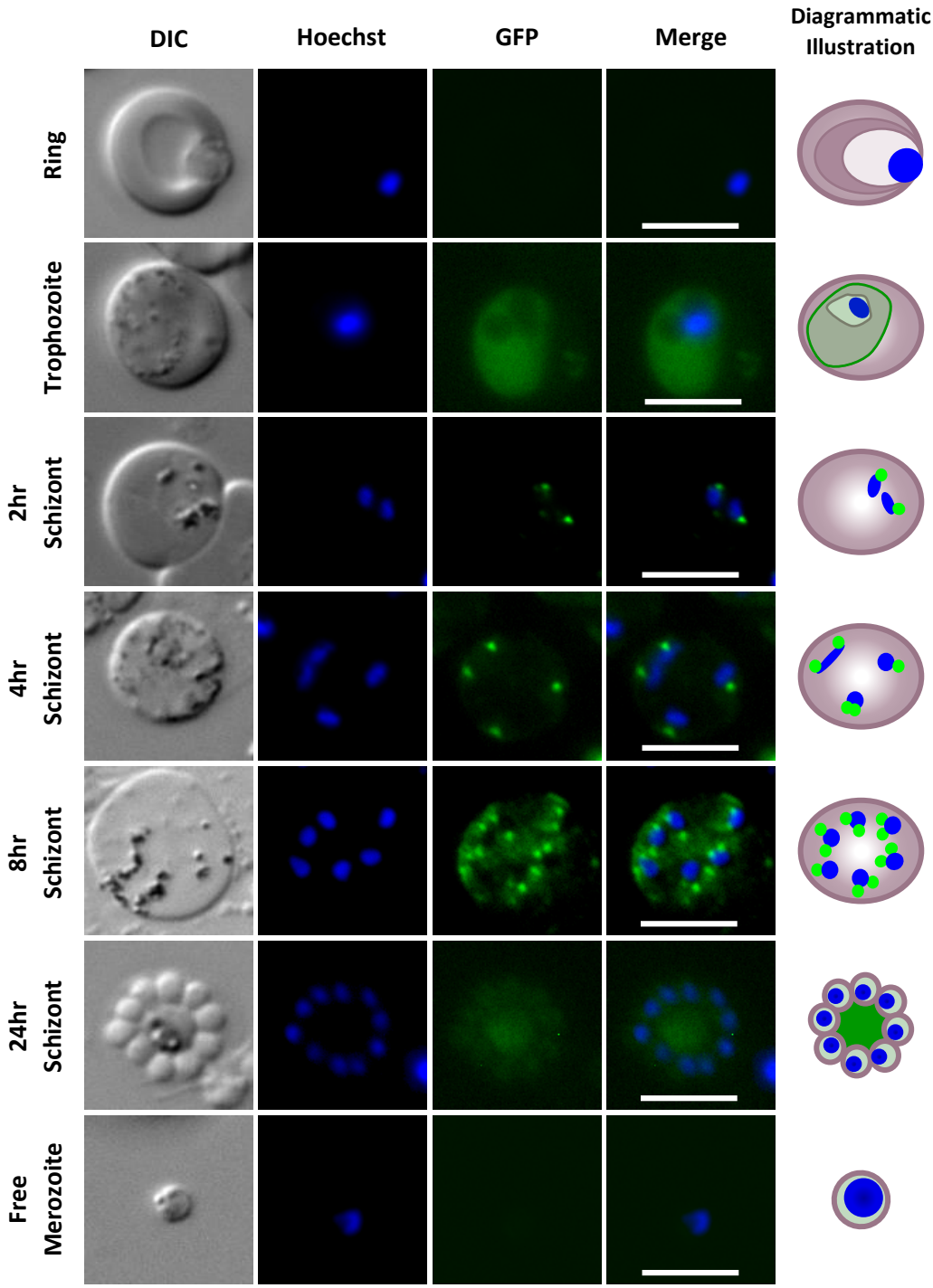


Figure 11 - NEK1-GFP expression (green) in intraerythrocytic asexual stages viewed under a fluorescent microscope.

Parasites were incubated in a schizont media with samples being withdrawn at desired time points. Initial parasite identification was achieved via the staining of the nuclei using Hoechst (blue), which in conjunction with the differential interreference contrast (DIC) channels, was also used for the recognition of specific stages by direct cell observation or by counting nuclear totals. Merge contains superimposed Hoechst and GFP channels, with scale bars representing 5 µm. The adjacent diagram represents a simplified view of the respective images.

4.1.4 NEK1 Localisation in Activated Male Gametocytes

Strong NEK1 expression was observed throughout male endoreduplication, during which foci predominantly localised in the perinuclear space of the central nucleus (Figure 12). Initially, a single NEK1-GFP dot was observed dividing into two separate entities approximately two minutes post activation, before separating to opposite cell hemispheres. Atypical focal division was then observed up to ten minutes post activation, which culminated in the formation of approximately eight NEK1 foci in total, encircling the nucleus. This corresponds to the expected nuclear ploidy at this time, implicating NEK1 as an important component in the functioning of the MTOC, responsible for the manipulation of nuclear genomes. Additionally, atypical focal division corresponds to the previously discussed atypical division of the MTOC. NEK1 foci were not observed during male exflagellation, however, strong GFP staining was seen in the cytoplasm of these later stages (Figure 13). No visible foci were observed in male microgametes after flagellar egress. Expression of NEK1 in these stages was inconsistent, with three phenotypes being documented; strong anterior expression, weak anterior expression or no NEK1 expression at all. Due to the limited number of observed exflagellating males, no conclusion was made on the likely pattern of NEK1 at this time point. More images are required for an accurate understanding of observed results.

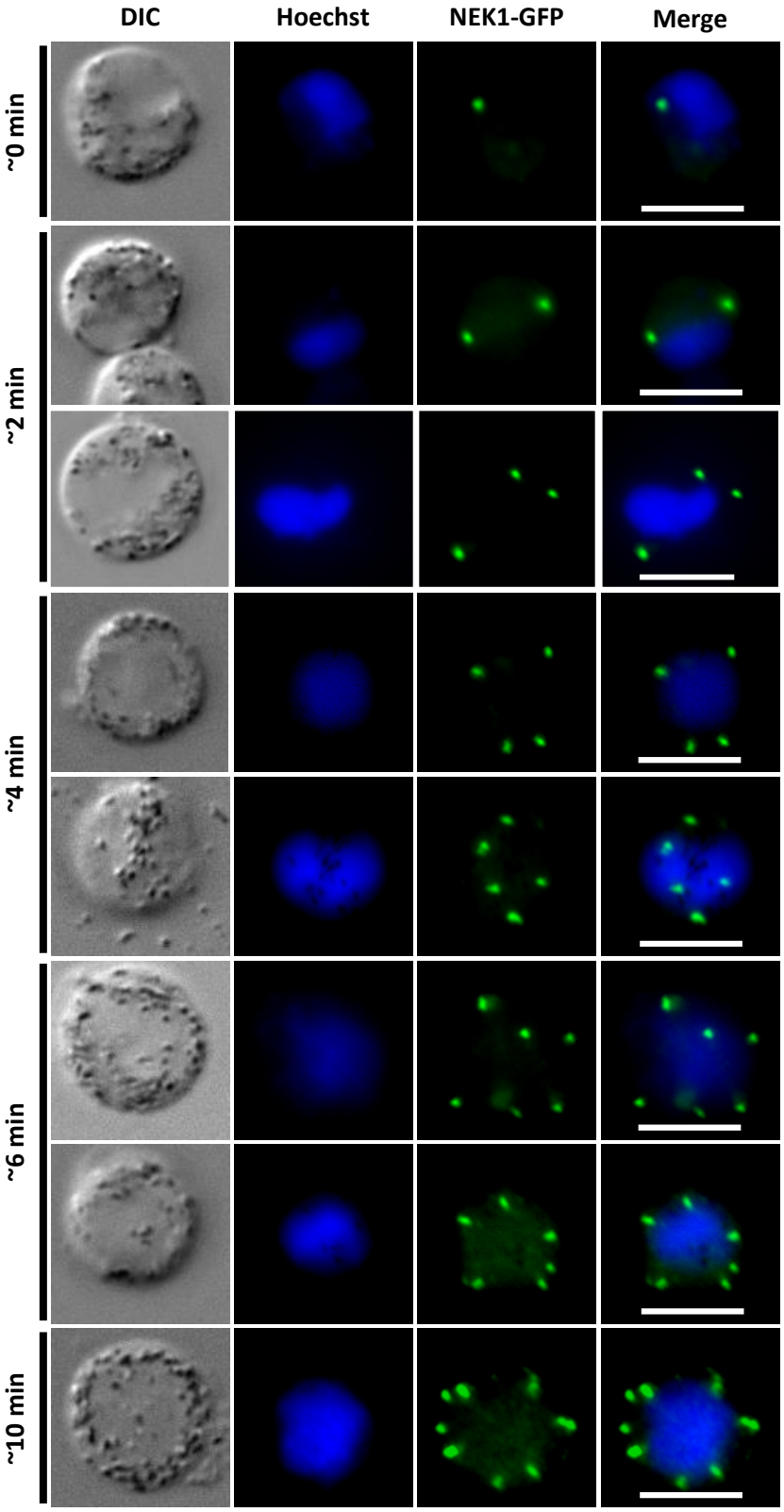


Figure 12 - Fluorescent microscopy of NEK1-GFP focal expression and localisation during male gametogenesis.

Male gametocytes were activated by the introduction of an ookinete media, which was mixed with the parasite directly on the slide. Observations of endoreduplication were observed within a 15-minute time window, with images being taken at minute intervals to document change in the parasite. Nuclei stained with Hoechst were used for the identification of the parasites and for the observations of NEK1 localisation relative to the nucleus. Merge comprises of Hoechst and NEK1-GFP channels, with additional scale bars representing 5 µm. Images of the male exflagellation process and the resultant microgametes are shown separately in Figure 13.

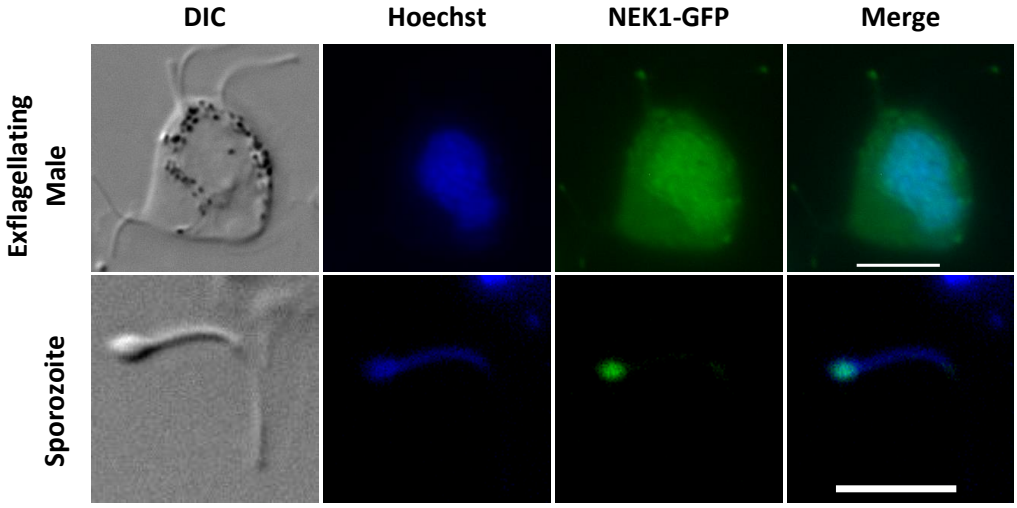


Figure 13 - NEK1-GFP expression in exflagellating males and the resultant flagella approximately ~15 minutes post activation, as seen using fluorescent microscopy.

Ookinete media containing Hoechst was used for male activation and nuclear staining. Merge comprises of the Hoechst and NEK1-GFP channels, with additional scale bars representing 5 µm. Few examples of the final stages of this process were obtained and thus more are required to understand the patterns of NEK1 expression in exflagellating males and the subsequent male microgametes.

4.1.5 NEK1 Localisation in Ookinete Stages

In contrast to male cells, no NEK1-GFP was observed in female gametes (Figure 14A), however, NEK1 foci were observed in a small subset of zygotes (Figure 14B). The number of cells displaying this phenotype was relatively small, albeit consistent, with NEK1 localising at the surface of the nucleus in examples where protein expression was reported. Interestingly, no NEK1 foci were detected in any of the subsequent stage I ookinetes, suggesting that the dot may have only been present in recently fertilised females, and subsequently degraded prior to the formation of said ookinete. NEK1 focal expression during the ookinete developmental stages was specific, only being observed at around 12.5 hours into ookinete development (Figure 15). Foci did not display any stage bias, with NEK1 expression being observed in Stage III and stage IV ookinetes, suggesting that NEK1 expression was not stage specific, however, more a factor of developmental time. Only a few examples of these specific stages were observed, thus

only a few examples of this NEK1 expression could be seen, however, during this process NEK1 foci were reported dividing in a similar manner to the foci observed during male gametogenesis. NEK1 expression at this time likely corresponds to the process of meiosis, in which diploid ookinetes developed into tetraploid mature stages prior to the formation of the oocyst on the midgut exterior. More examples of NEK1 expression in zygotes and ookinetes are required for an accurate conclusion.

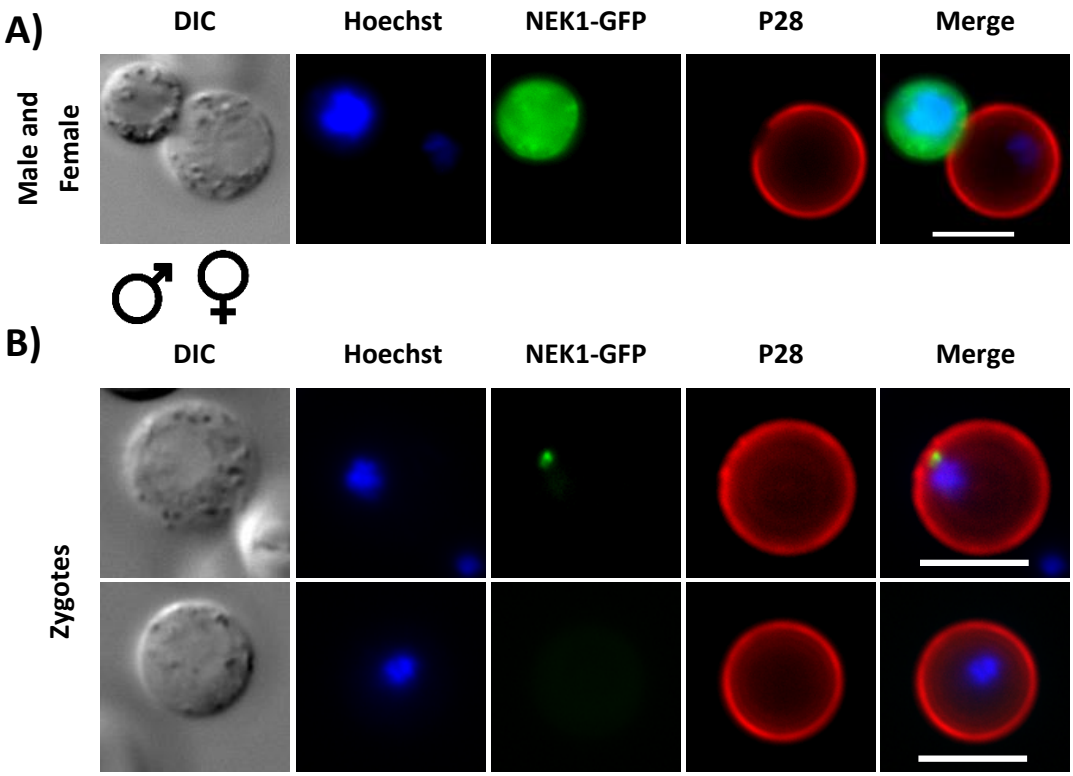


Figure 14 - NEK1-GFP expression in males compared to female gametocytes and the two zygote phenotypes observed.

Gamete activation and the subsequent fertilisation of females to form zygotes was achieved using an ookinete media containing Hoechst for nuclear staining. Cy3-conjugated P28 antibodies (red) were used to stain the P28 proteins specifically on female and zygote surfaces to aid in identification and observation of ookinete development. Merge comprises of the Hoechst, NEK1-GFP and P28 channels, with additional scale bars representing 5 μm.

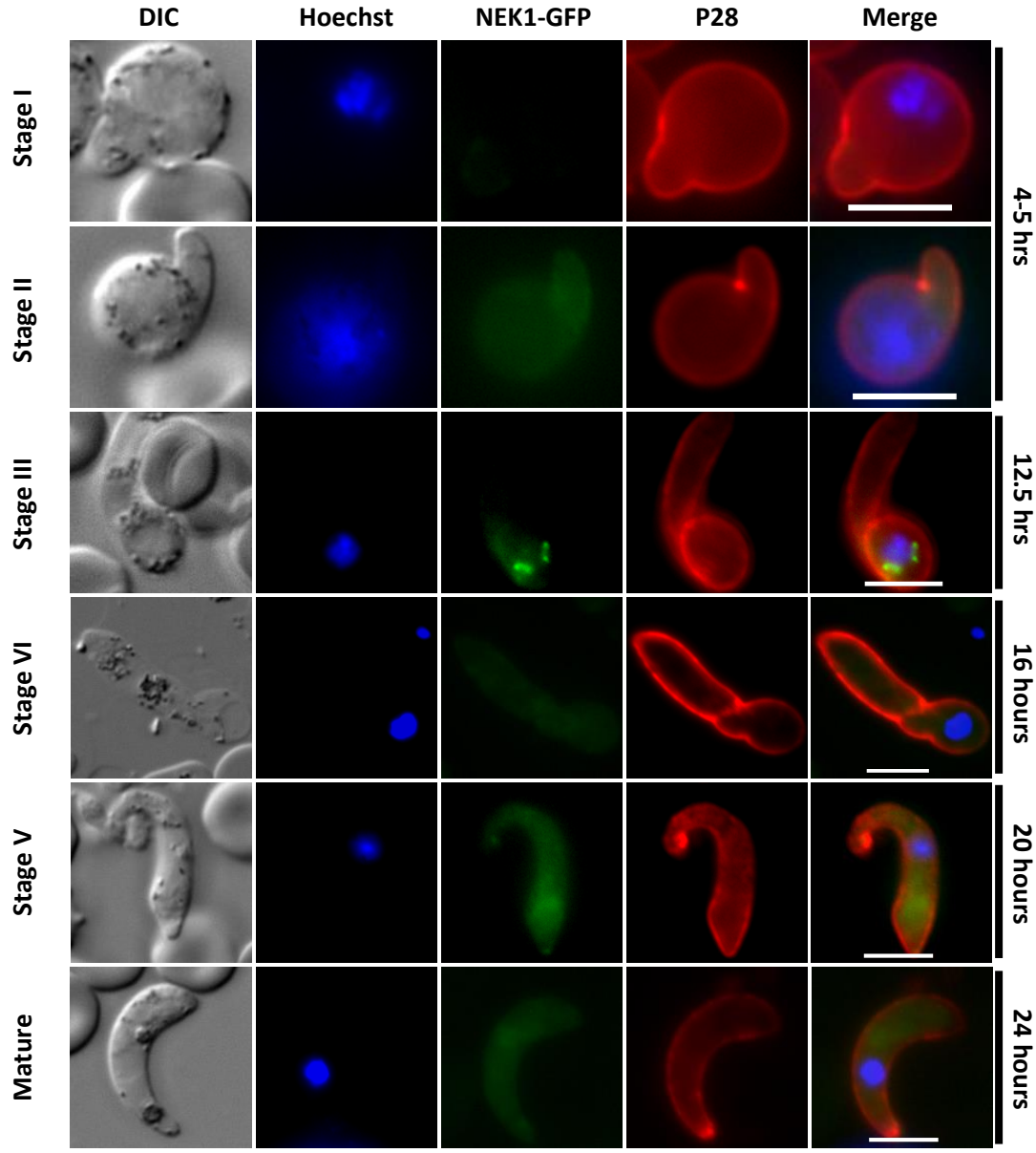


Figure 15 - NEK1-GFP expression during ookinete development.

Gamete activation and the subsequent fertilisation of females to form zygotes was achieved using an ookinete media containing Hoechst for nuclear staining. Samples were observed at predetermined time points over a 24-hour period to track ookinete progression over the six stages of development. Cy3-conjugated P28 antibodies were used to stain the P28 proteins specifically on ookinete surfaces to aid in identification and observation of development. Merge comprises of the Hoechst, NEK1-GFP and P28 channels, with additional scale bars representing 5 μm.

4.2 NEK1 Localises at Centriole-related Structures During Schizogony and Male Gametogenesis

To give credence to the previously implicated role of NEK1 in MTOC functioning, and to better define the location of NEK1 foci in relation to pre-established cellular structures, co-localisation studies using centrin and α-tubulin markers were carried out. This was achieved using immunofluorescence assay procedures with antibodies against NEK1, centrin (Cen-2) and α-tubulin. Samples were fixed at desired time points, and incubated with the appropriate antibodies to first bind to the proteins and provide the foundations on which the fluorescent antibodies could attach. Fluorescent microscopy was then used to observe the slides. NEK1 localisation was observed between centrin and α-tubulin markers in schizonts and male gametocytes respectively, however, no localisation was seen between α-tubulin and NEK1 during schizogony.

4.2.1 NEK1 Localises with Centrin-2 Markers

NEK1 proteins were not observed fully co-localising with centrin markers during asexual schizogony, however, in all instances NEK1 foci adjoined centrin dots and formed very close complexes (Figure 16A). Neither foci were observed in the absence of the other, with both maintaining a similar pattern of expression across the different stages, notably absent in ring, trophozoite and mature schizonts. Due to the inconsistency of observed examples, the exact location of NEK1 relative to centrin and the nucleus was not determined. However, centrin and NEK1 complexes were observed undergoing a distinct sequence of division prior to nuclear karyokinesis. The most recurrent NEK1:centrin arrangement observed was a 1:1 ratio of the respective foci (Figure 16B), with 1:2 configurations being the second most recorded. Observed 2:1 ratios of NEK1 and centrin were highly infrequent and were likely miscounts of unclear foci.

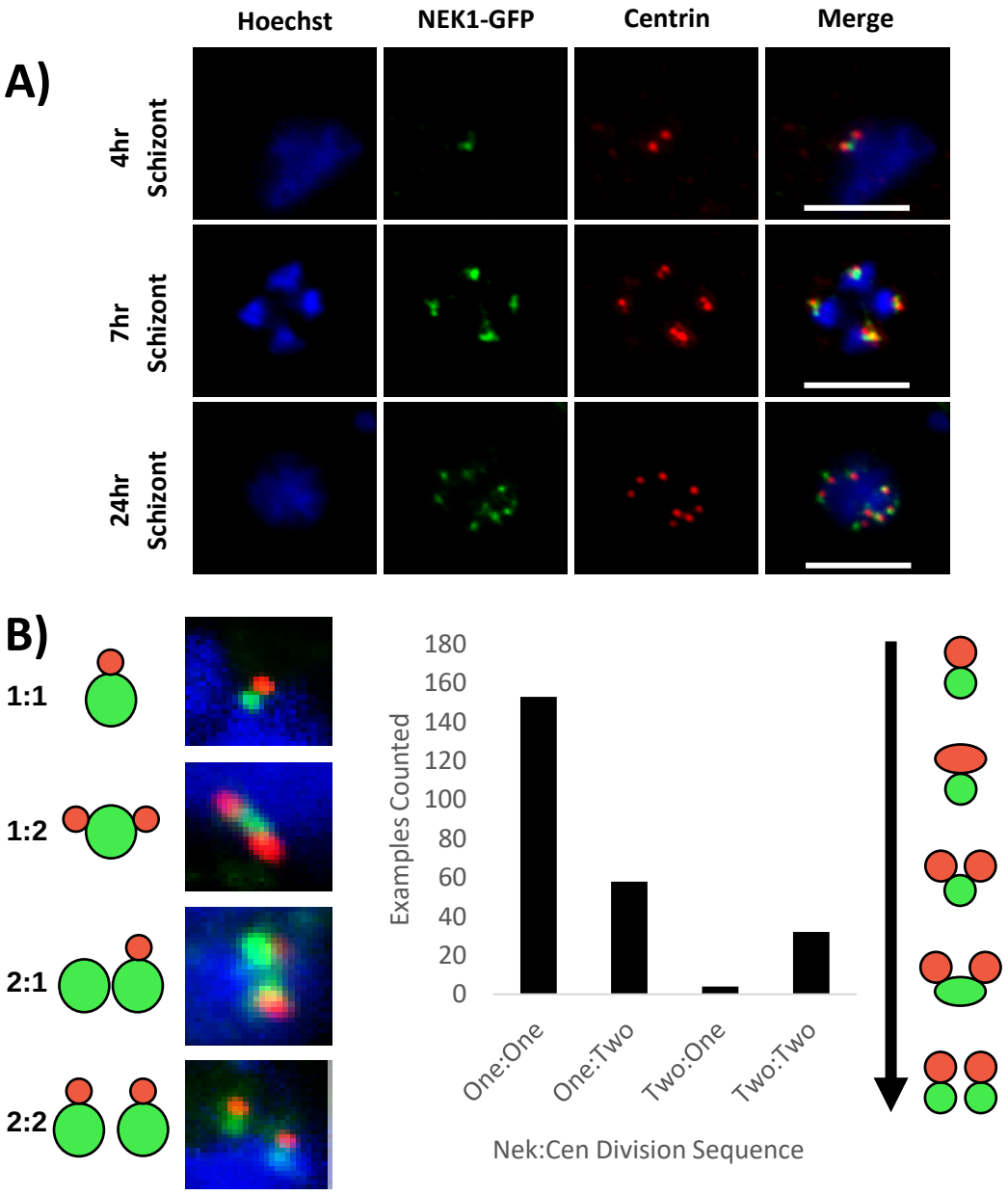


Figure 16 - Localisation studies using NEK1-GFP with centrin markers in fixed IFA blood stage schizonts.

Parasites were incubated in a schizont media, with samples being withdrawn at desired time points and fixed on slides for their preservation prior to the IFA procedure. **A)** Immunofluorescence assays were undertaken using centrin markers to assess the relationship between NEK1 and MTOC structures during early, mid and late schizogony. Hoechst was used for the observation of the nuclei relative to the proteins. Centrin markers used 588 mouse antibodies (red) for staining. Merge comprises of Hoechst, NEK1 and centrin channels, with 5 µm scale bars. **B)** Focal arrangements were categorised into the four groups predominantly observed in the samples (1:1, 1:2, 2:1 and 2:2) and were counted in 30 fields of view at 60x magnification. A simplified view of the NEK1:centrin sequence of division is present to the right of the graph, with the arrow indicating the direction of the process.

Centrin foci thus took primacy during division, demonstrating a sequence reminiscent of the previously described NEK1/nuclei association in asexual parasites (Figure 11). Centrin dots divided into two separate entities before the division of NEK1, resulting in 2:1 focal ratio. The division of NEK1 (2:2) and separation of these complexes resulted in the reestablishment of the original 1:1 configuration. As centrin represents the *Plasmodium* MTOC, the results suggest a strong association between NEK1 and this organelle during schizogony.

4.2.2 NEK1 Partially Colocalises with α-tubulin During the Dividing Stages of Gametogony, However, not Schizogony

In contrast to the localisation observed between centrin and NEK1, no localisation was observed in IFA samples using α-tubulin markers in asexual parasites (Figure 17). Mitotic spindles were clearly visible in the IFA samples, however, NEK1 foci were completely absent. Whilst this was expected in ring, trophozoite and mature stages, it had been previously demonstrated that strong NEK1 focal expression was evident in early and mid-stage schizonts (Figure 11). The absence of defined NEK1 foci suggests an error occurred during the IFA procedure. This was perhaps as a result of insufficient blocking procedures, excessive use of the rabbit 488 antibodies, or the insufficient cleaning of the wells after each incubation. Consequently, no direct patterns could be deduced from the results with regards to the localisation of NEK1 in relation to α-tubulin spindles. However, the close associations observed between the α-tubulin markers and the nuclei may be significant. Previously described patterns of NEK1 and centrin foci exposed a clear relationship between the two proteins, which localised to the periphery of the nuclei (Figure 16). It is therefore not implausible to suggest that successful NEK1 IFAs using α-tubulin markers would demonstrate a pattern of associations, reminiscent of that between the NEK1 foci and centrin, however, this is yet to be shown.

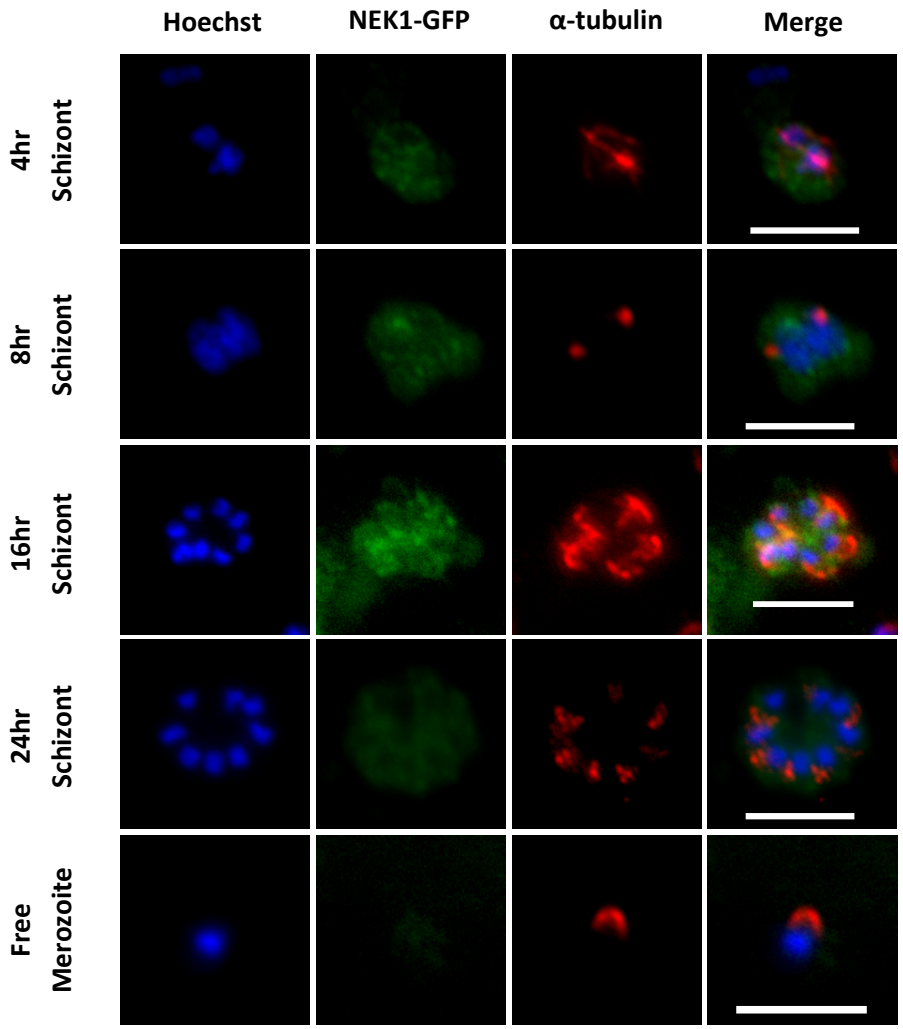


Figure 17 - Localisation studies using NEK1 and α-tubulin in fixed IFAs samples of blood stage schizonts.

Parasites were incubated in schizont media, with the withdrawal of samples occurring at the desired time points. Immunofluorescence assays were undertaken using α-tubulin markers to assess the relationship between NEK1 and mitotic spindles during early, mid and late schizogony. Hoechst staining was used for the observation of the nuclei relative to the proteins. α-tubulin markers used 588 mouse antibodies (red) for staining. Merge comprises of Hoechst, NEK1 and α-tubulin channels, with 5 µm scale bars.

Partial colocalization of NEK1 with α-tubulin was evident in male gametogenesis (Figure 18). NEK1 foci, in corroboration with their previously reported temporal patterns during endoreduplication (Figure 12), formed at the surface of the nucleus and proceeded to divide atypically. Initially, α-tubulin was distributed around the cellular periphery with no evidence of localisation, which was to be expected. After ~1.5 minutes, microtubules were observed extending across the cell, at which point NEK1 could be seen associated with their points of origin. The previously reported co-localisation between NEK1 and centrin benefits from these findings, as α-tubulin subunits (making up the mitotic spindles) are known to form at the MTOCs, just as NEK1 was observed doing during schizogony when it localised with centrin markers (Figure 16). By 8 minutes post activation, eight NEK1 foci were observed encircling the nucleus and associated with α-tubulin spindles, which at this point had formed cross structures spanning the lengths and widths of the cell. Interestingly, no localisation between the kinase and the axonemes, which are also made of α-tubulin subunits, was reported throughout the process, suggesting NEK1 is only associated with the mitotic spindles. Examples of exflagellating males were not observed, however, no NEK1 foci were observed during this process in previous observations (Figure 13), so regardless of whether α-tubulin markers could have been seen in this stage, no colocalization would have been evident.

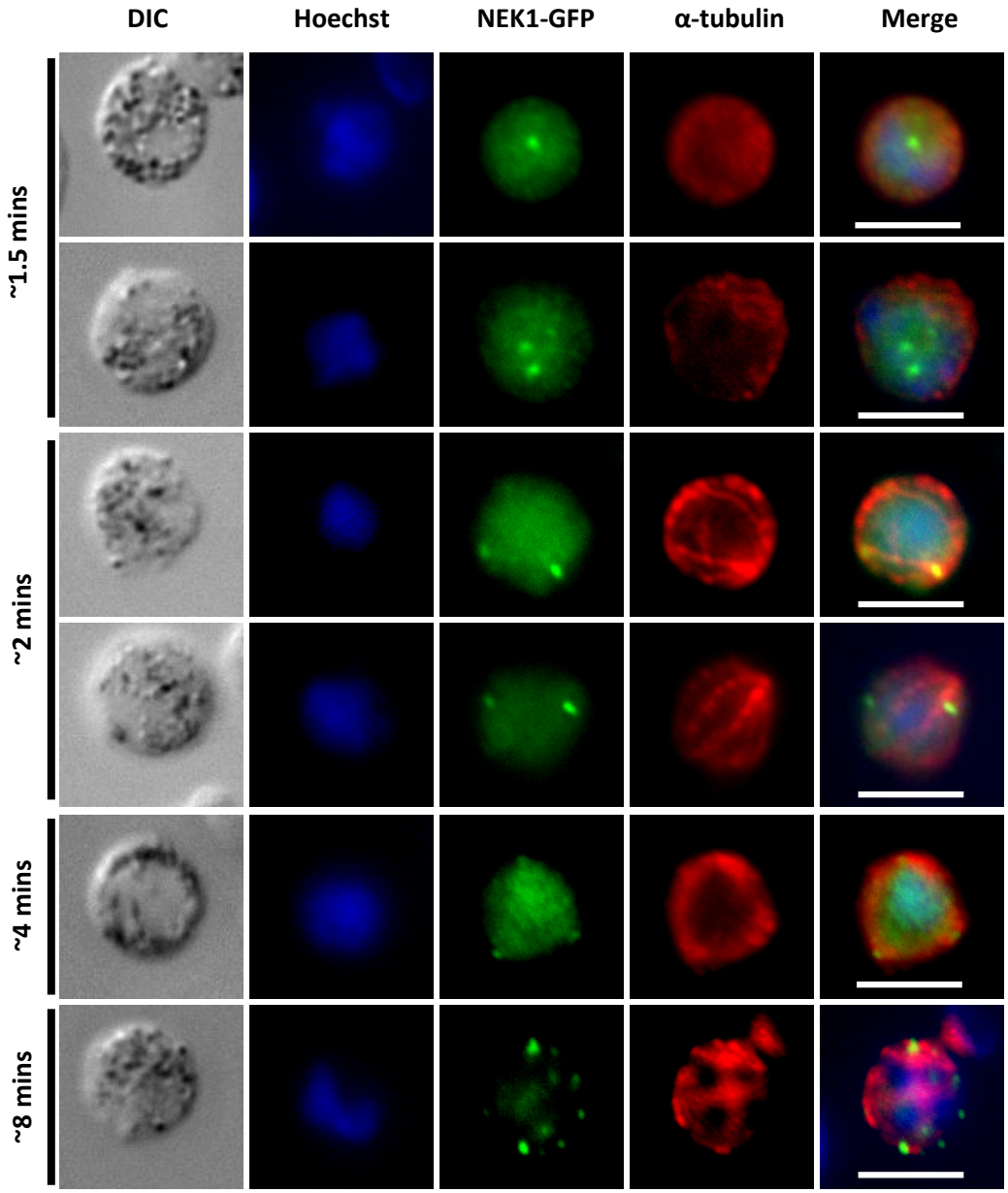


Figure 18 - Localisation studies using NEK1 and α-tubulin in fixed IFAs samples of activated male gametocytes.

Males were activated using an ookinete media and fixed at desired time points. Immunofluorescence assays were undertaken using α-tubulin markers to assess the relationship between NEK1 and mitotic spindles during male gametogenesis and exflagellation. Hoechst staining was used for the observation of the single nucleus relative to the proteins. α-tubulin markers used 588 mouse antibodies (red) for staining. Merge comprises of Hoechst, NEK1 and α-tubulin channels, with 5 µm scale bars. Images of later time points were not successfully observed.

4.2.3 NEK1 Localises with NDC80 and Shares a Similar Pattern of Focal Duplication During Genome Replication

Previous studies have identified NDC80 as a component of the *Plasmodium* outer kinetochores, which are known to attach to the centromeres during proliferation (Zeeshan et al., 2020). The reported localisation of NDC80 foci, corresponds to localisation of NEK1 foci previously demonstrated during blood stage schizogony (Figure 11). NDC80 foci form at the surface of the nuclei, and divide with respect to karyokinesis (Zeeshan et al., 2020). Patterns of NEK1 localisation relative to NDC80 could thus give a more accurate interpretation of the location of NEK1 relative to the MTOCs. Therefore, the spatio-temporal patterns of NEK1 relative to NDC80 during schizogony are shown here. Previously generated NDC80-mCherry parasite lines were selected for use in a cross with NEK1-GFP parasites in order to form a transgenic line expressing both fluorescent proteins. This inferred a significant benefit over IFA procedures, which was the ability to use live cell imaging to track the progression of the two proteins relative to each other throughout the proliferative stages.

The observed interactions between NEK1 and NDC80 were similar to those previously reported between NEK1 and centrin during blood stage schizogony (Figure 16). No complete colocalization was observed between NEK1 and NDC80, however, in all instances, NEK1 foci were observed adjacent to the kinetochore proteins with each nucleus inheriting a single NEK1 and NDC80 dot after karyokinesis (Figure 19). It was inferred from the images that NEK1 divided prior to the division of the NDC80 foci, as was to be expected considering NEK1 has been shown to be associated with the MTOCs which divide prior to the centromeres. Whilst NDC80 foci persisted throughout schizogony, NEK1 proteins were diffused in later stages, however, an association between both proteins was evident throughout the entire time NEK1 foci were visible.

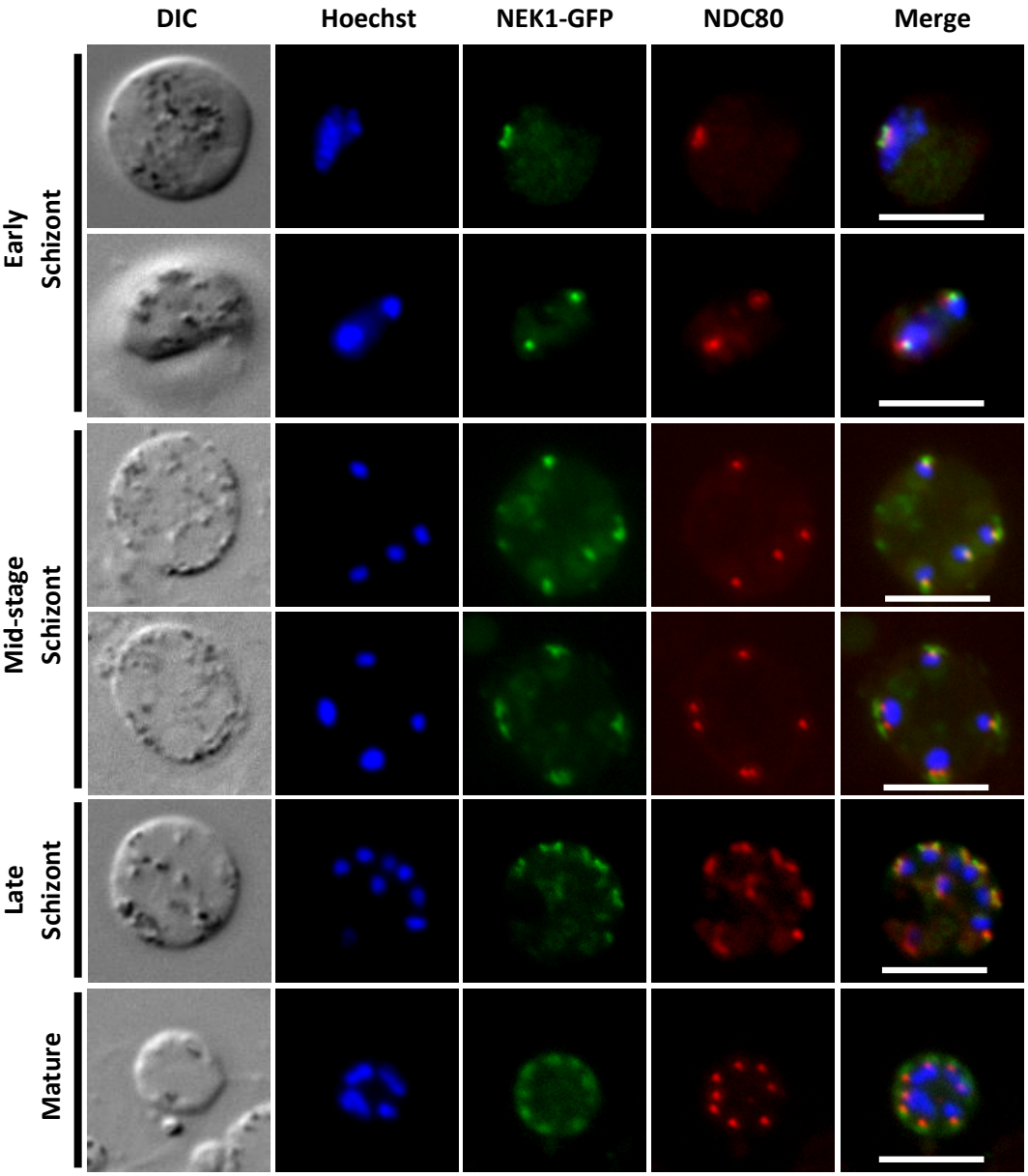


Figure 19 - Spatio-temporal patterns of NEK1-GFP relative to NDC80-mCherry proteins in live imaged cells.

A previously generated NDC80-mCherry (red) parasite line was crossed with the existing NEK1-GFP line to produce parasites expressing both GFP and mCherry fluorescent proteins for use in live cell imaging analyses. Hoechst and DIC channels were used for parasite and specific stage recognition. Merge consists of Hoechst, GFP and NDC80-mCherry channels with scale bars representing 5 µm.

Importantly, NEK1 foci were formed on the outside of NDC80 foci, and thus furthest from the nucleus, which was to be expected as the association of NDC80 with the centromeres would place them at the end of the α-tubulin mitotic spindles, and thus closest to the genomic material compared to the MTOC and thus NEK1.

Further investigation sought to use cross over techniques using NEK1 with other known *Plasmodium* proteins implicated in blood and mosquito stage proliferation. Attempts to cross NEK1-GFP with ARK2-mCherry, a kinase yet to be visualised in *Plasmodium*, kinesin-8B, a motor flagellar associated protein, and SAS4, a basal body protein, were attempted. ARK2 into NEK1 parasite lines, although initially successful, did not survive long enough to study localisation patterns, and kinesin-8B cross over attempts were in progress, however, put on hold due to the COVID-19 pandemic.

4.3 Proteomic Analysis Reveals a Large Number of Interactive Partnerships Between NEK1 and other Proteins Implicated in Cell Division and Axonemal Functioning

As a kinase implicated in the phosphorylation of the *Plasmodium* MTOC and its associated proteins, it is likely that NEK1 undergoes many protein-protein interactions. To investigate the possible interacting partners of NEK1, an immunoprecipitation assay was performed on activated male gametocytes prior to mass spectrometry. Male gametocytes were activated for 1.5 minutes in an Ookinete media and purified into pellets, before they were cross-linked by subjecting them to two incubations, the first in 37% formaldehyde and the second in 0.125 M glycine, both in PBS. Samples then underwent two consecutive washing steps in PBS. Immunoprecipitation was carried out using a GFP-Trap® A kit (Chromotek) as per the manufacturer's instructions. Briefly, the lysates were resuspended in lysis buffer with the addition of 1x protease inhibiter, before undergoing sonication. Beads were washed in dilution buffer with 20 µl added to each sample, which were then tumbled for 4 hours at 2°C. Beads were washed again in dilution

buffer with supernatant discarded. Completed samples were sent to Dr Andrew Bottrill and colleagues at The University of Warwick for MS. WT-GFP was used as a control in the MS, however, the Table below (Table 10) only presents the pulldown results from the NEK1-GFP samples.

4.3.1 NEK1 Interacts with a Number of Motor Proteins During Male Gametogenesis

The MS results revealed a number of conserved proteins interacting with NEK1 in male gametocytes, namely a large repertoire associated with the microtubules (Table 10). In total, eight dynein proteins were present, of which five were heavy chains with the remaining three consisting of two intermediate and a single β chain. Further microtubule associated proteins included the radial spoke protein 9 and the flagellar outer arm dynein-associated protein, structural components of the microtubule axoneme. Interestingly, the Armadillo-repeat protein was reported in addition to kinesin-8B and CDPK1, shifting the presumed role of NEK1 from MTOC dynamics to exflagellation and flagellar activity. Previous localisation studies reported a close association between NEK1 and centrin (Figure 16) which was further confirmed by the MS results, with centrin-1 and -2 proteins being present. Both proteins are components of the *Plasmodium's* basal bodies, in addition to the MTOCs. This is suggestive of a dual role of the kinase during male endoreduplication and succeeding exflagellation, however, this will be studied in greater depth later. Additionally, SRPK1 and Importin-7 were identified, the roles of which with regards to NEK1 will need to be studied in depth. A number of interactors were ejected from the table, including 13 conserved proteins of unknown function and 5 WD repeat containing-proteins (Appendix D).

It should be noted that only one MS procedure was successfully carried out, with the other attempt failing as a result of an unintentionally high concentration of schizonts present in the sample. Due to the COVID-19 pandemic, not enough time was available to repeat the

experiment to produce more reliable results. As such, the results should be considered preliminary until such time as more data is available for cross referencing.

Table 10 – Mass spectrometry results of NEK1-GFP in male gametocytes.

A protein pull-down involving cross-linking and lysis steps produced GFP-Trap beads containing NEK1 and its associated interacting partners, which was sent off for mass spectrometry analysis. Results are ordered by peptides from highest to lowest. Some results were ejected from the table on the grounds of not being relevant to endomitosis, including 13 conserved proteins of unknown function in addition to 5 WD repeat-containing proteins. Another MS is required to confidentially confirm and increase the reliability of the present results.

Accession Number	Identified Proteins	Molecular Weight	Peptides
PBANKA_1443000	NIMA related kinase 1, putative	108 kDa	32
PBANKA_0507300	Dynein heavy chain, putative	624 kDa	30
PBANKA_0416100	Dynein heavy chain, putative	685 kDa	27
PBANKA_0925400	Dynein heavy chain, putative	605 kDa	24
PBANKA_1405000	MORN repeat protein, putative	150 kDa	13
PBANKA_0202700	Kinesin-8B, putative	169 kDa	11
PBANKA_0917400	Armadillo-repeat protein PF16	58 kDa	9
PBANKA_0601200	Dynein heavy chain, putative	666 kDa	7
PBANKA_1329200	Dynein beta chain, putative	766 kDa	7
PBANKA_1310400	Centrin-2, putative	19 kDa	6
PBANKA_1018300	Dynein intermediate chain, putative	70 kDa	6
PBANKA_0615700	Dynein heavy chain, putative	623 kDa	6
PBANKA_1458800	Kinesin, putative	165 kDa	6
PBANKA_1431500	Radial spoke head protein 9, putative	42 kDa	5
PBANKA_0822900	Dynein intermediate chain, putative	94 kDa	5
PBANKA_0314200	Calcium-dependent protein kinase 1	61 kDa	4
PBANKA_0401100	Serine/threonine protein kinase, putative	154 kDa	4
PBANKA_0803600	Importin-7, putative	144 kDa	3
PBANKA_0206300	Centrin-1, putative	20 kDa	3
PBANKA_0504300	Flagellar outer arm dynein-associated protein, putative	12 kDa	3

4.4 Functional Analysis of NEK1 Implicates it as an Essential Kinases for *Plasmodium* Sexual Development

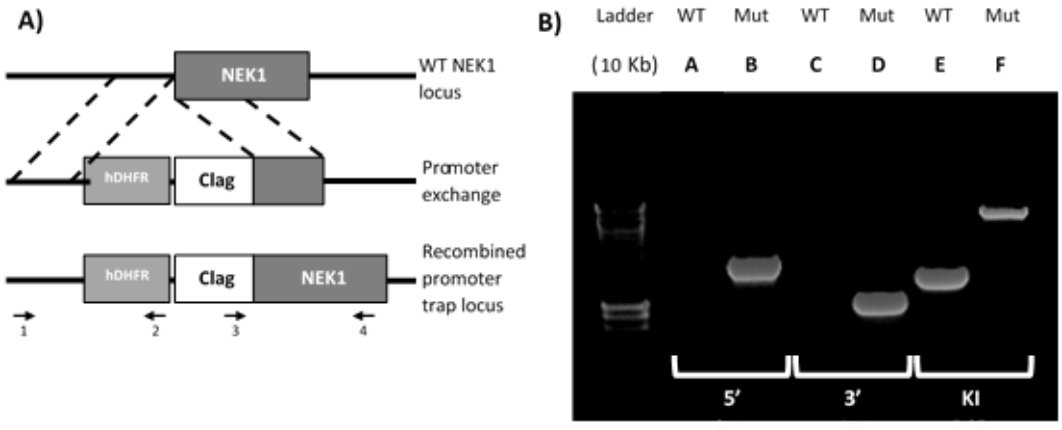
4.4.1 Analysis of NEK1 Function in Gametogenesis and Ookinete Formation

The function of NEK1 in the proliferative stages was identified using a conditional knockdown construct placed upstream of the NEK1 locus and thus in charge of its expression. The need to undertake such an approach was governed by the non-redundant nature of NEK1, previously described in the asexual stages of parasite proliferation. Therefore, this method was adopted in order to promote NEK1 transcription during asexual development, so that the parasite might progress into sexual maturity, yet circumvent any such transcription of the kinase during sexual proliferation. Such a technique works off of the basis that Clag1 (cytoadherence linked asexual gene) is only present in asexual parasites (Sebastian et al., 2012), thus allowing for the promotion of NEK1clag transcription specific to these stages. Consequently, the absence of Clag1 in the mosquito stages prevents the promotion of NEK1 transcription. Through the observation of cell viability in the absence of NEK1, the possible roles of the kinase can be deduced and potentially applied to other proliferative stages.

4.4.2 Confirmation of Clag1 Integration into the NEK1 Gene for use in Conditional Knockdown

NEK1clag parasite lines had previously been generated in the lab by double homologous recombination (see Table 9 for primers). Successful integration had been confirmed at the time of their generation; however, a diagnostic PCR was repeated on the isolated gDNA of asexual NEK1clag parasites (extracted from frozen blood aliquots) to confirm the sample contained the desired PTD tagged NEK1 locus before committing to its use (Figure 20). The 5' end integration was confirmed using 5' IntPtD014 and 5' IntRV primers, which bind upstream of the construct and inside of the hDHFR selectable marker respectively, the latter region not being present in the WT. The 3' end integration was confirmed using

3’ IntClag and 3’ IntPTD014 primers, which bind in the clag1 and NEK1 respectively, the former not being present in the WT. Gene knock-in confirmation used 5’ IntPTD014 and 3’ IntPTD014 primers. Both binding sites are present in WT and NEK1clag DNA, however, as the latter construct contains hDHFR, the clag1 promoter trap and NEK1, it is heavier than the WT thus explaining its position in the gel-electrophoresis relative to the rest. A qRT-PCR was used to determine whether successful downregulation of NEK1 had been achieved in the NEK1clag gametocytes, relative to the NEK1clag schizonts, and the equivalent WT gametocytes.



C)

gDNA	Forward primer	Reverse primer	Binding sites
WT (A)	5' IntPTD014	5' IntRv	1+2
NEK1clag (B)	5' IntPTD014	5' IntRv	1+2
WT (C)	3' IntClag	3' IntPTD014	3+4
NEK1clag (D)	3' IntClag	3' IntPTD014	3+4
WT (E)	5' IntPTD014	3' IntPTD014	1+4
NEK1clag (F)	5' IntPTD014	3' IntPTD014	1+4

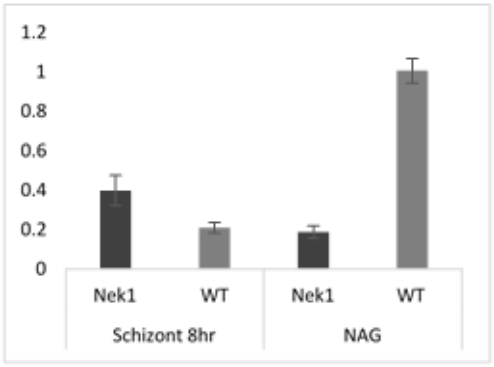


Figure 20 - Genotypic analysis of NEK1clag genes to confirm successful integration.

A) Schematic representation of the double homologous recombination procedure used to insert the NEK1 locus downstream and under the control of a clag1 promoter trap. The numbers below the recombined promoter trap locus represent the binding sites for the primers used in the diagnostic PCR. **B)** Gel-electrophoresis of the diagnostic PCR. Primer 1 (5' IntPTD014) and primer 2 (5' IntRv) bind at the regions labelled 1 and 2 on the schematic respectively, and were used to confirm the integration of the selectable marker (hDHFR). Primer 2 failed to bind to WT gDNA as the marker was not present, preventing amplification and thus a resultant band in the WT (A) lane. Primer 3 (3' IntClag) and primer 4 (3' IntPTD014) bind at 3 and 4 respectively, and were used to determine whether the clag1 promoter trap had integrated into the NEK1 locus. WT lacks this promoter trap, and so primer 3 was unable to bind to the gDNA, resulting in an absent band in the WT (C) lane. Primer 1 and primer 4 were used to determine gene knock-in. Primer 1 was able to bind upstream and inside of the NEK1 WT locus, and so a band was present in the WT (E) lane. The band in the mutant (F) lane was much heavier as the region between site 1 and 4 in the NEK1clag locus contained the hDHFR cassette, promoter trap and the NEK1 gene itself. **C)** Table containing all the primers used and their binding sites. **D)** qRT- PCR demonstrating the downregulation of NEK1 in NEK1clag parasites compared to WT non-activated gametocytes. There was no downregulation of NEK1 in NEK1clag schizonts grown for 8 hours.

4.4.3 Nek1 is Essential for the Progression of the Sexual Stages

To determine the importance of NEK1 in the sexual stages of *P. berghei*, observations of NEK1clag and wild-type control parasites were made from the onset of male exflagellation to oocyst formation using live cell microscopy in order to track progress. In addition, ookinete and oocyst counts were undertaken to assess the impact of the formation of these stages in the absence of NEK1. To achieve this, ookinete stages were categorised into either non-mature (stage V and below) or mature cells, with the intention of observing the difference in conversion from non-mature to mature ookinetes in NEK1clag compared to WT. Additionally, oocyst counts involved the extraction and observation of the mosquito midguts at day 7 and day 21 of oocyst development, in order to count the number of cells present for WT and NEK1clag respectively. Light microscopy was used to observe the number of exflagellating males for both parasites. Exflagellation centres, rosette structures formed by the association of emerging microgametes with surrounding cells, were counted as a single exflagellating male, due to the difficulty of resolving the individuals within the cluster under the light microscope. Finally, qRT-PCR analyses using RNA isolated from non-activated NEK1clag and WT gametocytes were used to assess the impact of downregulated NEK1 on various other pre-established proteins involved in gametocyte proliferation. These consisted of NEK2, NEK3, CDPK4, SRPK1, MAPk2, SAS6, kinesin-8B and ARK2.

4.4.4 NEK1 is Essential for Male Exflagellation

No male exflagellation was observed in the NEK1clag parasites, in contrast to 123 observed in the WT (Figure 21). Due to the previously implicated role of NEK1 in male endoreduplication, and the above-mentioned patterns of NEK1 localisation with the suspected MTOCs in male gametocytes (Figure 12), it was expected that the downregulation of the protein would prevent male exflagellation. Whilst the preliminary observations made using the light microscope confirmed this result with zero examples

recorded, subsequent observations using fluorescent microscopy confirmed the presence of male flagella in NEK1clag samples, albeit in observably lower frequencies compared to WT. Further evidence for male exflagellation in NEK1clag was provided by the observation of zygote stages, evidently formed by the fusing of male microgametes with female macrogametes, which will be discussed further. As a result, the counts made using the light microscope were not representative of all NEK1clag samples.

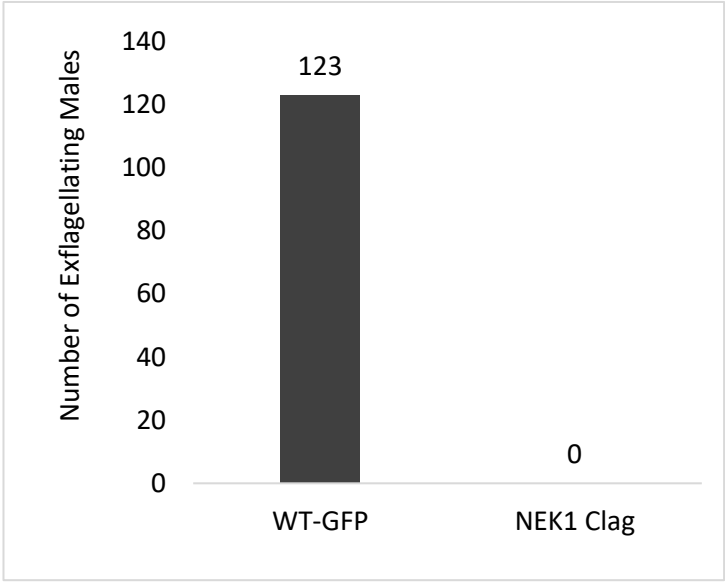


Figure 21 - Number of NEK1clag and WT exflagellating males observed after activation.

Males were activated by the addition of an ookinete media directly to the slide. Counts were made using a light microscope at 40x magnification. Free flagella were not counted, only those cells that were visibly undergoing exflagellation, or in clusters known as exflagellating centres were acknowledged. The results collected were preliminary and thus inaccurate, which was compounded by the confirmation of NEK1clag flagella using fluorescent microscopy.

Further analyses with regards to the impact of NEK1clag on male exflagellation, are required before solid conclusions can be drawn. It would be insightful to observe the process of exflagellation in NEK1clag males, to identify possible defects in microgamete egression. Furthermore, observations of the resultant flagella would serve to elucidate whether NEK1clag examples differ in morphology and motility compared to their WT

counterparts. However, it can be deduced that the downregulation of NEK1clag in the mutant parasites, did significantly reduce male exflagellation.

4.4.5 No Ookinete Development was observed in NEK1clag Parasites

A significant reduction in the number of mature ookinetes was observed between WT and NEK1clag parasites (Figure 22A). Of the 217 observed WT ookinetes, 119 had matured to stage VI after 24 hours of development, with the remaining 90 parasites existing as a combination of stage III, IV and V (55% conversion). In contrast to this, of the 145 NEK1clag examples observed after 24 hours, 143 had failed to develop into mature ookinetes, remaining as either unfertilised females or non-mature stages (1.4% conversion) (Figure 22B). Due to their similar morphology, the number of females compared to zygotes was difficult to determine, both being stained with Cy3-conjugated P28 antibodies, however, it is likely that most were the former due to the lack of any previously observed male exflagellation. Regardless of this, no such difficultly was encountered in the identification of stage I ookinetes, which were easily distinguishable, and served as evidence of exflagellation in NEK1clag parasites. No visual deformities were recorded in the NEK1clag zygotes or stage I parasites, however, all stage I ookinetes appeared to have arrested early in their development. This was evidenced by the fact that none of the stage I's possessed large projecting membranes from which the "banana" shaped ookinete would subsequently develop from, instead only being observed with a small protrusion as seen in Figure 22B. The two supposedly mature ookinete stages observed, whilst possessing the long bodies associated with mature ookinete morphology, did not completely resemble their WT equivalents. It is possible that these were miscounts of Cy3 antibody artifacts, or perhaps malformed and amalgamated ookinete stages.

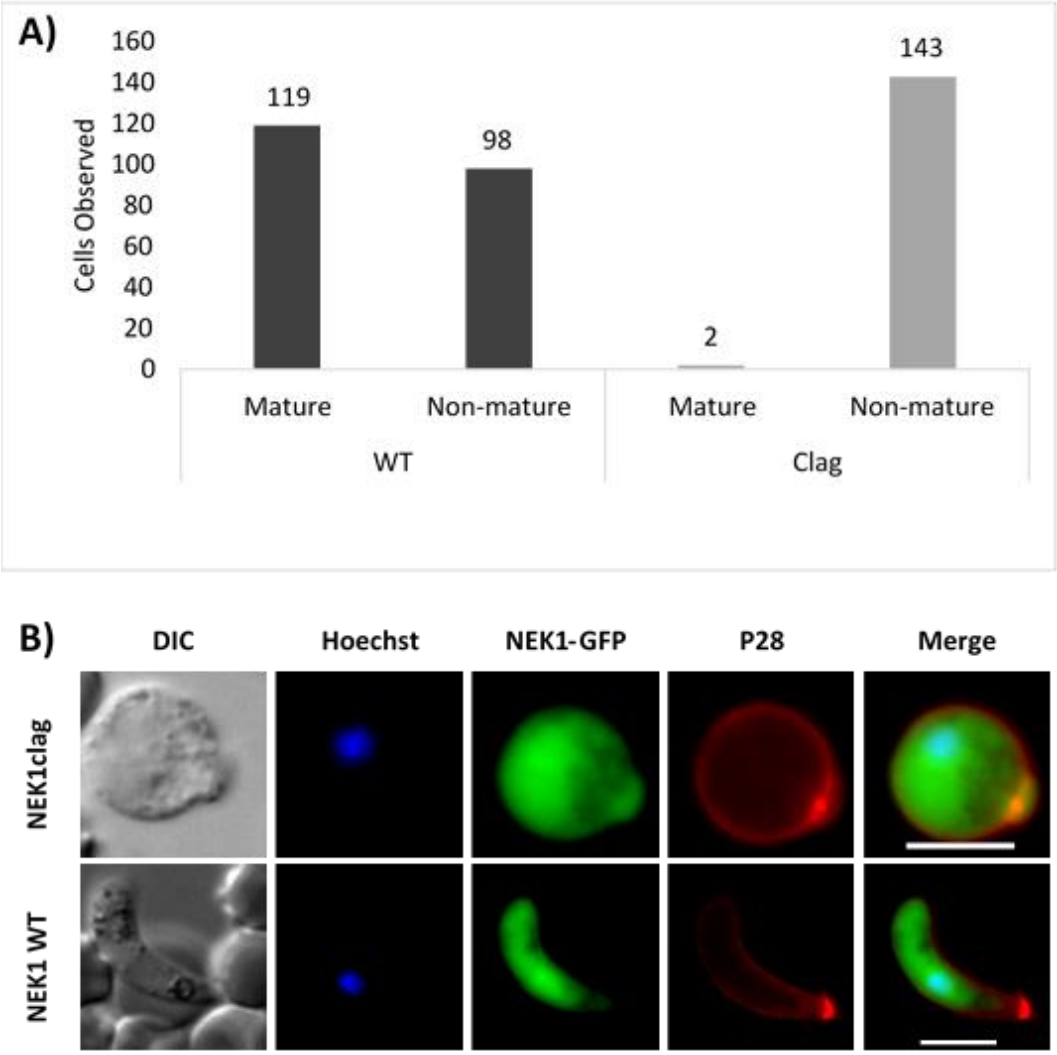


Figure 22 - NEK1clag and WT ookinete development and phenotypic analysis.

A) Wild-type and NEK1clag ookinetes were categorised as either non-mature (stage V and below) or mature ookinetes and subsequently counted at 60x magnification in 30 fields of view. Observations were made using fluorescent microscopy with Cy3-conjugated P28 antibodies and Hoechst to identify ookinetes and classify specific stages according to cell morphology. **B)** Images of the most commonly observed WT and NEK1clag ookinete stage after 24 hours of development. Merge contains the Hoechst, NEK1-GFP and Cy3-conjugated P28 antibody channels, with scale bars representing 5 µm.

4.4.6 No Oocyst Formation was Observed in NEK1clag Parasites

Concurrent with the previous observations of mutant ookinete development, no NEK1clag oocysts were observed after 7 and 21 days of in vitro development (Figure 23). In contrast, 350 and 121 WT oocysts were counted at day 7 and day 21 respectively. Most of the mutant ookinetes did not progress beyond stage I, and thus did not develop into motile stages capable of the relocation and implantation into the midgut exterior wall, required for oocyst formation. The large decline in WT oocysts observed between days 7

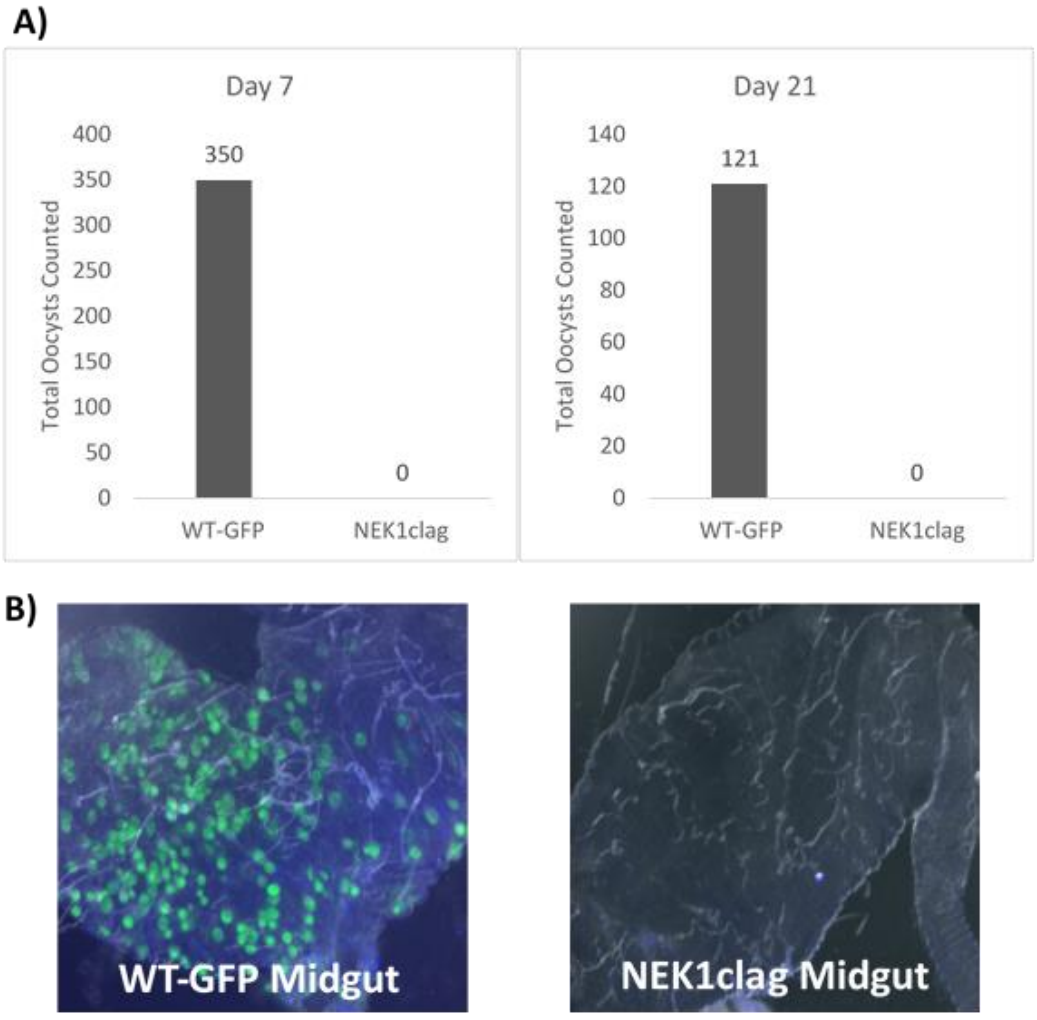


Figure 23 - NEK1clag and WT oocyst development.

A) Oocyst counts at day 7 and day 21 of development inside mosquito host. Midguts were extracted and analysed using fluorescent microscopy whereupon totals were counted. **B)** Side-by-side comparison of day 21 observations of WT and NEK1clag oocysts inside mosquito midguts. No oocysts were observed in any of the NEK1clag midguts, with those in the WT appearing healthy.

and 21 was as a result of the natural variation in parasitaemia between different mosquito samples, and the bottleneck nature of *Plasmodium* oocyst development due to high parasite mortality caused by the mosquito's immune defences.

4.4.7 NEK1 may act as an Upstream Regulator of MAPk2

In the three qRT-PCR tests, NEK1clag expression was successfully downregulated in the mutant non-activated gametocytes (NAGs), compared to that of the WT (Figure 24). No significant difference was observed in the expression of NEK2, however, NEK3 expression was subject to a large standard deviation (Figure 24A). No previous research has implicated NEK1 as an upstream regulator of the other NIMA-related kinases in *Plasmodium*, so it is unlikely that NEK1clag was responsible for this result. Regardless of this, a repeat of the NEK3 result is still required to increase the overall reliability of the qRT-PCR analysis. In addition, no difference in CDPK4, SRPK1, SAS6, kinesin-8B or ARK2 expression was observed in the NEK1clag NAGs (Figure 22B+22C). In contrast however, a significant reduction of MAPk2 expression was observed between the NEK1clag and the WT ($t=.0373$, $p= .05$) (Figure 24C). This confirmed the previously suggested role of NEK1 as an upstream regulator of MAPk2 proteins, as demonstrated by Dorin-Semblat et al. (2011). The subsequent downregulation of NEK1clag thus impacted the transcription and expression of the MAPk2 protein.

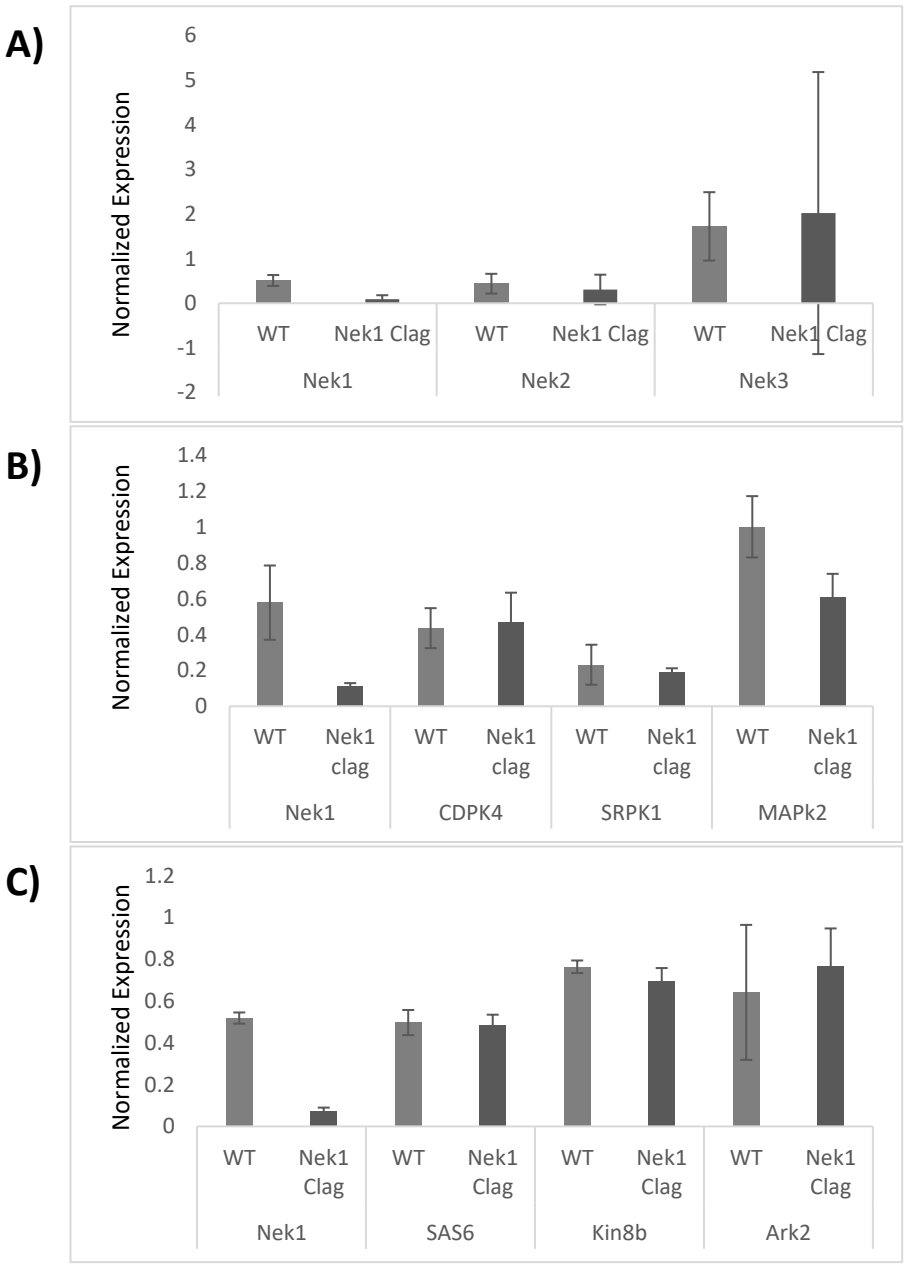


Figure 24 - Normalized expression of cDNA encoding proteins implicated in male gametogenesis, in the presence or absence of NEK1 wild-type and NEK1clag respectively.

Expression of transcript was examined by qRT-PCR tests on RNA extracted from WT-GFP and NEK1clag non-activated male gametocytes, with amplification being measured using SYBR green dye. Expression is normalised using Arginine-tRNA and HSP70 control genes with standard deviation error bars. MAPk2 expression was significantly reduced in NEK1clag NAGs compared to that of WT (t=.0373, p=.05).

5.0 Discussion

The mammalian NIMA-related Kinases represent a family of 11 proteins concerned with a number of cellular processes ranging from mitotic regulation, axonemal maintenance and DDR (Fry et al., 2012; O'Regan et al., 2007). Defects in these mechanisms are known contributors to human disease, which has resulted in a heightened interested in the NEK proteins, especially those concerned with various cancers (Peres de Oliveira et al., 2020). In comparison to what is known of mammalian NEKs, the *Plasmodium* equivalents (NEK1-4) are poorly understood. Previous research, as evidenced by novel attempts to knockout the genes, have implicated them as essential regulators of the *Plasmodium* cell cycle, with NEK1 in particular demonstrating global expression in the proliferative stages (Tewari et al., 2010). As such, the desirability of NEK1 as a target for non-invasive anti-malarial strategies has increased, owed to the ability to disrupt the protein at multiple stages of the parasite's development.

The present study characterises the temporal patterns of the NEK1 protein in the proliferative stages, consisting of blood stage schizogony, mosquito stage gametogenesis and ookinesis, in greater detail than has previously been achieved and with more emphasis on the elucidation of the role of NEK1 in *Plasmodium*. Here it is reported that NEK1 is present in the cytosol during all proliferative stages of the life cycle, where it specifically localises in the perinuclear space as distinct foci. In addition, NEK1 proteins are reported undergoing a highly specific and predictable temporal sequence of atypical focal division in endomitosis and endoreduplication, particularly in the latter which has not yet been investigated. Strong evidence is provided in this thesis in favour of an association between NEK1 proteins and the *Plasmodium* MTOC, further demonstrated by co-localisation studies using cell division markers such as centrin and α-tubulin. By demonstrating the importance of the non-redundant NEK1 protein in *P. berghei,* this

study increases the fundamental knowledge of the NIMA-related Kinases as a potential target for therapeutic interventionist strategies against Apicomplexan parasites.

5.1 Localisation and Expression of NEK1 in Proliferative Stages

Initial attempts to characterise the *P. berghei* male and female proteomes for the purpose of identifying possible gender-specific proteins, resulted in the recognition of NEK1 as a male gametocyte specific transcript (Khan et al., 2005). More recent reports have conversely indicated that NEK1 is not only present in both asexual and sexual cycles, but is also essential for their completion (Dorin-Semblat et al., 2011; Tewari et al., 2010). Interestingly, NEK1-GFP is observably more distinct and abundant in male gametocytes compared to schizonts. Whilst fluorescent microscopic techniques are qualitive in nature and thus not appropriate for the attempted quantitation of the protein kinase, the more distinct GFP phenotypes in male gametocytes, evidenced in live cell imaging, raises an interesting question with regards to the levels of NEK1 expression in the proliferative stages. Preliminary qRT-PCR results used to confirm the downregulation of NEK1clag (discussed later), exhibit a dramatically increased level of WT-GFP NEK1 mRNA in the non-activated gametocytes compared to that of eight-hour schizonts. To confidently confirm this, it would be prudent to conduct a dedicated qRT-PCR to determine the transcript levels of NEK1-GFP in these stages. However, it has been suggested that an up-regulation of NEK1 specific to the microgametes is as a result of the need to undergo the rapid completion of up to eight endoreduplicative divisions prior to exflagellation (Tewari et al., 2010). Despite this, the level of NEK1 expression in NAGs is rather unexpected, as observations of activated male gametogenesis suggested a de novo synthesis of the protein. The gametes exposure to the mosquito's immune defences are deleterious to the parasite (Smith et al., 2014) and thus endoreduplication and succeeding exflagellation occur within a rapid 15-minute window to expedite female fertilisation (Guinet et al., 1996; Sinden, 2009). It therefore seems likely that the accumulation of the kinase in

NAGs, allows for the immediate translation of the transcript upon the activation of the parasite to supply the rapid endoreduplicative process.

NEK1 is not observed expressing in the ring or early trophozoite parasites. These stages exist in a state of quiescence representing the G_0 phase and, as such, do not synthesize important cell cycle regulators (Arnot et al., 2011; Ishiyama et al., 2008). Conversely, diffused cytosolic NEK1 proteins are observed in mid-to-late trophozoites which suggests an upregulation of the protein in a similar nature to that seen in the gametes. This finding is validated by previous observations in trophozoite stages (Carvalho et al., 2013). Late trophozoites are characterised by the formation of visible hemozoin crystals, a by-product of cytoplasmic digestion for the synthesis of proteins involved in G_1 and S phases (Arnot et al., 2011). Therefore, it is suggested that NEK1 is one such protein synthesised at this point, evidenced by the GFP expression.

NEK1 focal formation is indicative of the initiation of schizogony, demonstrated by the immediate onset of karyokinesis, at which point GFP signals are strong. Mature schizonts are characterised by the radial arrangement of the nuclei to form a syncytium, at which point division has ceased, potentially explaining the diffused NEK1 protein and absence of focal localisation. To determine the exact expressive patterns of NEK1 throughout schizogony, time-specific qRT-PCR procedures can be carried out, in which schizont cultures are split into early (2-6 hours) mid (7-14 hours), late (15-19 hours) and mature (20+ hours) samples. This would provide an estimate of the temporal expression of NEK1, however, due to the asynchronous nature of parasite division and thus inconsistent rates of parasite maturation, it would be difficult to quantify the kinase at a specific schizont stage.

During schizogony, NEK1 localises to the perinuclear space where it divides with respect to nuclear ploidy. The separation of the foci to opposite nuclear hemispheres is

accompanied by karyokinesis, and the equal distribution of NEK1 between the two new nuclei. Likewise, the foci of gametogenesis localise to the same location, however, divide into eight dots corresponding to the number of expected genomes within the single nucleus (8N), before karyokinesis and exflagellation. The characterisation of NEK1 in these stages is highly indicative of an association between the kinase and the *Plasmodium* microtubule organising centres. As a caveat of closed mitotic division, the Apicomplexan MTOC must be associated with the nuclear membrane, which remains intact throughout the process. As such, an alliance between the MTOC and the nuclear pore complex is necessary to allow for the nucleation of the mitotic spindles, which are anchored at the MTOC for the purpose of genomic manipulation during mitosis (Aikawa, 1967; Bannister et al., 2000a). Thus, the localisation of NEK1 to the perinuclear space, where it is visible as highly distinct and specific foci throughout much of schizogony and gametogenesis, correlates to the location of putative MTOC activity.

Toxoplasma gondii, another Apicomplexan parasite subject to extensive study, undergo a variant mitosis known as endodyogeny, a closed mitotic system characterised by the formation of two daughter cells inside the mother (Striepen et al., 2007). The location of the MTOC has previously been identified in the cytoplasm of the parasite associated with the nuclear lamina (Gubbels et al., 2006). Chen and Gubbels (2013) identified the temporal patterns of NEK1 in the tachyzoite stage, confirming its localisation to the region of established MTOC activity. Additionally, Mammalian NEK2, the *Plasmodium* NEK1 ortholog, is observed localising to the centrosomes prior to the onset of mitotic division (Hames et al., 2005; Hames and Fry, 2002).

Further support is gained from the specific sequences of NEK1 focal division within asexual and sexual proliferation. NEK1 divides atypically during endomitosis, corresponding to MTOC division. This is also evident in gametogenesis, however, karyokinesis does not

occur until the end of endoreduplication, resulting in a mononucleate arrangement with radially dispersed atypically dividing foci. This process of atypical mitotic division has been implicated as an adaptation to allow for the quicker and more efficient egression of daughter cells, than would be possible if undergoing synchronous geometric nuclei duplication as demonstrated in endopolygeny (Gerald et al., 2011; Vaishnava et al., 2005). MTOC division is an unequal process, resulting in the formation of an immature daughter and a mature mother. This dimorphism is responsible for the observed asynchronicity of *Plasmodium* division, as the daughter MTOC is required to undergo a period of maturation to form the functioning organelle (Matthews et al., 2018). This is consistent with human centrioles, representing the MTOC, which form pericentriolar structures from the mother, serving as an immature version that is incapable of division (Nigg and Holland, 2018).

Interestingly, Arnot et al. (2011) reported that the preformation of the MTOC occurs in early trophozoite stages, existing as a cytoplasmic organelle associated with the nuclear membrane. This raises questions with regards to the role of NEK1 during this process, as NEK1 foci do not form in this stage, and cytosolic expression is not observed until the formation of the mid-to-late trophozoite. This suggests that NEK1 is not involved in MTOC formation, but may be involved in its later duplication, however, more evidence is required to confirm this. NEK1 focal division occurs by the elongation of the protein until its split and separation. This correlates to the theoretical formation of daughter microtubule organising centres, however, this process is poorly understood in *Plasmodium.* In yeast, spindle pole body (SPB) duplication (the MTOC equivalent), occurs by the formation of a satellite adjacent to the mother, separated by an electron dense structure known as a bridge. From this, the daughter SPB is formed in parallel to the mother at the boundary between G_1 and S phases and eventually separates to opposite nuclear hemispheres (Crasta and Surana, 2006). The formation of the *Plasmodium* daughter MTOC is also believed to occur in parallel with the pre-existing mother,

evidenced by side-by-side tubulin staining structures observed in this study and earlier by Arnot et al. (2011), in addition to the aforementioned elongation and separation of the NEK1.

The expression of NEK1 foci in a minority of the zygote stages is surprising; although sporadic, it is consistent across multiple samples suggesting it is not an artefact. NEK1 is male gametocyte-specific and so any evidence of the kinase in zygote stages is likely to have been contributed by the microgamete upon its fertilisation of the female. It has been demonstrated that the MTOC, along with the basal body are packaged into the microgamete prior to egression (Sinden, 1991). As NEK1 has previously been demonstrated associating with the MTOC during gametogenesis, it is suggested here that the observed dot in the zygote stages may be the male donated microtubule organising centre. If the organelle is donated to the female, perhaps in order to assist in later meiosis, then the presence of NEK1 may be explained by its prior incidence in the microgametes. Microscopy of flagella revealed traces of NEK1-GFP fluorescence, however, this observation was highly inconsistent. In *Chlamydomonas*, the NEK equivalent, FA2p, localises to the basal bodies (additionally functioning as MTOCs) at the proximal ends of the axoneme as distinct foci (Mahjoub et al., 2004). However, NEK1-GFP was diffused in flagella with no evidence of localisation at the head of the cell where the proximal end of the axoneme is located, suggesting no association with either the *Plasmodium* BB or MTOC is present at this time. It is clear that more work is required on the elucidation of NEK1 expression specific to the flagella in order to understand its exact role.

Additionally, it is suggested that this phenotype could be present in all zygotes immediately after the fusion of the gametes, with the subsequent breakdown or diffusion of the NEK1 protein, not observed again until the onset of meiosis, explaining the absence

in other zygotes. However, as the parasite line was transgenic and not clonal, the presence of WT zygotes and flagella which did not express NEK1-GFP could have been mistaken for mutant cells lacking this phenotype. The fertilisation event was not documented in this project and so it would be insightful to observe. To confirm the presence of the MTOC in the zygote, NEK1-GFP mutants can be genetically crossed with SAS4 or SAS6 fluorescing proteins. These are established components of the basal bodies and MTOCs of *Plasmodium* male gametocytes, and would confirm whether the foci are associated with the latter organelle in zygotes (Carvalho-Santos et al., 2010; Marques et al., 2015; Sinden et al., 2010; Zheng et al., 2014). It would also serve to investigate whether an MTOC is present in the preceding female, to give credibility to the hypothesis that the organelle is intentionally donated and perhaps involved in later meiosis.

Our study of NEK1 during the meiotic stages of ookinete differentiation revealed NEK1 focal expression in stage III and IV ookinetes at around 12.5 hours after fertilisation. Only a few of these studies reported this phenotype, however, the focal arrangement was reminiscent of that seen during gametogenesis. This expression corresponds to the meiotic event known to occur in *Plasmodium* ookinetes around this time (McKenzie et al., 2001). Correspondingly, the Human NEK2 protein has also been implicated in meiosis and its expression has been shown to peak dramatically in the testis during the pachytene stage (Arama et al., 1998). It would be beneficial to observe the whole meiotic event for the purpose of documenting the patterns of NEK1 localisation throughout. It is highly probable however, that a single NEK1 dot is present from the onset which divides into two and then four, matching the expected ploidy. Remarkably, the example image depicts two NEK1 foci simultaneously dividing into four and thus not atypically. This could potentially be as a result of the need to undergo meiotic recombination between homologous chromosomes (Mlambo et al., 2012). This occurs after the first round of chromosome segregation, which does in fact correspond to the two NEK1 foci observed

in the ookinete. The further division of these two foci into four dots is at the same time indicative of the second round of segregation, where sister chromatids are separated to form four haploid genomes (Mlambo et al., 2012). However, more evidence is required to be able to confirm this synchronised division of NEK1.

5.2 Colocalization of NEK1 Proteins

The consistent localisation of NEK1 to the perinuclear space, in conjunction with the specific patterns of focal division reported in all proliferative stages, are strong indications that NEK1 is indeed interacting with the *Plasmodium* MTOC. All supporting evidence thus far has focussed on the localisation of NEK1 to the region of putative MTOC activity. In order to fully realise the interactions between the kinase and the MTOC, then the use of protein markers representing the microtubule organising centres and their associated mitotic spindles was necessary.

Our observations using *Pb*CEN-2 markers with NEK1-GFP, demonstrate comparable developmental profiles throughout schizogony. Whilst no complete colocalization is reported, NEK1 foci are adjoined to the protein marker in all instances, forming a very close associative complex. The visualisation of these colocalised proteins provides far more than just the validation of their associative nature, additionally exposing new dynamics between the kinase and the MTOC. Centrin proteins form on the interior of NEK1-GFP foci in most instances. As no complete colocalization is present, it suggests that NEK1 and centrin operate in different regions of the MTOC. The architecture of this organelle is poorly understood, however, the yeast SPB is considered structurally analogous to the centriole-equivalents of *Plasmodium* (Arnot et al., 2011). The SPB is made of three vertically stacked segments consisting of the outer plaque, the central plaque which is flanked by the half-bridges and the inner plaque on which the mitotic spindles are anchored (Kilmartin, 2014). NEK1-GFP is presumably operating in the vicinity

of the outer plaque, whilst centrin is incorporated with the inner workings of the organelle.

Centrin proteins have been implicated as major components involved in the duplication and separation of the centrosomes in numerous eukaryotic organisms (Azimzadeh and Bornens, 2007). Four centrins have been identified in *P. falciparum* (*Pf*CEN-1, -2, -3 and -4), which demonstrate stage specific patterns of expression dictated by their transcriptional regulation (Mahajan et al., 2008). Centrin-2 displays increased levels of expression in the mature schizonts where it localises at the MTOCs (Mahajan et al., 2008). Little is known of the mechanistic role of these proteins in malaria parasites. The centrin equivalent in yeast (Cdc31p), forms a complex with Sfi1 at the half-bridges of the SPB and has been implicated as essential for SPB duplication (Crasta and Surana, 2006; Kilmartin, 2014; Spang et al., 1993). Presumably, *Pb*CEN-2 operates in the same vicinity in *Plasmodium*, associated with the half-bridges and the central plaque region of the organelle, hence the lack of complete colocalization with NEK1.

The recruitment of ARK1 to the MTOC has previously been demonstrated by the use of α-tubulin markers; ARK1 foci flank the intra-nuclear mitotic spindles of recently duplicated MTOCs, and thus are presumably associated with the inner plaque of the structure (Carvalho et al., 2013; Reininger et al., 2011). Consequently, the protein offers the perfect marker to allow for the relative study of NEK1 and centrin, which can be achieved by genetically crossing ARK1-mCherry parasites with NEK1-GFP. Provided NEK1 and centrin are localised to the outer and central MTOC segments respectively, then it would be expected that ARK1 and NEK1 foci would flank the centrin marker. A NEK1 into ARK2 line was bred for the purpose of studying the relative localisation of the proteins, however, the line did not survive and insufficient time was available to repeat the cross due to the impact of the COVID-19 pandemic on laboratory access. *Toxoplasma* ARK2 and ARK3

localise to the inner and outer plaques of the tachyzoite MTOC respectively, whilst *P. falciparum* ARK3 localises to the outer regions of budding schizonts (Berry et al., 2016; Reininger et al., 2011). The *Plasmodium* ARK2 gene has not yet been visualised in the parasite. Unlike ARK1 and ARK3, it is unique to the *Plasmodium* genus and not an ortholog of other Apicomplexan equivalents (Carvalho et al., 2013) and, as such, no comparisons can be drawn.

Centrin foci divide by the elongation and the separation of the protein into two new entities, conforming to the aforementioned process of NEK1 focal duplication. Interestingly, centrin foci and thus MTOCs are demonstrated dividing prior to NEK1 in all instances. It is suggested here that the division of centrin foci and thus the MTOC can only occur as a result of the phosphorylation of essential proteins by NEK1. As such, NEK1 foci are not observed duplicating until it has completed this necessary phosphorylation which coincides with the full separation of centrin foci. This is perhaps suggestive of a direct NEK1 involvement in the process of MTOC bridge disjunction and the separation of the two entities, however, the exact role of the kinase with regards to this process remains unexplored. Human NEK2a has been implicated in the process of centrosomal disjunction. The kinase forms a complex with C-Nap1 (Fry, 2002), a coiled-coil protein thought to provide a site of attachment for the centriolar linking structures (Crasta and Surana, 2006). The phosphorylation of C-Nap1 by NEK2a, displaces it from the centrioles and thus promotes disjunction (Fry, 2002). The roles of NEK2a may be similar to that of the *Plasmodium* NEK1 protein, however, no C-NAP1 equivalents have been identified in the parasite. More importantly however, *Toxoplasma gondii* Cep250 (homologous to human C-Nap1), does not colocalise with *Tg*NEK1, and is not impacted by its deletion, suggesting this association in Apicomplexa is absent (Chen and Gubbels, 2015, 2019).

Attempts to demonstrate the localisation of α-tubulin with NEK1-GFP using IFAs were unsuccessful in schizont stages. The α-tubulin spindles were observed in all images, seemingly operating as intended, however, NEK1 foci were not visible during schizogony. The overwhelming presence of diffused cytosolic NEK1-GFP in the images is suggestive of an error made during the IFA procedures, perhaps in the form of the excessive use of fluorescent antibodies combined with the insufficient washing of wells between incubations. The microtubules are hollow cylinders formed of dimers consisting of associated α-tubulin and β-tubulin monomers (Nogales and Downing, 2008) and perform a wide range of tasks including the maintenance of cell polarity and importantly the division of the parasite (Spreng et al., 2019). Gerald et al. (2011), using 3D confocal microscopy of centrin and α-tubulin markers, clearly demonstrated the localisation of the microtubules to the interior of the MTOCs. The co-localisation of NEK1-GFP with α-tubulin is predicted to mirror this spindle-MTOC complex, with NEK1 foci taking the position of the centrin. This experiment needs to be repeated in order to confirm this model of colocalization in schizogony, perhaps through the use super resolution or 3D confocal microscopy, in order to observe this process in much finer detail as was demonstrated by Gerald et al. (2011).

The partial colocalization of α-tubulin with NEK1 in male activated gametocytes corresponds to the previously described relationship expected between the proteins during schizogony. Whilst the images are sufficient enough to confirm this relationship, the necessary use of multiple fixed IFA samples to build a chronological sequence of events during endoreplication does not provide an adequate means of understanding the temporal-dynamics between NEK1 and the spindle. It is recommended that a line of NEK1 into kinesin-8fX parasites are generated to observe the real-time dynamics of spindle formation with respect to NEK1. Kinesin-8X are motor proteins associated with the microtubules, implicated in the roles of intracellular transport, motility and cell division.

Zeeshan et al. (2019b) demonstrated the localisation of kinesin-8X to the microtubules and MTOCs, where it displayed similar temporal dynamics to the former during endoreduplication, culminating in the formation of foci corresponding to nuclear ploidy. The described dynamics of kinesin-8X during gametogenesis resembles that of NEK1, however, this is yet to be seen.

Our demonstration of localisation between NEK1 and NDC80 (kinetochore marker), revealed a similar developmental profile throughout schizogony. Concurrent with NEK1-centrin complexes, NDC80 foci are always associated with the interior of NEK1-GFP and undergo a specific sequence of division. NDC80 is one of four protein constituents that make up the NDC80 complex, a major structural component of the kinetochore that links the outer and inner disk-like assemblies associated with the microtubules and centromeres (Ciferri et al., 2007; Zeeshan et al., 2020). The structure consists of two globular heterodimers composed of NDC80-NUF2 (microtubule associated) and SPC24-SPC25 (centromere associated) subcomplexes, separated by coiled-coil chains which overlap at the tetramerization domain (Ciferri et al., 2007). The additional kinetochore cross-linking structures, KNL1/SPC105, are bound by MTW1/MIS12 to the base of the NDC80 complex in the inner kinetochore, forming the so called KMN network (Ciferri et al., 2005). This association with the kinetochores explains the interior localisation of the protein relative to NEK1, as the kinetochores represent the point of attachment between the spindle and centromeres. Additionally, the primacy of NEK1 division relative to NDC80 is as a result of NEK1s association with the MTOC, the division of which is the one of first events involved in *Plasmodium* mitosis, whereas kinetochore separation and thus NDC80 focal division does not occur until anaphase (Zeeshan et al., 2020). What remains unclear however, is whether the phosphorylative action of NEK1 is in anyway linked to the attachment and separation of these structures. Human NEK2 is responsible for the phosphorylation of HEC1 proteins (human NDC80), implicated as essential for the

maintenance of chromosomal integrity by the promotion of stable microtubule-centromere attachments and the faithful segregation of the chromosomes during anaphase (Chen et al., 2002; Du et al., 2008). As NDC80 is highly conserved between species (Akiyoshi and Gull, 2013), it seems possible that the *Plasmodium* NEK equivalents may be involved in a similar process of chromosome segregation. However, no evidence has been put forward in support of this and centromere-kinetochore interactions as a whole are not fully understood in *Plasmodium*.

5.3 Interacting Partners of NEK1

The patterns of NEK1 localisation determined by fluorescent microscopy expose a surface level interaction between NEK1 and the regulatory structures of *Plasmodium* proliferation. In order to understand the exact role of the kinase with respect to mitotic division, the identification of the unobserved interacting partners of NEK1 is vital. This was achieved by protein pulldown procedures of NEK1 in activated male gametocytes, and the subsequent MS of the resultant complex.

The interaction between NEK1 and kinesin-8B is significant as it implicates the kinase in basal body dynamics. Kinesin-8B is a known protein of the BBs and has been identified as essential for their formation and correct axonemal assembly (Zeeshan et al., 2019a). Additionally, confirmed interaction between NEK1 and both centrin-1 and -2 validates its hypothesized association with the MTOCs, previously only evidenced by colocalization. More importantly however, centrin-1 and -2 have been identified as constituents of the BBs (Talman et al., 2014) which, combined with a kinesin-8B association, is indicative of an interaction between these organelles and NEK1.

Our proteomics data suggested that a number of dynein heavy chains were interacting with NEK1 in male activated gametocytes. The heavy chain is a subcomplex of the dynein motor protein which, depending on the class, is generally either associated with the

cytoplasmic microtubules or the ciliary axonemes (Vale, 2003). The C-terminus of the heavy dyneins interact with light and intermediate chains responsible for motor regulation and cargo tethering, whereas the N-terminus is the region of ATP hydrolytic action where chemical energy is transferred into mechanical force (Asai and Koonce, 2001). Remarkably, the data suggests that NEK1 is specifically axoneme dynein-associated. NEK1 interacts with two outer-arm dynein (OAD) β heavy chains and an OAD α heavy chain, in addition to two intermediate chains and the flagellar outer arm dynein-associated protein, all components of the outer-arm motor proteins of the axoneme as predicted in the male proteome (Talman et al., 2014). Additionally, the presence of an inner-arm dynein β heavy chain is indicative of an association with inner-arm motor proteins (Talman et al., 2014). In conjunction with NEK1/dynein interactions, the Armadillo-repeat protein PF16, with which NEK1 was also associated, is a component of the central C1 and C2 axonemal microtubules implicated in the maintenance of the central apparatus (Straschil et al., 2010; Talman et al., 2014). The deletion of this protein results in the significant decrease in axonemal integrity and subsequent motility. This suggests that by interacting with PF16, NEK1 may play an important role in microtubule uniformity (Straschil et al., 2010).

Importantly, the lack of any established cytoplasmic dynein subcomplexes suggests NEK1 is not involved in the phosphorylation of cytoplasmic motor proteins, responsible for microtubule associated transportation of cellular cargos. However, it should be noted that Talman et al. (2014) failed to identify any cytoplasmic light or heavy chains in the *P. berghei* proteome, which they suggested was as a result of an absence of cargo conveyance along the axonemes. This is explained by the cytoplasmic assembled nature of the axonemes which do not require the use of an intraflegellar transport system for their construction (Sinden et al., 2010). The formation of the mitotic spindles remains poorly understood especially with regards to NEK1. Kinesin-8X, a kinesin implicated in the

formation of the mitotic spindles in *Plasmodium*, does not interact with NEK1 as according to the pulldown results, further suggesting that NEK1s association with the motor proteins is restricted to the dyneins of the axoneme.

NEK1/MORN repeat protein interactions may play a role in the egress of the microgamete stages. The roles of MORN1 during male *Plasmodium* gametogenesis are not understood, however, the protein has been demonstrated localising to the region of merozoite budding during schizogony, in addition to the apical and posterior ends of *Toxoplasma* mother cells *(Gubbels et al., 2006; Kono et al., 2016).* It suggested that the protein forms a region of attachment for the IMC and plasma membrane, necessary for the process of nuclear division in addition to daughter cell budding (Gubbels et al., 2006; Kono et al., 2016). Perhaps the interaction between NEK1 and MORN1 is required for the similar egression of the microgametes, the representation of which using protein makers would be very insightful for future fluorescent microscopy-based research.

5.4 Functional Analysis of NEK1 in *Plasmodium berghei*

It is clear that NEK1 plays a significant role in the regulation of *Plasmodium* proliferation indicating connections with various cell division machinery. To determine its function in the gametocytes, reverse genetic techniques were utilised to observe gametogenesis in the absence of NEK1. Previous studies have demonstrated that NEK1 plays a vital role in the asexual proliferation of *Plasmodium* parasites (Dorin-Semblat et al., 2011), so the use of specific protein knockdowns at targeted life stages was required. The addition of a clag1 promoter trap upstream of the NEK1 gene allowed for stage specific-expression, due to the promoter's tight restriction in gametogenesis but not schizogony (Saini et al., 2017; Sebastian et al., 2012). This technique had been demonstrated with CDPK1 to examine ookinete development in its absence (Sebastian et al., 2012).

The use of conditional knockdowns using NEK1clag implicates NEK1 as an essential kinase in male endoreplication, with clag samples demonstrating a significant reduction in exflagellating males. It is not clear what NEK1clag specifically impacts as the lack of microgamete formation can be attributed to either a failure of the previous endoreplication step or exflagellation itself. However, as NEK1 has been shown to be associated with multiple proteins and is considered a general cell cycle regulator (Invergo et al., 2017; Tewari et al., 2010), it is likely that its disruption impacts more than just a single process. NEK1s colocalization with the MTOC and non-redundant nature in asexual stages implicates the kinase as essential for MTOC mediated endomitosis. By interreacting with centrin-1 and -2, demonstrating colocalization with the MTOCs, and also being essential in sexual stages, NEK1 presumably plays the same role in MTOC mediated endoreduplication. The formation of MTOC structures during trophozoite stages in the absence of NEK1-GFP (Arnot et al., 2011) implies NEK1 is concerned with MTOC duplication and separation specifically, and so perhaps NEK1clag impedes this process and thus mitosis as a whole.

The disruption of the basal bodies demonstrated by kinesin-8B knockouts prevents exflagellation (Zeeshan et al., 2019a). Ultra-structure TEM studies have indicated that the structure and function of the BB is linked to the MTOC, coinciding with their recruitment at these organelles (Francia et al., 2015; Zeeshan et al., 2019a). NEK1s interactive partnership with kinesin-8B and the aforementioned centrins in addition to the shared focal dynamics, implicates NEK1 as a mediator of BB formation and possible separation. The NEKC protein of *Trypanosoma brucei* has been implicated in BB separation, however, this parasite lacks centriole-equivalent structures, with the BB itself responsible for mitotic spindle manipulation (Pradel et al., 2006). It is unknown whether this distinction is important to NEK proteins, however, the similar structure and dynamics between the BBs and MTOCs suggests that it is not. The breadth of an organism's NEK repertoire

correlates to the complexity of the machines required for axonemal assembly due to the diversification of proteins to fulfil specialised needs (Fry et al., 2017; Quarmby and Mahjoub, 2005). *Giardia lamblia* encode 198 NEK proteins for four flagella, whereas *Chlamydomonas* species encode ten NEK proteins for a single flagellum (Fry et al., 2017; Manning et al., 2011). Contrastingly, *Plasmodia* encode only four NEK proteins, reflecting the simplicity of microgamete flagella, and evidencing the potential dual-purpose nature of NEK1 in both BB and MTOC processes due to the restricted number of kinases.

It has been previously demonstrated that NEK1 acts as an upstream regulator of MAPk2 expression (Dorin et al., 2001), confirmed by the downregulation of the protein mRNA in NEK1clag mutant NAGs. This is significant as MAPk2 has been implicated as an essential protein involved in the explosive egression of the microgametes from the male gametocyte (Tewari et al., 2005; Wierk et al., 2013). The extent of this impact on microgamete formation is not known as the presumed disruption of both MTOC mediated endoreduplication and BB formation in the absence of NEK1, is likely enough to have prevented exflagellation in the first place. In contrast, SRPK1 has been implicated in the mediation of mRNA alternative splicing within the first minutes of gametocyte activation (Invergo et al., 2017; Tewari et al., 2010). NEK1 was found to be an interacting partner of this kinase, and due to its supposed operation from the onset of endoreduplication, its potential disruption in NEK1clag mutants is presumably quite damaging to the process as a whole. This is evidenced by SRPK1 knockout studies demonstrating significant decreases in the successful completion of endoreduplication (Invergo et al., 2017).

A number of NEK1clag flagella were observed in fluorescent microscopy despite no evidence of male exflagellation being reported. It is not thought that this is evidence of exflagellation in the absence of NEK1, rather the presence of minute but sufficient traces of the kinase due to the nature of knockdown procedures as opposed to knockout. Auxin-

inducible degron (AID) techniques were planned, however, insufficient time was available to undertake them due to the COVID-19 pandemic. This involves the generation of an AID-tagged NEK1 protein which, when exposed to the auxin plant hormone, causes the recognition of the AID by TIR1 F-box proteins, mediating ubiquitination and its subsequent degradation (Balestra et al., 2020; Philip and Waters, 2015).

The few flagella observed did not appear defective, though no motility was reported. Basal body and PF16 disruption, as is potentially the case in NEK1clag parasites, does not thwart axonemal assembly. However, it does prevent the formation of the 9+2 arrangement of the doublet microtubules, in addition to the impairment of flagellar motility to varying degrees (Depoix et al., 2020; Straschil et al., 2010). As such, in order to identify the effects of NEK1clag on flagella, ultra-structure studies of the axoneme are required to observe potential defects. NEK1 is not thought to be involved in direct axonemal assembly however, evidenced by the lack of association between the kinase and light axonemal dynein chains, which are believed to be important to assembly but are functionally redundant in motility (Talman et al., 2014).

Nevertheless, it is suggested that NEK1 may play a direct role in flagella motility, evidenced by the previously demonstrated presence of dispersed NEK1 residue throughout microgametes, in combination with the interactive partnership between NEK1 and axonemal related heavy dyneins. Flagellar motility is an ATP demanding process, likely requiring a kinase such as NEK1 for the phosphorylation of dynein N-termini to facilitate the transfer of phosphates from ATP. It should be noted however, that the pulldown that exposed these interactions between the kinase and the dyneins was conducted at around 1.5 minutes post male activation, and as such, axonemal formation would have been in its infancy. It remains unclear why NEK1 would be associated with the axonemal dyneins at this time as no evidence suggests that the movement of these

structures is required during their cytoplasmic formation. However, as the axonemes form a basket around the nucleus as they are assembled (Zeeshan et al., 2019a), it is suggested that dynein mediated oscillations in axonemes prevent obstructions between neighbouring microtubules and may assist in the packaging of the axoneme into the flagella during exflagellation.

The discovery of NEK1clag zygotes was surprising. As previously mentioned, it is not thought that endoreduplication or exflagellation is possible in the absence of NEK1, with observed outliers likely having originated from systems where NEK1 downregulation was not sufficient. Furthermore, it remains a mystery as to why stage I ookinetes arrested. If sufficient NEK1 was available to allow for endoreduplication, exflagellation and hypothesized flagella motility, then why was there not a sufficient amount to allow for the progression of the ookinetes and later formation of oocysts? This is especially perplexing when considering the fact that the ookinetes did not manage to progress to at least stage III or IV forms which is where NEK1 plays a visible role in presumed MTOC mediated meiosis. CDPK1 was identified as a NEK1 interacting partner and is abundant in the ookinete stages. Downregulation of this kinase results in the arrestation of ookinetes which appear “retort” in shape, and has led to the implication that CDPK1 is important in the regulation of cellular morphogenesis by unidentified means in addition to the de-repression of various transcripts that are crucial for mature ookinete formation (Sebastian et al., 2012). Regardless, if zygotes were successfully fertilised, then how is it that the potential disruption of CDPK1 in NEK1clag parasites occurred? Furthermore, not even NEK1clag ookinetes were able to advance to the point where they took on the retort morphology demonstrated by Sebastian et al. (2012). It is highly likely that further unidentified impacts are caused to ookinetes in the downregulated NEK1 parasites, which of course encourages further investigation. However, it is worth noting that had knockout techniques been used, it is unlikely that ookinetes would have been observed in the first

place. Perhaps the targeted degradation of NEK1 during ookinesis by aforementioned AID techniques is required to observe the effects of an absence of NEK1 on ookinetes instead of attempting to observe the examples that were not intentionally formed in the first place.

5.5 Concluding Remarks

This study of the *P. berghei* NIMA-related kinase 1 sought to deliver an in-depth assessment of the roles of the protein throughout the proliferative stages, evidenced by fluorescent microscopy, colocalization studies, protein pull-downs and knockdown procedures. NEK1 displays highly distinct patterns of localisation relative to the nucleus and undergoes a specific sequence of division with respect to nuclear karyokinesis in schizogony. Furthermore, NEK1 focal dynamics closely mirror those of the MTOC, as evidenced by centrin markers in all proliferate stages. It can be argued with reasonable confidence that NEK1 is involved in the duplication and separation of the MTOC, which itself is a crucial regulator of atypical endomitosis and endoreduplication. Additionally, the roles of NEK1 in gametogenesis have been somewhat identified, proposing that the kinase may be involved in basal body formation, axonemal regulation by its interaction with implicated proteins and the mediation of phosphate transfer required for flagella motility. Whilst this study was conducted with the intention of resolving the function NEK1, its extensive interactions with other proteins in addition to the impacts its absence has on both schizogony and gametogenesis, has raised many additional questions that are in need of further investigation.

To conclude, this study has highlighted the importance of NEK1 during schizogony, gametogenesis and ookinesis. The delicate nature of *Plasmodium* proliferation, teamed with the non-redundancy of NEK1 in multiple life stages, makes the kinase a very promising target for the disruption of both asexual and sexual replication. It is hoped that further research into NEK1 could allow for the development of various non-invasive anti-malarial strategies to compromise the protein and subsequently prevent the successful completion of the parasite's lifecycle.

References

Aikawa, M. (1967). Ultrastructure of the pellicular complex of Plasmodium fallax. J Cell Biol *35*, 103-113.

Akiyoshi, B., and Gull, K. (2013). Evolutionary cell biology of chromosome segregation: insights from trypanosomes. Open Biol *3*, 130023.

Andersen, J.S., Wilkinson, C.J., Mayor, T., Mortensen, P., Nigg, E.A., and Mann, M. (2003). Proteomic characterization of the human centrosome by protein correlation profiling. Nature *426*, 570-574.

Arama, E., Yanai, A., Kilfin, G., Bernstein, A., and Motro, B. (1998). Murine NIMA-related kinases are expressed in patterns suggesting distinct functions in gametogenesis and a role in the nervous system. Oncogene *16*, 1813-1823.

Arnone, J.T., Walters, A.D., and Cohen-Fix, O. (2013). The dynamic nature of the nuclear envelope: lessons from closed mitosis. Nucleus *4*, 261-266.

Arnot, D.E., Ronander, E., and Bengtsson, D.C. (2011). The progression of the intra-erythrocytic cell cycle of Plasmodium falciparum and the role of the centriolar plaques in asynchronous mitotic division during schizogony. Int J Parasitol *41*, 71-80.

Asai, D.J., and Koonce, M.P. (2001). The dynein heavy chain: structure, mechanics and evolution. Trends Cell Biol *11*, 196-202.

Avidor-Reiss, T., and Gopalakrishnan, J. (2013). Cell Cycle Regulation of the Centrosome and Cilium. Drug Discov Today Dis Mech *10*, e119-e124.

Azimzadeh, J., and Bornens, M. (2007). Structure and duplication of the centrosome. J Cell Sci *120*, 2139-2142.

Baer, K., Klotz, C., Kappe, S.H., Schnieder, T., and Frevert, U. (2007). Release of hepatic Plasmodium yoelii merozoites into the pulmonary microvasculature. PLoS Pathog *3*, e171.

Balestra, A.C., Zeeshan, M., Rea, E., Pasquarello, C., Brusini, L., Mourier, T., Subudhi, A.K., Klages, N., Arboit, P., Pandey, R.*, et al.* (2020). A divergent cyclin/cyclin-dependent kinase complex controls the atypical replication of a malaria parasite during gametogony and transmission. Elife *9*.

Bannister, L.H., Hopkins, J.M., Dluzewski, A.R., Margos, G., Williams, I.T., Blackman, M.J., Kocken, C.H., Thomas, A.W., and Mitchell, G.H. (2003). Plasmodium falciparum apical membrane antigen 1 (PfAMA-1) is translocated within micronemes along subpellicular microtubules during merozoite development. J Cell Sci *116*, 3825-3834.

Bannister, L.H., Hopkins, J.M., Fowler, R.E., Krishna, S., and Mitchell, G.H. (2000a). A brief illustrated guide to the ultrastructure of Plasmodium falciparum asexual blood stages. Parasitol Today *16*, 427-433.

Bannister, L.H., Hopkins, J.M., Fowler, R.E., Krishna, S., and Mitchell, G.H. (2000b). Ultrastructure of rhoptry development in Plasmodium falciparum erythrocytic schizonts. Parasitology *121 (Pt 3)*, 273-287.

Bannister, L.H., Hopkins, J.M., Margos, G., Dluzewski, A.R., and Mitchell, G.H. (2004). Three-dimensional ultrastructure of the ring stage of Plasmodium falciparum: evidence for export pathways. Microsc Microanal *10*, 551-562.

Bannister, L.H., and Sherman, I.W. (2009). *Plasmodium*. eLS, 1-12.

Barbash, O., and Diehl, J. (2008). Regulation of the Cell Cycle. In The Molecular Basis of Cancer, J. Mendelsohn, P. Howley, M. Israel, J. Gray, and C. Thompson, eds., pp. 177-188.

Barnwell, J.W. (2001). Hepatic Kupffer cells: the portal that permits infection of hepatocytes by malarial sporozoites? Hepatology *33*, 1331-1333.

Beeson, J.G., Drew, D.R., Boyle, M.J., Feng, G., Fowkes, F.J., and Richards, J.S. (2016). Merozoite surface proteins in red blood cell invasion, immunity and vaccines against malaria. FEMS Microbiol Rev *40*, 343-372.

Belham, C., Roig, J., Caldwell, J.A., Aoyama, Y., Kemp, B.E., Comb, M., and Avruch, J. (2003). A mitotic cascade of NIMA family kinases. Nercc1/Nek9 activates the Nek6 and Nek7 kinases. J Biol Chem *278*, 34897-34909.

Bennink, S., Kiesow, M.J., and Pradel, G. (2016). The development of malaria parasites in the mosquito midgut. Cell Microbiol *18*, 905-918.

Berry, L., Chen, C.T., Reininger, L., Carvalho, T.G., El Hajj, H., Morlon-Guyot, J., Bordat, Y., Lebrun, M., Gubbels, M.J., Doerig, C*., et al.* (2016). The conserved apicomplexan Aurora kinase TgArk3 is involved in endodyogeny, duplication rate and parasite virulence. Cell Microbiol *18*, 1106-1120.

Bertran, M.T., Sdelci, S., Regue, L., Avruch, J., Caelles, C., and Roig, J. (2011). Nek9 is a Plk1-activated kinase that controls early centrosome separation through Nek6/7 and Eg5. EMBO J *30*, 2634-2647.

Besteiro, S., Dubremetz, J.F., and Lebrun, M. (2011). The moving junction of apicomplexan parasites: a key structure for invasion. Cell Microbiol *13*, 797-805.

Billker, O., Shaw, M.K., Margos, G., and Sinden, R.E. (1997). The roles of temperature, pH and mosquito factors as triggers of male and female gametogenesis of Plasmodium berghei in vitro. Parasitology *115 (Pt 1)*, 1-7.

Black, M.W., and Boothroyd, J.C. (2000). Lytic cycle of Toxoplasma gondii. Microbiol Mol Biol Rev *64*, 607-623.

Bracchi-Ricard, V., Barik, S., Delvecchio, C., Doerig, C., Chakrabarti, R., and Chakrabarti, D. (2000). PfPK6, a novel cyclin-dependent kinase/mitogen-activated protein kinase-related protein kinase from Plasmodium falciparum. Biochem J *347 Pt 1*, 255-263.

Briggs, L.J., Davidge, J.A., Wickstead, B., Ginger, M.L., and Gull, K. (2004). More than one way to build a flagellum: comparative genomics of parasitic protozoa. Curr Biol *14*, R611-612.

Brooks, C.F., Francia, M.E., Gissot, M., Croken, M.M., Kim, K., and Striepen, B. (2011). Toxoplasma gondii sequesters centromeres to a specific nuclear region throughout the cell cycle. Proc Natl Acad Sci U S A *108*, 3767-3772.

Brown, R.W., Sharma, A.I., and Engman, D.M. (2017). Dynamic protein S-palmitoylation mediates parasite life cycle progression and diverse mechanisms of virulence. Crit Rev Biochem Mol Biol *52*, 145-162.

Bui, H.T.N., Niederwieser, I., Bird, M.J., Dai, W., Brancucci, N.M.B., Moes, S., Jenoe, P., Lucet, I.S., Doerig, C., and Voss, T.S. (2019). Mapping and functional analysis of heterochromatin protein 1 phosphorylation in the malaria parasite Plasmodium falciparum. Sci Rep *9*, 16720.

Burda, P.C., Caldelari, R., and Heussler, V.T. (2017). Manipulation of the Host Cell Membrane during Plasmodium Liver Stage Egress. mBio *8*.

Carvalho-Santos, Z., Machado, P., Branco, P., Tavares-Cadete, F., Rodrigues-Martins, A., Pereira-Leal, J.B., and Bettencourt-Dias, M. (2010). Stepwise evolution of the centriole-assembly pathway. J Cell Sci *123*, 1414-1426.

Carvalho, T.G., Doerig, C., and Reininger, L. (2013). Nima- and Aurora-related kinases of malaria parasites. Biochim Biophys Acta *1834*, 1336-1345.

CDC (2019). CDC - Parasites - Malaria.

Chen, C.T., and Gubbels, M.J. (2013). The Toxoplasma gondii centrosome is the platform for internal daughter budding as revealed by a Nek1 kinase mutant. J Cell Sci *126*, 3344-3355.

Chen, C.T., and Gubbels, M.J. (2015). Apicomplexan cell cycle flexibility: centrosome controls the clutch. Trends Parasitol *31*, 229-230.

Chen, C.T., and Gubbels, M.J. (2019). TgCep250 is dynamically processed through the division cycle and is essential for structural integrity of the Toxoplasma centrosome. Mol Biol Cell *30*, 1160-1169.

Chen, Y., Jirage, D., Caridha, D., Kathcart, A.K., Cortes, E.A., Dennull, R.A., Geyer, J.A., Prigge, S.T., and Waters, N.C. (2006). Identification of an effector protein and gain-of-function mutants that activate Pfmrk, a malarial cyclin-dependent protein kinase. Mol Biochem Parasitol *149*, 48-57.

Chen, Y., Riley, D.J., Zheng, L., Chen, P.L., and Lee, W.H. (2002). Phosphorylation of the mitotic regulator protein Hec1 by Nek2 kinase is essential for faithful chromosome segregation. J Biol Chem *277*, 49408-49416.

Ciferri, C., De Luca, J., Monzani, S., Ferrari, K.J., Ristic, D., Wyman, C., Stark, H., Kilmartin, J., Salmon, E.D., and Musacchio, A. (2005). Architecture of the human ndc80-hec1 complex, a critical constituent of the outer kinetochore. J Biol Chem *280*, 29088-29095.

Ciferri, C., Musacchio, A., and Petrovic, A. (2007). The Ndc80 complex: hub of kinetochore activity. FEBS Lett *581*, 2862-2869.

Coleman, B.I., Skillman, K.M., Jiang, R.H.Y., Childs, L.M., Altenhofen, L.M., Ganter, M., Leung, Y., Goldowitz, I., Kafsack, B.F.C., Marti, M.*, et al.* (2014). A Plasmodium falciparum histone deacetylase regulates antigenic variation and gametocyte conversion. Cell Host Microbe *16*, 177-186.

Cooper, G.M. (2000). The Cell: A Molecular Approach, 2nd edn (Sunderland (MA): Sinauer Associates).

Coppi, A., Tewari, R., Bishop, J.R., Bennett, B.L., Lawrence, R., Esko, J.D., Billker, O., and Sinnis, P. (2007). Heparan sulfate proteoglycans provide a signal to Plasmodium sporozoites to stop migrating and productively invade host cells. Cell Host Microbe *2*, 316-327.

Costa-Guda, J., and Arnold, A. (2013). Hyperparathyroidism. In Genetics of Bone Biology and Skeletal Disease, R. Thakker, M. Whyte, J. Eisman, and T. Igarashi, eds. (Academic Press), pp. 397-408.

Crasta, K., and Surana, U. (2006). Disjunction of conjoined twins: Cdk1, Cdh1 and separation of centrosomes. Cell Div *1*, 12.

Crutcher, J., and Hoffman, S. (1996). Malaria. In Medical Microbiology, S. Baron, ed. (University of Texas Medical Branch).

Das, S., Hertrich, N., Perrin, A.J., Withers-Martinez, C., Collins, C.R., Jones, M.L., Watermeyer, J.M., Fobes, E.T., Martin, S.R., Saibil, H.R.*, et al.* (2015). Processing of Plasmodium falciparum Merozoite Surface Protein MSP1 Activates a Spectrin-Binding Function Enabling Parasite Egress from RBCs. Cell Host Microbe *18*, 433-444.

De Souza, C.P., and Osmani, S.A. (2007). Mitosis, not just open or closed. Eukaryot Cell *6*, 1521-1527.

Depoix, D., Marques, S.R., Ferguson, D.J., Chaouch, S., Duguet, T., Sinden, R.E., Grellier, P., and Kohl, L. (2020). Vital role for Plasmodium berghei Kinesin8B in axoneme assembly during male gamete formation and mosquito transmission. Cell Microbiol *22*, e13121.

Deshmukh, A.S., Agarwal, M., Mehra, P., Gupta, A., Gupta, N., Doerig, C.D., and Dhar, S.K. (2015). Regulation of Plasmodium falciparum Origin Recognition Complex subunit 1 (PfORC1) function through phosphorylation mediated by CDK-like kinase PK5. Mol Microbiol *98*, 17-33.

Doerig, C., Doerig, C., Horrocks, P., Coyle, J., Carlton, J., Sultan, A., Arnot, D., and Carter, R. (1995). Pfcrk-1, a developmentally regulated cdc2-related protein kinase of Plasmodium falciparum. Mol Biochem Parasitol *70*, 167-174.

Dorin-Semblat, D., Carvalho, T.G., nivez, m.-P., Halbert, J., Poullet, P., Semblat, J.-P., Goldring, J., Chakrabarti, D., Mehra, P., Dhar, S*., et al.* (2013). An atypical cyclin-dependent kinase controls Plasmodium falciparum proliferation rate.

Dorin-Semblat, D., Schmitt, S., Semblat, J.P., Sicard, A., Reininger, L., Goldring, D., Patterson, S., Quashie, N., Chakrabarti, D., Meijer, L*., et al.* (2011). Plasmodium falciparum NIMA-related kinase Pfnek-1: sex specificity and assessment of essentiality for the erythrocytic asexual cycle. Microbiology *157*, 2785-2794.

Dorin, D., Le Roch, K., Sallicandro, P., Alano, P., Parzy, D., Poullet, P., Meijer, L., and Doerig, C. (2001). Pfnek-1, a NIMA-related kinase from the human malaria parasite Plasmodium falciparum Biochemical properties and possible involvement in MAPK regulation. Eur J Biochem *268*, 2600-2608.

Du, J., Cai, X., Yao, J., Ding, X., Wu, Q., Pei, S., Jiang, K., Zhang, Y., Wang, W., Shi, Y*., et al.* (2008). The mitotic checkpoint kinase NEK2A regulates kinetochore microtubule attachment stability. Oncogene *27*, 4107-4114.

Dwivedi, A., Reynes, C., Kuehn, A., Roche, D.B., Khim, N., Hebrard, M., Milanesi, S., Rivals, E., Frutos, R., Menard, D*., et al.* (2017). Functional analysis of Plasmodium falciparum subpopulations associated with artemisinin resistance in Cambodia. Malar J *16*, 493.

Eksi, S., Morahan, B.J., Haile, Y., Furuya, T., Jiang, H., Ali, O., Xu, H., Kiattibutr, K., Suri, A., Czesny, B*., et al.* (2012). Plasmodium falciparum gametocyte development 1 (Pfgdv1) and gametocytogenesis early gene identification and commitment to sexual development. PLoS Pathog *8*, e1002964.

Filarsky, M., Fraschka, S.A., Niederwieser, I., Brancucci, N.M.B., Carrington, E., Carrio, E., Moes, S., Jenoe, P., Bartfai, R., and Voss, T.S. (2018). GDV1 induces sexual commitment of malaria parasites by antagonizing HP1-dependent gene silencing. Science *359*, 1259-1263.

Francia, M.E., Dubremetz, J.F., and Morrissette, N.S. (2015). Basal body structure and composition in the apicomplexans Toxoplasma and Plasmodium. Cilia *5*, 3.

Francia, M.E., and Striepen, B. (2014). Cell division in apicomplexan parasites. Nat Rev Microbiol *12*, 125-136.

Fry, A.M. (2002). The Nek2 protein kinase: a novel regulator of centrosome structure. Oncogene *21*, 6184-6194.

Fry, A.M., Bayliss, R., and Roig, J. (2017). Mitotic Regulation by NEK Kinase Networks. Front Cell Dev Biol *5*, 102.

Fry, A.M., Meraldi, P., and Nigg, E.A. (1998). A centrosomal function for the human Nek2 protein kinase, a member of the NIMA family of cell cycle regulators. EMBO J *17*, 470-481.

Fry, A.M., O'Regan, L., Sabir, S.R., and Bayliss, R. (2012). Cell cycle regulation by the NEK family of protein kinases. J Cell Sci *125*, 4423-4433.

Fry, A.M., Schultz, S.J., Bartek, J., and Nigg, E.A. (1995). Substrate specificity and cell cycle regulation of the Nek2 protein kinase, a potential human homolog of the mitotic regulator NIMA of Aspergillus nidulans. J Biol Chem *270*, 12899-12905.

Ganter, M., Goldberg, J.M., Dvorin, J.D., Paulo, J.A., King, J.G., Tripathi, A.K., Paul, A.S., Yang, J., Coppens, I., Jiang, R.H.*, et al.* (2017). Plasmodium falciparum CRK4 directs continuous rounds of DNA replication during schizogony. Nat Microbiol *2*, 17017.

Geleta, G., and Ketema, T. (2016). Severe Malaria Associated with Plasmodium falciparum and P. vivax among Children in Pawe Hospital, Northwest Ethiopia. Malar Res Treat *2016*, 1240962.

Gerald, N., Mahajan, B., and Kumar, S. (2011). Mitosis in the human malaria parasite Plasmodium falciparum. Eukaryot Cell *10*, 474-482.

Ghosh, K., and Ghosh, K. (2007). Pathogenesis of anemia in malaria: a concise review. Parasitol Res *101*, 1463-1469.

Govindasamy, K., Jebiwott, S., Jaijyan, D.K., Davidow, A., Ojo, K.K., Van Voorhis, W.C., Brochet, M., Billker, O., and Bhanot, P. (2016). Invasion of hepatocytes by Plasmodium sporozoites requires cGMP-dependent protein kinase and calcium dependent protein kinase 4. Mol Microbiol *102*, 349-363.

Gubbels, M.J., Vaishnava, S., Boot, N., Dubremetz, J.F., and Striepen, B. (2006). A MORN-repeat protein is a dynamic component of the Toxoplasma gondii cell division apparatus. J Cell Sci *119*, 2236-2245.

Guinet, F., Dvorak, J.A., Fujioka, H., Keister, D.B., Muratova, O., Kaslow, D.C., Aikawa, M., Vaidya, A.B., and Wellems, T.E. (1996). A developmental defect in Plasmodium falciparum male gametogenesis. J Cell Biol *135*, 269-278.

Gunalan, K., Lo, E., Hostetler, J.B., Yewhalaw, D., Mu, J., Neafsey, D.E., Yan, G., and Miller, L.H. (2016). Role of Plasmodium vivax Duffy-binding protein 1 in invasion of Duffy-null Africans. Proc Natl Acad Sci U S A *113*, 6271-6276.

Guttery, D.S., Holder, A.A., and Tewari, R. (2012). Sexual development in Plasmodium: lessons from functional analyses. PLoS Pathog *8*, e1002404.

Guttery, D.S., Roques, M., Holder, A.A., and Tewari, R. (2015). Commit and Transmit: Molecular Players in Plasmodium Sexual Development and Zygote Differentiation. Trends in Parasitology *31*, 676-685.

Halbert, J., Ayong, L., Equinet, L., Le Roch, K., Hardy, M., Goldring, D., Reininger, L., Waters, N., Chakrabarti, D., and Doerig, C. (2010). A Plasmodium falciparum transcriptional cyclin-dependent kinase-related kinase with a crucial role in parasite proliferation associates with histone deacetylase activity. Eukaryot Cell *9*, 952-959.

Hames, R.S., Crookes, R.E., Straatman, K.R., Merdes, A., Hayes, M.J., Faragher, A.J., and Fry, A.M. (2005). Dynamic recruitment of Nek2 kinase to the centrosome involves microtubules, PCM-1, and localized proteasomal degradation. Mol Biol Cell *16*, 1711-1724.

Hames, R.S., and Fry, A.M. (2002). Alternative splice variants of the human centrosome kinase Nek2 exhibit distinct patterns of expression in mitosis. Biochem J *361*, 77-85.

Hames, R.S., Wattam, S.L., Yamano, H., Bacchieri, R., and Fry, A.M. (2001). APC/C-mediated destruction of the centrosomal kinase Nek2A occurs in early mitosis and depends upon a cyclin A-type D-box. EMBO J *20*, 7117-7127.

Harding, C.R., and Frischknecht, F. (2020). The Riveting Cellular Structures of Apicomplexan Parasites. Trends Parasitol.

Hisaeda, H., Yasutomo, K., and Himeno, K. (2005). Malaria: immune evasion by parasites. Int J Biochem Cell Biol *37*, 700-706.

Hopp, C.S., and Sinnis, P. (2015). The innate and adaptive response to mosquito saliva and Plasmodium sporozoites in the skin. Ann N Y Acad Sci *1342*, 37-43.

Howes, R.E., Battle, K.E., Mendis, K.N., Smith, D.L., Cibulskis, R.E., Baird, J.K., and Hay, S.I. (2016). Global Epidemiology of Plasmodium vivax. Am J Trop Med Hyg *95*, 15-34.

Hu, K., Mann, T., Striepen, B., Beckers, C.J., Roos, D.S., and Murray, J.M. (2002). Daughter cell assembly in the protozoan parasite Toxoplasma gondii. Mol Biol Cell *13*, 593-606.

Invergo, B.M., Brochet, M., Yu, L., Choudhary, J., Beltrao, P., and Billker, O. (2017). Sub-minute Phosphoregulation of Cell Cycle Systems during Plasmodium Gamete Formation. Cell Rep *21*, 2017-2029.

Ishiyama, A., Otoguro, K., Namatame, M., Nishihara, A., Furusawa, T., Takahashi, Y., Masuma, R., Shiomi, K., and Omura, S. (2008). Simaomicin alpha: effects on the cell cycle of synchronized, cultured Plasmodium falciparum. J Antibiot (Tokyo) *61*, 254-257.

Janse, C.J., Mons, B., Rouwenhorst, R.J., Van der Klooster, P.F., Overdulve, J.P., and Van der Kaay, H.J. (1985). In vitro formation of ookinetes and functional maturity of Plasmodium berghei gametocytes. Parasitology *91 (Pt 1)*, 19-29.

Jaskiewicz, E., Jodlowska, M., Kaczmarek, R., and Zerka, A. (2019). Erythrocyte glycophorins as receptors for Plasmodium merozoites. Parasit Vectors *12*, 317.

Josling, G.A., and Llinas, M. (2015). Sexual development in Plasmodium parasites: knowing when it's time to commit. Nat Rev Microbiol *13*, 573-587.

Kafsack, B.F., Rovira-Graells, N., Clark, T.G., Bancells, C., Crowley, V.M., Campino, S.G., Williams, A.E., Drought, L.G., Kwiatkowski, D.P., Baker, D.A.*, et al.* (2014). A transcriptional switch underlies commitment to sexual development in malaria parasites. Nature *507*, 248-252.

Kats, L.M., Black, C.G., Proellocks, N.I., and Coppel, R.L. (2006). Plasmodium rhoptries: how things went pear-shaped. Trends Parasitol *22*, 269-276.

Khan, S.M., Franke-Fayard, B., Mair, G.R., Lasonder, E., Janse, C.J., Mann, M., and Waters, A.P. (2005). Proteome analysis of separated male and female gametocytes reveals novel sex-specific Plasmodium biology. Cell *121*, 675-687.

Khodjakov, A., and Rieder, C.L. (2001). Centrosomes enhance the fidelity of cytokinesis in vertebrates and are required for cell cycle progression. J Cell Biol *153*, 237-242.

Kilmartin, J.V. (2014). Lessons from yeast: the spindle pole body and the centrosome. Philos Trans R Soc Lond B Biol Sci *369*.

Kim, K., and Weiss, L.M. (2004). Toxoplasma gondii: the model apicomplexan. Int J Parasitol *34*, 423-432.

Koch, M., and Baum, J. (2016). The mechanics of malaria parasite invasion of the human erythrocyte - towards a reassessment of the host cell contribution. Cell Microbiol *18*, 319-329.

Kono, M., Heincke, D., Wilcke, L., Wong, T.W., Bruns, C., Herrmann, S., Spielmann, T., and Gilberger, T.W. (2016). Pellicle formation in the malaria parasite. J Cell Sci *129*, 673-680.

Kuehn, A., and Pradel, G. (2010). The coming-out of malaria gametocytes. J Biomed Biotechnol *2010*, 976827.

Lal, K., Prieto, J.H., Bromley, E., Sanderson, S.J., Yates, J.R., 3rd, Wastling, J.M., Tomley, F.M., and Sinden, R.E. (2009). Characterisation of Plasmodium invasive organelles; an ookinete microneme proteome. Proteomics *9*, 1142-1151.

Langhi, D.M., Jr., and Bordin, J.O. (2006). Duffy blood group and malaria. Hematology *11*, 389-398.

Le Roch, K., Sestier, C., Dorin, D., Waters, N., Kappes, B., Chakrabarti, D., Meijer, L., and Doerig, C. (2000). Activation of a Plasmodium falciparum cdc2-related kinase by heterologous p25 and cyclin H. Functional characterization of a P. falciparum cyclin homologue. J Biol Chem *275*, 8952-8958.

Lye, Y.M., Chan, M., and Sim, T.S. (2006). Pfnek3: an atypical activator of a MAP kinase in Plasmodium falciparum. FEBS Lett *580*, 6083-6092.

Mahajan, B., Selvapandiyan, A., Gerald, N.J., Majam, V., Zheng, H., Wickramarachchi, T., Tiwari, J., Fujioka, H., Moch, J.K., Kumar, N.*, et al.* (2008). Centrins, cell cycle regulation proteins in human malaria parasite Plasmodium falciparum. J Biol Chem *283*, 31871-31883.

Mahjoub, M.R., Qasim Rasi, M., and Quarmby, L.M. (2004). A NIMA-related kinase, Fa2p, localizes to a novel site in the proximal cilia of Chlamydomonas and mouse kidney cells. Mol Biol Cell *15*, 5172-5186.

Maier, A.G., Duraisingh, M.T., Reeder, J.C., Patel, S.S., Kazura, J.W., Zimmerman, P.A., and Cowman, A.F. (2003). Plasmodium falciparum erythrocyte invasion through glycophorin C and selection for Gerbich negativity in human populations. Nat Med *9*, 87-92.

Manning, G., Reiner, D.S., Lauwaet, T., Dacre, M., Smith, A., Zhai, Y., Svard, S., and Gillin, F.D. (2011). The minimal kinome of Giardia lamblia illuminates early kinase evolution and unique parasite biology. Genome Biol *12*, R66.

Marques, S.R., Ramakrishnan, C., Carzaniga, R., Blagborough, A.M., Delves, M.J., Talman, A.M., and Sinden, R.E. (2015). An essential role of the basal body protein SAS-6 in Plasmodium male gamete development and malaria transmission. Cell Microbiol *17*, 191-206.

Matthews, H., Duffy, C.W., and Merrick, C.J. (2018). Checks and balances? DNA replication and the cell cycle in Plasmodium. Parasit Vectors *11*, 216.

McKenzie, F.E., Ferreira, M.U., Baird, J.K., Snounou, G., and Bossert, W.H. (2001). Meiotic recombination, cross-reactivity, and persistence in Plasmodium falciparum. Evolution *55*, 1299-1307.

Melo Hanchuk, T.D., Papa, P.F., La Guardia, P.G., Vercesi, A.E., and Kobarg, J. (2015). Nek5 interacts with mitochondrial proteins and interferes negatively in mitochondrial mediated cell death and respiration. Cell Signal *27*, 1168-1177.

Menard, R., Tavares, J., Cockburn, I., Markus, M., Zavala, F., and Amino, R. (2013). Looking under the skin: the first steps in malarial infection and immunity. Nat Rev Microbiol *11*, 701-712.

Menkin-Smith, L., and Winders, W.T. (2020). Malaria (Plasmodium Vivax). In StatPearls (Treasure Island (FL)).

Michalik, P. (2009). On the occurrence of the 9+0 axonemal pattern in the spermatozoa of sheetweb spiders (Araneae, Linyphiidae). Journal of Arachnology *33*, 569-572.

Mitchell, D.R. (2004). Speculations on the evolution of 9+2 organelles and the role of central pair microtubules. Biol Cell *96*, 691-696.

Mlambo, G., Coppens, I., and Kumar, N. (2012). Aberrant sporogonic development of Dmc1 (a meiotic recombinase) deficient Plasmodium berghei parasites. PLoS One *7*, e52480.

Moritz, M., Braunfeld, M.B., Guenebaut, V., Heuser, J., and Agard, D.A. (2000). Structure of the gamma-tubulin ring complex: a template for microtubule nucleation. Nat Cell Biol *2*, 365-370.

Morris, N.R. (1975). Mitotic mutants of Aspergillus nidulans. Genet Res *26*, 237-254.

Nigg, E.A., and Holland, A.J. (2018). Once and only once: mechanisms of centriole duplication and their deregulation in disease. Nat Rev Mol Cell Biol *19*, 297-312.

Nogales, E., and Downing, K. (2008). Tubulin and Microtubule Structures. In The Role of Microtubules in Cell Biology, Neurobiology and Oncology T. Fojo, ed. (Humana Press).

O'Regan, L., Blot, J., and Fry, A.M. (2007). Mitotic regulation by NIMA-related kinases. Cell Div *2*, 25.

O'Regan, L., and Fry, A.M. (2009). The Nek6 and Nek7 protein kinases are required for robust mitotic spindle formation and cytokinesis. Mol Cell Biol *29*, 3975-3990.

O'Regan, L., Sampson, J., and Fry, A.M. (2015a). Hsp70 proteins in mitosis and disease. Oncotarget *6*, 32293-32294.

O'Regan, L., Sampson, J., Richards, M.W., Knebel, A., Roth, D., Hood, F.E., Straube, A., Royle, S.J., Bayliss, R., and Fry, A.M. (2015b). Hsp72 is targeted to the mitotic spindle by Nek6 to promote K-fiber assembly and mitotic progression. J Cell Biol *209*, 349-358.

Oakley, B.R., and Morris, N.R. (1983). A mutation in Aspergillus nidulans that blocks the transition from interphase to prophase. J Cell Biol *96*, 1155-1158.

Osmani, S.A., Pu, R.T., and Morris, N.R. (1988). Mitotic induction and maintenance by overexpression of a G2-specific gene that encodes a potential protein kinase. Cell *53*, 237-244.

Peres de Oliveira, A., Kazuo Issayama, L., Betim Pavan, I.C., Riback Silva, F., Diniz Melo-Hanchuk, T., Moreira Simabuco, F., and Kobarg, J. (2020). Checking NEKs: Overcoming a Bottleneck in Human Diseases. Molecules *25*.

Philip, N., and Waters, A.P. (2015). Conditional Degradation of Plasmodium Calcineurin Reveals Functions in Parasite Colonization of both Host and Vector. Cell Host Microbe *18*, 122-131.

Posfai, D., Sylvester, K., Reddy, A., Ganley, J.G., Wirth, J., Cullen, Q.E., Dave, T., Kato, N., Dave, S.S., and Derbyshire, E.R. (2018). Plasmodium parasite exploits host aquaporin-3 during liver stage malaria infection. PLoS Pathog *14*, e1007057.

Pradel, L.C., Bonhivers, M., Landrein, N., and Robinson, D.R. (2006). NIMA-related kinase TbNRKC is involved in basal body separation in Trypanosoma brucei. J Cell Sci *119*, 1852-1863.

Quarmby, L.M., and Mahjoub, M.R. (2005). Caught Nek-ing: cilia and centrioles. J Cell Sci *118*, 5161-5169.

Rangarajan, R., Bei, A., Henry, N., Madamet, M., Parzy, D., Nivez, M.P., Doerig, C., and Sultan, A. (2006). Pbcrk-1, the Plasmodium berghei orthologue of P. falciparum cdc-2 related kinase-1 (Pfcrk-1), is essential for completion of the intraerythrocytic asexual cycle. Exp Parasitol *112*, 202-207.

Rapley, J., Nicolas, M., Groen, A., Regue, L., Bertran, M.T., Caelles, C., Avruch, J., and Roig, J. (2008). The NIMA-family kinase Nek6 phosphorylates the kinesin Eg5 at a novel site necessary for mitotic spindle formation. J Cell Sci *121*, 3912-3921.

Rea, E., Le Roch, K.G., and Tewari, R. (2018). Sex in Plasmodium falciparum: Silence Play between GDV1 and HP1. Trends Parasitol *34*, 450-452.

Reininger, L., Billker, O., Tewari, R., Mukhopadhyay, A., Fennell, C., Dorin-Semblat, D., Doerig, C., Goldring, D., Harmse, L., Ranford-Cartwright, L.*, et al.* (2005). A NIMA-related protein kinase is essential for completion of the sexual cycle of malaria parasites. J Biol Chem *280*, 31957-31964.

Reininger, L., Garcia, M., Tomlins, A., Muller, S., and Doerig, C. (2012). The Plasmodium falciparum, Nima-related kinase Pfnek-4: a marker for asexual parasites committed to sexual differentiation. Malar J *11*, 250.

Reininger, L., Tewari, R., Fennell, C., Holland, Z., Goldring, D., Ranford-Cartwright, L., Billker, O., and Doerig, C. (2009). An essential role for the Plasmodium Nek-2 Nima-related protein kinase in the sexual development of malaria parasites. J Biol Chem *284*, 20858-20868.

Reininger, L., Wilkes, J.M., Bourgade, H., Miranda-Saavedra, D., and Doerig, C. (2011). An essential Aurora-related kinase transiently associates with spindle pole bodies during Plasmodium falciparum erythrocytic schizogony. Mol Microbiol *79*, 205-221.

Risco-Castillo, V., Topcu, S., Marinach, C., Manzoni, G., Bigorgne, A.E., Briquet, S., Baudin, X., Lebrun, M., Dubremetz, J.F., and Silvie, O. (2015). Malaria Sporozoites Traverse Host Cells within Transient Vacuoles. Cell Host Microbe *18*, 593-603.

Robbins, J.A., Absalon, S., Streva, V.A., and Dvorin, J.D. (2017). The Malaria Parasite Cyclin H Homolog PfCyc1 Is Required for Efficient Cytokinesis in Blood-Stage Plasmodium falciparum. mBio *8*.

Roig, J., Groen, A., Caldwell, J., and Avruch, J. (2005). Active Nercc1 protein kinase concentrates at centrosomes early in mitosis and is necessary for proper spindle assembly. Mol Biol Cell *16*, 4827-4840.

Roig, J., Mikhailov, A., Belham, C., and Avruch, J. (2002). Nercc1, a mammalian NIMA-family kinase, binds the Ran GTPase and regulates mitotic progression. Genes Dev *16*, 1640-1658.

Roos, D.S., Crawford, M.J., Donald, R.G., Fohl, L.M., Hager, K.M., Kissinger, J.C., Reynolds, M.G., Striepen, B., and Sullivan, W.J., Jr. (1999). Transport and trafficking: Toxoplasma as a model for Plasmodium. Novartis Found Symp *226*, 176-195; discussion 195-178.

Roques, M., Stanway, R.R., Rea, E.I., Markus, R., Brady, D., Holder, A.A., Guttery, D.S., and Tewari, R. (2019). Plasmodium centrin PbCEN-4 localizes to the putative MTOC and is dispensable for malaria parasite proliferation. Biol Open *8*.

Roques, M., Wall, R.J., Douglass, A.P., Ramaprasad, A., Ferguson, D.J., Kaindama, M.L., Brusini, L., Joshi, N., Rchiad, Z., Brady, D.*, et al.* (2015). Plasmodium P-Type Cyclin CYC3 Modulates Endomitotic Growth during Oocyst Development in Mosquitoes. PLoS Pathog *11*, e1005273.

Roskams, T., Moshage, H., De Vos, R., Guido, D., Yap, P., and Desmet, V. (1995). Heparan sulfate proteoglycan expression in normal human liver. Hepatology *21*, 950-958.

Rossetto, D., Avvakumov, N., and Cote, J. (2012). Histone phosphorylation: a chromatin modification involved in diverse nuclear events. Epigenetics *7*, 1098-1108.

Saini, E., Zeeshan, M., Brady, D., Pandey, R., Kaiser, G., Koreny, L., Kumar, P., Thakur, V., Tatiya, S., Katris, N.J*., et al.* (2017). Photosensitized INA-Labelled protein 1 (PhIL1) is novel component of the inner membrane complex and is required for Plasmodium parasite development. Sci Rep *7*, 15577.

Sarrazin, S., Lamanna, W.C., and Esko, J.D. (2011). Heparan sulfate proteoglycans. Cold Spring Harb Perspect Biol *3*.

Sdelci, S., Bertran, M.T., and Roig, J. (2011). Nek9, Nek6, Nek7 and the separation of centrosomes. Cell Cycle *10*, 3816-3817.

Sdelci, S., Schutz, M., Pinyol, R., Bertran, M.T., Regue, L., Caelles, C., Vernos, I., and Roig, J. (2012). Nek9 phosphorylation of NEDD1/GCP-WD contributes to Plk1 control of gamma-tubulin recruitment to the mitotic centrosome. Curr Biol *22*, 1516-1523.

Sebastian, S., Brochet, M., Collins, M.O., Schwach, F., Jones, M.L., Goulding, D., Rayner, J.C., Choudhary, J.S., and Billker, O. (2012). A Plasmodium calcium-dependent protein kinase controls zygote development and transmission by translationally activating repressed mRNAs. Cell Host Microbe *12*, 9-19.

Shahabuddin, M. (1998). Plasmodium ookinete development in the mosquito midgut: a case of reciprocal manipulation. Parasitology *116 Suppl*, S83-93.

Sinden, R.E. (1991). Mitosis and meiosis in malarial parasites. Acta Leiden *60*, 19-27.

Sinden, R.E. (2009). Malaria, sexual development and transmission: retrospect and prospect. Parasitology *136*, 1427-1434.

Sinden, R.E., Canning, E.U., and Spain, B. (1976). Gametogenesis and fertilization in Plasmodium yoelii nigeriensis: a transmission electron microscope study. Proc R Soc Lond B Biol Sci *193*, 55-76.

Sinden, R.E., Talman, A., Marques, S.R., Wass, M.N., and Sternberg, M.J. (2010). The flagellum in malarial parasites. Curr Opin Microbiol *13*, 491-500.

Smith, E.F., and Lefebvre, P.A. (1997). The role of central apparatus components in flagellar motility and microtubule assembly. Cell Motil Cytoskeleton *38*, 1-8.

Smith, R.C., Vega-Rodriguez, J., and Jacobs-Lorena, M. (2014). The Plasmodium bottleneck: malaria parasite losses in the mosquito vector. Mem Inst Oswaldo Cruz *109*, 644-661.

Solyakov, L., Halbert, J., Alam, M.M., Semblat, J.P., Dorin-Semblat, D., Reininger, L., Bottrill, A.R., Mistry, S., Abdi, A., Fennell, C*., et al.* (2011). Global kinomic and phospho-proteomic analyses of the human malaria parasite Plasmodium falciparum. Nat Commun *2*, 565.

Spang, A., Courtney, I., Fackler, U., Matzner, M., and Schiebel, E. (1993). The calcium-binding protein cell division cycle 31 of Saccharomyces cerevisiae is a component of the half bridge of the spindle pole body. J Cell Biol *123*, 405-416.

Spreng, B., Fleckenstein, H., Kubler, P., Di Biagio, C., Benz, M., Patra, P., Schwarz, U.S., Cyrklaff, M., and Frischknecht, F. (2019). Microtubule number and length determine cellular shape and function in Plasmodium. EMBO J *38*, e100984.

Straschil, U., Talman, A.M., Ferguson, D.J., Bunting, K.A., Xu, Z., Bailes, E., Sinden, R.E., Holder, A.A., Smith, E.F., Coates, J.C*., et al.* (2010). The Armadillo repeat protein PF16 is essential for flagellar structure and function in Plasmodium male gametes. PLoS One *5*, e12901.

Striepen, B., Jordan, C.N., Reiff, S., and van Dooren, G.G. (2007). Building the perfect parasite: cell division in apicomplexa. PLoS Pathog *3*, e78.

Sturm, A., Amino, R., van de Sand, C., Regen, T., Retzlaff, S., Rennenberg, A., Krueger, A., Pollok, J.M., Menard, R., and Heussler, V.T. (2006). Manipulation of host hepatocytes by the malaria parasite for delivery into liver sinusoids. Science *313*, 1287-1290.

Talman, A.M., Domarle, O., McKenzie, F.E., Ariey, F., and Robert, V. (2004). Gametocytogenesis: the puberty of Plasmodium falciparum. Malar J *3*, 24.

Talman, A.M., Prieto, J.H., Marques, S., Ubaida-Mohien, C., Lawniczak, M., Wass, M.N., Xu, T., Frank, R., Ecker, A., Stanway, R.S.*, et al.* (2014). Proteomic analysis of the Plasmodium male gamete reveals the key role for glycolysis in flagellar motility. Malar J *13*, 315.

Terzakis, J.A., Vanderberg, J.P., Foley, D., and Shustak, S. (1979). Exoerythrocytic merozoites of Plasmodium berghei in rat hepatic Kupffer cells. J Protozool *26*, 385-389.

Tewari, R., Dorin, D., Moon, R., Doerig, C., and Billker, O. (2005). An atypical mitogen-activated protein kinase controls cytokinesis and flagellar motility during male gamete formation in a malaria parasite. Mol Microbiol *58*, 1253-1263.

Tewari, R., Straschil, U., Bateman, A., Bohme, U., Cherevach, I., Gong, P., Pain, A., and Billker, O. (2010). The systematic functional analysis of Plasmodium protein kinases identifies essential regulators of mosquito transmission. Cell Host Microbe *8*, 377-387.

Trampuz, A., Jereb, M., Muzlovic, I., and Prabhu, R.M. (2003). Clinical review: Severe malaria. Crit Care *7*, 315-323.

Tuteja, R. (2007). Malaria - an overview. FEBS J *274*, 4670-4679.

Usui, M., Prajapati, S.K., Ayanful-Torgby, R., Acquah, F.K., Cudjoe, E., Kakaney, C., Amponsah, J.A., Obboh, E.K., Reddy, D.K., Barbeau, M.C.*, et al.* (2019). Plasmodium falciparum sexual differentiation in malaria patients is associated with host factors and GDV1-dependent genes. Nat Commun *10*, 2140.

Vaishnava, S., Morrison, D.P., Gaji, R.Y., Murray, J.M., Entzeroth, R., Howe, D.K., and Striepen, B. (2005). Plastid segregation and cell division in the apicomplexan parasite Sarcocystis neurona. J Cell Sci *118*, 3397-3407.

Vale, R.D. (2003). The molecular motor toolbox for intracellular transport. Cell *112*, 467-480.

Vaughan, A.M., and Kappe, S.H.I. (2017). Malaria Parasite Liver Infection and Exoerythrocytic Biology. Cold Spring Harb Perspect Med *7*.

Wall, R.J., Ferguson, D.J.P., Freville, A., Franke-Fayard, B., Brady, D., Zeeshan, M., Bottrill, A.R., Wheatley, S., Fry, A.M., Janse, C.J.*, et al.* (2018). Plasmodium APC3 mediates chromosome condensation and cytokinesis during atypical mitosis in male gametogenesis. Sci Rep *8*, 5610.

Wall, R.J., Roques, M., Katris, N.J., Koreny, L., Stanway, R.R., Brady, D., Waller, R.F., and Tewari, R. (2016). SAS6-like protein in Plasmodium indicates that conoid-associated apical complex proteins persist in invasive stages within the mosquito vector. Sci Rep *6*, 28604.

White, M.W., and Suvorova, E.S. (2018). Apicomplexa Cell Cycles: Something Old, Borrowed, Lost, and New. Trends Parasitol *34*, 759-771.

WHO (2015). Control and elimination of Plasmodium vivax malaria – A technical brief.

WHO (2019). Malaria.

Wierk, J.K., Langbehn, A., Kamper, M., Richter, S., Burda, P.C., Heussler, V.T., and Deschermeier, C. (2013). Plasmodium berghei MAPK1 displays differential and dynamic subcellular localizations during liver stage development. PLoS One *8*, e59755.

Wiese, C., Goldberg, M.W., Allen, T.D., and Wilson, K.L. (1997). Nuclear envelope assembly in Xenopus extracts visualized by scanning EM reveals a transport-dependent 'envelope smoothing' event. J Cell Sci *110 (Pt 13)*, 1489-1502.

Willems, E., Dedobbeleer, M., Digregorio, M., Lombard, A., Lumapat, P.N., and Rogister, B. (2018). The functional diversity of Aurora kinases: a comprehensive review. Cell Div *13*, 7.

Wilson, L.G., Carter, L.M., and Reece, S.E. (2013). High-speed holographic microscopy of malaria parasites reveals ambidextrous flagellar waveforms. Proc Natl Acad Sci U S A *110*, 18769-18774.

Zeeshan, M., Ferguson, D.J., Abel, S., Burrrell, A., Rea, E., Brady, D., Daniel, E., Delves, M., Vaughan, S., Holder, A.A*., et al.* (2019a). Kinesin-8B controls basal body function and flagellum formation and is key to malaria transmission. Life Sci Alliance *2*.

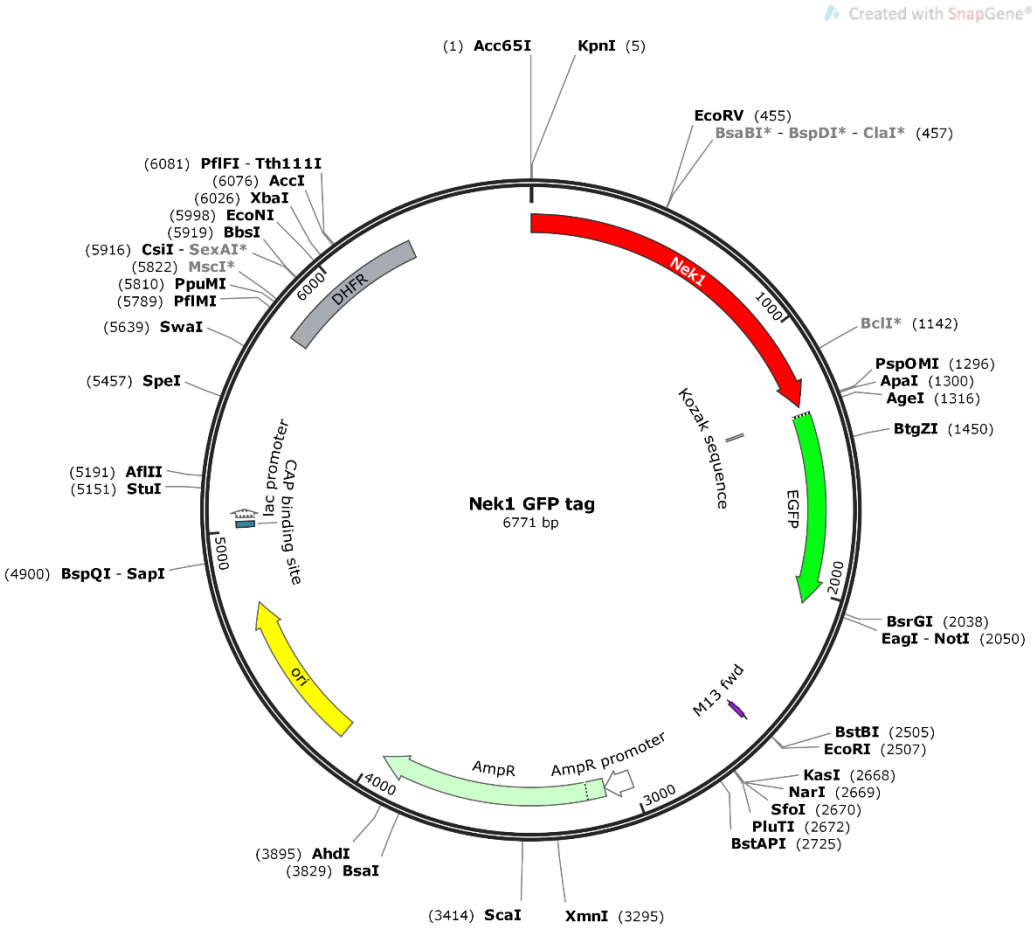
Zeeshan, M., Pandey, R., Ferguson, D.J.P., Tromer, E.C., Markus, R., Abel, S., Brady, D., Daniel, E., Limenitakis, R., Bottrill, A.R*., et al.* (2020). Real-time dynamics of Plasmodium NDC80 reveals unusual modes of chromosome segregation during parasite proliferation. J Cell Sci *134*.

Zeeshan, M., Shilliday, F., Liu, T., Abel, S., Mourier, T., Ferguson, D.J.P., Rea, E., Stanway, R.R., Roques, M., Williams, D*., et al.* (2019b). Plasmodium kinesin-8X associates with mitotic spindles and is essential for oocyst development during parasite proliferation and transmission. PLoS Pathog *15*, e1008048.

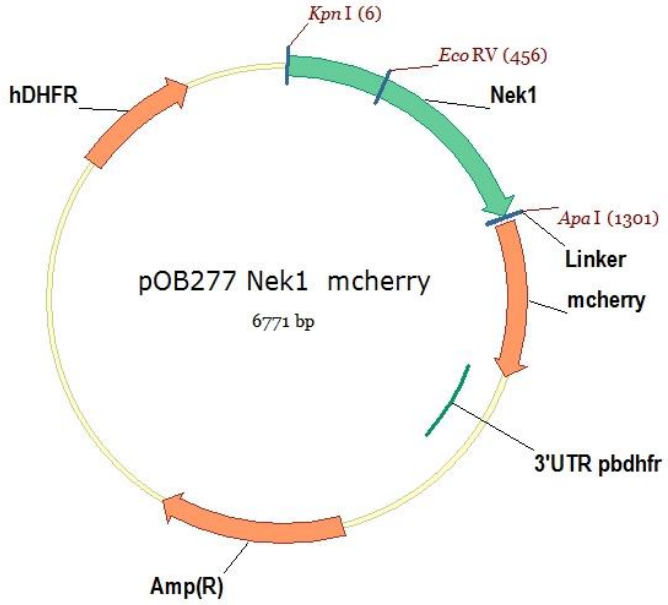
Zheng, X., Gooi, L.M., Wason, A., Gabriel, E., Mehrjardi, N.Z., Yang, Q., Zhang, X., Debec, A., Basiri, M.L., Avidor-Reiss, T*., et al.* (2014). Conserved TCP domain of Sas-4/CPAP is essential for pericentriolar material tethering during centrosome biogenesis. Proc Natl Acad Sci U S A *111*, E354-363.

Appendices

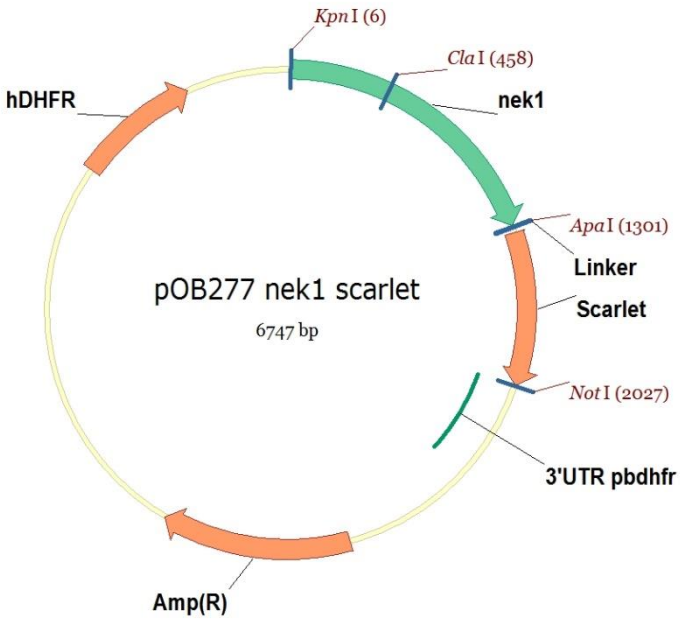
Appendix A| pOB277 vector containing a GFP fluorescing tag. Vectors were transformed into *E. coli* in order to clone the NEK1 C-terminus region, which were digested out of the plasmid using Apa1 and Kpn1 enzymes and separated using gel electrophoresis. Purified C-termini were thus available for ligation into vectors containing mCherry and Scarlet tags.



Appendix B| pOB277 mCherry vector diagram including the restriction enzymes, in which the NEK1 C-terminus region was ligated to produce the construct. Vectors contain hDHFR and Ampicillin cassettes to infer resistance to the drugs and promote selective growth of cells with containing the desired vector.



Appendix C| pOB277 Scarlet vector diagram including the restriction enzymes, in which the NEK1 C-terminus region was ligated to produce the construct. Vectors contain hDHFR and Ampicillin cassettes to infer resistance to the drugs and promote selective growth of cells with containing the desired vector.



Appendix D| Complete table of NEK1 interacting partners identified in mass spectrometry analyses. Accession numbers in red are those that were ejected from Table 10.

Accession Number	Identified Proteins	Molecular Weight	Peptides
PBANKA_1443000	NIMA related kinase 1, putative	108 kDa	32
PBANKA_0507300	dynein heavy chain, putative	624 kDa	30
PBANKA_0416100	dynein heavy chain, putative	685 kDa	27
PBANKA_0925400	dynein heavy chain, putative	605 kDa	24
PBANKA_1405000	MORN repeat protein, putative	150 kDa	13
PBANKA_1320100	conserved Plasmodium protein, unknown function	93 kDa	13
PBANKA_0202700	kinesin-8, putative	169 kDa	11
PBANKA_1035700	WD repeat-containing protein 65, putative	170 kDa	11
PBANKA_0917400	armadillo repeat protein PF16	58 kDa	9
PBANKA_0601200	dynein heavy chain, putative	666 kDa	7
PBANKA_0801500	conserved Plasmodium protein, unknown function	89 kDa	7
PBANKA_1329200	dynein beta chain, putative	766 kDa	7
PBANKA_1361500	WD repeat-containing protein 16, putative	85 kDa	7
PBANKA_1310400	centrin-2, putative	19 kDa	6
PBANKA_1018300	dynein intermediate chain, putative	70 kDa	6
PBANKA_0102700	conserved Plasmodium protein, unknown function	45 kDa	6
PBANKA_0615700	dynein heavy chain, putative	623 kDa	6
PBANKA_1125300	conserved Plasmodium protein, unknown function	107 kDa	6
PBANKA_1458800	kinesin, putative	165 kDa	6
PBANKA_0906900	conserved Plasmodium protein, unknown function	273 kDa	6
PBANKA_1308000	conserved Plasmodium protein, unknown function	792 kDa	5
PBANKA_0939300	conserved Plasmodium protein, unknown function	129 kDa	5
PBANKA_0719700	conserved Plasmodium protein, unknown function	89 kDa	5
PBANKA_1431500	radial spoke head protein 9, putative	42 kDa	5
PBANKA_0822900	dynein intermediate chain, putative	94 kDa	5
PBANKA_1033700	conserved Plasmodium protein, unknown function	36 kDa	5
PBANKA_1110300	WD repeat-containing protein, putative	73 kDa	5
PBANKA_0314200	calcium-dependent protein kinase 1	61 kDa	4
PBANKA_0401100	serine/threonine protein kinase, putative	154 kDa	4
PBANKA_0415800	WD repeat-containing protein 66, putative	131 kDa	4
PBANKA_0507800	conserved protein, unknown function	60 kDa	4
PBANKA_0509700	conserved Plasmodium protein, unknown function	567 kDa	4
PBANKA_1428300	WD repeat-containing protein, putative	145 kDa	4
PBANKA_0803600	importin-7, putative	144 kDa	3
PBANKA_0206300	centrin-1, putative	20 kDa	3
PBANKA_0504300	flagellar outer arm dynein-associated protein, putative	12 kDa	3
PBANKA_1331300	conserved Plasmodium protein, unknown function	223 kDa	3
PBANKA_0711000	conserved Plasmodium protein, unknown function	160 kDa	3